Università degli Studi di Napoli "Federico II"

Facoltà di Scienze Matematiche Fisiche e Naturali

On the robustness of holonomic quantum computation

Cosmo Lupo

Ph.D. in Physics

Dottorato di Ricerca in Fisica Fondamentale ed Applicata

- XX Ciclo -

Supervisor:
Prof. Giuseppe Marmo

Coordinatore:
Prof. Gennaro Miele

anno accademico 2006/2007

Abstract

Besides standard *dynamical* schemes to realize a quantum computer, there are particular approaches which are based on intrinsic properties of quantum systems, leading to the definition of *topological* computation and *holonomic*, or *geometric*, computation. The holonomic approach can be viewed as the application of *non-Abelian geometric phases* to quantum information processing, it is believed to be *fault-tolerant* with respect of certain kind of *parametric noise*. Here we discuss the issue of robustness of holonomic quantum gates under parametric noise: we distinguish between *geometric* and *dynamical* effects of cancelation, which can appear in different contexts. A so-called *standard argument* in favor of the stability of noisy holonomic quantum gates is reviewed and extended to more general settings. New geometric effects that describe the behavior of noisy holonomic gates are presented. These effects lead to a *refining* of the *optimal strategy* to achieve a robust computation.

[...] I have no illusions of power, as to the scope and prospect of my attitude.
But, the minor role of my act and statement is a simple way of affirming that
in the face of a growing enormity which I consider intolerable,
I will exercise my own tiny act of disobedience to be able to look straight
into the eyes of my grandchildren and my students and say that I did know.

DANIEL AMIT
(from the letter to the American Physical Society, April 2003)

Contents

Preface

The present Dissertation collects part of the activity done during the doctorate at the University of Napoli "Federico II" regarding the issue of the *robustness of holonomic computation*. That is not the only subject to which my research activity was devoted during the last three years: two other main research interests were the *characterization of bi-partite and multi-partite entanglement* and the study of *linear-optical schemes for quantum computation*.
Finally, in order to allow a more concise and self-contained presentation, I decided to devote my Dissertation to a single topic.

The activity devoted to the characterization of quantum correlations started during my Master Thesis, when, under the supervising of Giuseppe Marmo, we studied bi-partite entanglement in the framework of the geometric approach to quantum mechanics. The collaboration with Volodya Man'ko yielded three joint publications on *Journal of Physics A* [Lu05, Lu06, Lu07]. In [Lu05], together with George Sudarshan, we proposed and studied a simple generalization of the operation of the partial transpose, called the *partial scaling transform*, which was considered for the study of bi-partite and multi-partite entanglement. In [Lu06] and [Lu07], we made use of the tomographic description of quantum mechanics to analyze the violations of Bell-like inequalities for systems with discrete levels. After my visiting period at the Max Planck institute for quantum optics, discussions about the entanglement in Matrix Product States led to the study of the *Realignment Criterion* and its possible generalizations; some preliminary results on that subject are available on the web in [Lu07+]. Further developments of are now in progress in collaboration with Paolo Aniello (see [An07']).

The activities regarding linear-optical schemes for quantum computing started in our group with Ruben Coen Cagli, who wrote his Master Thesis and published two papers on that subject. With Paolo Aniello and Mario Napolitano, we continued that line of research which led to the publication of the paper [An06] in a special issue of *Open System and Information Dynamics* related to the conference TQMFA, hosted in Palermo in 2005. The collaboration with Matteo Paris also led to the publication of another paper [An07] on that subject in *European Physical Journal D*.

The holonomic approach to quantum computing can be viewed as an application of geometric phases to quantum information processing. The interest in holonomic computation began with a series of seminar lectures given by Paolo Zanardi at the University of Napoli in the early 2004. The interest turned into activity after the appearance of a paper by Giuseppe Florio *et al.* [Fl06]. That paper yielded the right inspiration that led me, together with Paolo Aniello, Mario Napolitano and Giuseppe Florio, to the publication of the paper [Lu07'] on *Physical Review A*, concerning the issue of the robustness of holonomic computation under parametric noise. The content of that paper is contained in the chapter 3 of the present Dissertation. Other original considerations and results regarding

that subject are presented here for the first time in the chapters 4 and 5.

Few months ago, during a conference in Palermo, while I was already working at that subject, I had the opportunity to know that there is a planned experiment, whose aim will be to experimentally verify the robustness of geometric phases (see the Ph.D. Dissertation by Stefan Filipp [Fi06], now working at the Atominstitut der Österreichischen Universitäten in Wien, in the group of Helmut Rauch). I sincerely hope that the ideas and the calculations presented here can be useful for the interpretation of the experimental results.

Introduction

The word "holonomy" comes from the Greek roots *holos* and *nomos*, literarily meaning a "global rule". In differential geometry a holonomy in a principal fibre bundle is a consequence of the presence of a connection one-form with a non-vanishing curvature [Na05]. In physics, holonomies are a manifestation of gauge theories, example are the geometric phases described by S. Pancharatnam in [Pa56], by M. Berry and B. Simon in [Be84, Si83], by Y. Aharonov and J. Anandan in [AA87].

The application of quantum holonomies to the scopes of *quantum information processing* [NC00, Be04] leads to a particular approach which is known as *holonomic*, or *geometric* quantum computation. One of the most important challenges for the realization of quantum information tasks is the implementation of quantum logic gates that are *robust* in the presence of perturbations. An important issue is the analysis of the various kinds of errors than can affect computations or communications. In general, one can consider sources of error that can reduce or even destroy the efficacy of a specific operation.

The holonomic approach presents several complications with respect to other standard, dynamical schemes. The proper balance is determined by the fact that geometric phases are believed to be intrinsically *fault tolerant* with respect to some kind of errors.

Two kinds of source of errors can be distinguished: the first kind is a quantum noise, which is a consequence of the interaction of the system of interest with an environment of quantum degrees of freedom; the second kind is a classical noise, emerging from the interaction of the classical fields that are used to experimentally control the system with an environment of classical degrees of freedom. That kind of classical noise will be also called *parametric noise*. The subject of the present contribution is the study of the behavior of holonomic gates in the presence of parametric noise. To take in consideration only the classical noise can be viewed as a great limitation, since the most general noise is of quantum nature. Nevertheless, the restriction to the classical noise is motivated by the fact that it is with respect of that kind of errors that the holonomic computation is believed to be robust. A critical analysis of the issue of robustness of holonomic computation in the presence of parametric noise is indeed the main task of the present Dissertation.

The Thesis is organized in the following way:

- The first chapter contains a brief introduction to quantum information science. There is no ambition of giving a complete presentation of the field. The aim of the chapter is to communicate to the reader the flavor of some general ideas on which the field of quantum information science is based. We will review the Deutsch's algorithm as an example of the computational speed-up that can be obtained to solve classical problems with a quantum approach. The emphasis is on the role played by quantum interference. If it is true, quoting Richard Feynman, that the double-slit experiment contains all the mystery of quantum theory, it can be as well useful to

explain the core of quantum parallelism.

- In the second chapter, we present the main topic of the Dissertation, which is the *holonomic* scheme for quantum computing. Since that scheme is a straightforward application of quantum geometric phases (non-Abelian Berry's phases) to quantum computing, the chapter will review how geometric phases can be observed in quantum (and classical) mechanics. That will lead to the applications in quantum information processing. Starting with the description of geometric phases in classical optics, after we consider the geometric phases that appear in quantum mechanics in correspondence with a cyclic evolution and in the adiabatic case. The case of non-Abelian holonomies will lead to the applications for quantum information tasks. The proposal of a fully geometric computation with trapped ions will be considered in more details as a case study. The chapter ends with a review of the argument of robustness of holonomic gates, and in general geometric phases, in the presence of parametric noise and in the adiabatic limit. It is worth remarking that that robustness argument is related to the perturbations induced by the noise at the first order in its amplitude.

- Chapter three is devoted to the discussion of the behavior of non-adiabatic geometric phases. We discuss a peculiar example, in which a holonomic but non-adiabatic gate mimics the dynamics in the adiabatic regime. The attention will be focused on the efficacy of the gate in the presence of parametric noise, and we will pose the question whether the robustness of the geometric phases can be stated also in the non-adiabatic case. That will lead to the distinction between geometric and dynamical effects of cancelation of the noise. This chapter is mainly based on the paper [Lu07'].

- The robustness of geometric gates under parametric noise is discussed in the chapter four focusing on a simple *toy model*. The system under consideration is a semi-classical particle in the presence of a static magnetic field. If the particle moves along a closed loop, it acquires a phase factor which is only determined by the gauge potential and the given loop. Despite its simplicity, that model presents all the features that are peculiar of holonomic transformations. Indeed, that discussion is useful to understand the behavior of geometric phases in the presence of parametric noise, since in the adiabatic limit the dynamics can be completely determined by the underlying geometry. That geometric behavior is largely independent of the details of the system under consideration. The results, obtained analytically and numerically, leads to the individuation and the comprehension of the perturbative effects of the parametric noise at the second order in the noise amplitude.

- Finally, in chapter five, we analyze the behavior of geometric phases in the presence of parametric noise with respect to a given case study. The case study corresponds to the proposal of the geometric NOT gate with trapped ions. The results obtained for the toy model are numerically confirmed in that model.

Finally, few indications to the reader. Part of my efforts in the development of the present Dissertation was in order to make it understandable for a vast audience. Sadly, that task was rather demanding for the scope of a Ph.D. Thesis. More realistically, I may say that the only skills required to understand this Dissertation are a basic knowledge of non-relativistic quantum mechanics, some elements of differential geometry and, of course, the ability to read English at least at same level the author can write.

Chapter 1

Processing quantum information

The aim of this chapter is to give a general introduction to *quantum information processing*, or *quantum computation* in a lose sense. The presentation will be brief and far to be complete or self-consistent. The emphasis will be given on some of the basic aspects of quantum computation, the ambitious of the writer is not to be clear or exhaustive, but more simply to communicate the *flavor* of what a quantum computation is without going in the details of the rich field of quantum information theory. Hence, the presentation is rather general and is intended for a reader with a basic knowledge of non-relativistic quantum mechanics.

The basic idea in *quantum information science* is that information can be encoded in the state of a quantum mechanical system (read: a physical system whose behavior is explained by the principle of quantum theory at the best of our knowledge). Hence, given a *input* state $|\psi_{\text{in}}\rangle$, which expresses the configuration of some quantum system in a pure state, a *quantum algorithm* is nothing more than the physical transformation that the system experiences. Hence, by the principles of quantum mechanics, a quantum algorithm is a unitary transformation which maps an *input* state into an *output* state:

$$|\psi_{\text{in}}\rangle \ \longrightarrow \ |\psi_{\text{out}}\rangle = U|\psi_{\text{in}}\rangle \ . \tag{1.1}$$

The evolution of an ideally isolated quantum system is described by the non-autonomous Schrödinger equation

$$i\hbar\frac{d}{dt}|\psi(t)\rangle = H(t)|\psi(s)\rangle \ , \tag{1.2}$$

with the initial condition $|\psi(0)\rangle = |\psi_{\text{in}}\rangle$. Hence the unitary evolutor is formally written as

$$U = \mathbf{T}\exp\left(-\frac{i}{\hbar}\int_0^T H(t)dt\right) \ , \tag{1.3}$$

where $\mathbf{T}$ stands for the time-ordering, and T is the *operational time* of the computation.

1.1 Is information physical?

Encoding, storing, processing, sharing and decoding information have a fundamental role for the personal and cultural growth of the single human beings as well as for the development of the human societies. Through the history and in several contexts, human beings and communities have made use of different physical supports to encode, store and share information. In each context, each of those activities is motivated by some specific social problem. One can ask whether there is any relationship

between the physical support and the social content of information. Mural painting in prehistoric era had some important social meaning which we can only imagine nowadays. From a certain point of view, one may say that that social content is independent of the chemistry of the organic colors or the techniques used to obtained them. On the other hand, what is not irrelevant for the social content was the knowledge that people had and that allowed them to take advantage of those techniques to paint the walls of a cave, hence allowing the community to encode information with a social relevance in the physical medium, communicate and share that information with their contemporaries and with us after thousands of years. That kind of consideration can be extended to any kind of situation furnished by our history, without substantial differences whether we are talking about ink and paper, press, vinyl, magnetic tape or digital support. We can argue that there is a dialectic exchange between science and society also from the information point of view: the physical support and the available technologies do influence what kind of information people can and need to encode, to process and share.

Hence, a (rather philosophical) question that may be posed is about the social potentialities of encoding information in quantum systems. At the moment, obviously, we don't know how that technological opportunity could change the paradigm of information in the present (so-called) information-society. The easiest answer is to mention quantum cryptography, or the computational potentialities of quantum algorithms. Nevertheless, I can imagine that the advantages, or the changes, caused by the entrance of quantum mechanical systems in the everyday technology can be even more deep and unpredictable. The Moore's law is often mentioned to justify the entrance of the quantum theory in the framework of information technology as following from the extrapolation of an exponential law. Nevertheless, it is worth noticing that the paradigmatic difference between classical and quantum physics suggests a radical change which is *qualitative* prior than merely *quantitative*.

A brief introduction to some aspects of these qualitative changes is the subject of the following sections.

1.2 Digital or analog? Particle or wave?

Digital systems make use of a set of discrete variables to encode information, a typical example is a binary variable which takes discrete values in $\{0, 1\}$, often physically realized by voltage levels. An elementary *bit* of information can be also realized by a quantum mechanical system in a straight-forward way. One can for instance take in consideration a particle with spin-$1/2$, to which a Hilbert space $\mathcal{H} \cong \mathbb{C}^2$ is associated. A pair of orthogonal vectors in $\mathcal{H}$ can in principle be used to codify a classical bit of information. If the particle is in the presence of a static magnetic field oriented along the z direction, the system Hamiltonian is written as

$$H = B\sigma_z \ , \tag{1.4}$$

as a consequence, the natural choice is to select the two eigenstates of σ_z as a basis for the information encoding. Having in mind the quantum realization of a classical bit, we denote the ground and the excited states respectively as $|0\rangle$ and $|1\rangle$. Thus, we can realize a classical bit on a quantum support: *if* the energy is measured, the system is either in the state $|0\rangle$ or $|1\rangle$.

The peculiarities of the quantum theory start to play a role when one takes in consideration a second observable which does not commute with the Hamiltonian. For instance, an observable pro-

portional to σ_x defines a different notion of a classical bit, namely:

$$|0'\rangle = \frac{|0\rangle - |1\rangle}{\sqrt{2}} \tag{1.5}$$

$$|1'\rangle = \frac{|0\rangle + |1\rangle}{\sqrt{2}} . \tag{1.6}$$

A more general operator is written as $X = V^\dagger \sigma_z V$, where V is a unitary operator in the corresponding Hilbert space. If V has the following matrix expression

$$V \equiv \begin{bmatrix} \alpha & \beta \\ -\beta^* & \alpha^* \end{bmatrix} , \tag{1.7}$$

in the basis $\{|0\rangle, |1\rangle\}$ determined by σ_z, the basis of eigenvectors of X is written as

$$|0_V\rangle = \alpha|0\rangle - \beta^*|1\rangle \tag{1.8}$$

$$|1_V\rangle = \beta|0\rangle + \alpha^*|1\rangle . \tag{1.9}$$

That ambiguity in the choice of the basis is at the core of the definition of the quantum analogue of the classical bit, commonly known as the *qubit*.

The usual way to deal with a qubit is to fix a preferred basis (say $\{|0\rangle, |1\rangle\}$), hopefully determined by the eigenstates of a physically relevant observable such as the Hamiltonian. In that *computational* basis a generic (pure) state of the qubit is determined by a coherent superposition of the computational states:

$$|\psi\rangle = a|0\rangle + b|1\rangle \text{ with } a, b \in \mathbb{C}^2 . \tag{1.10}$$

Hence, while the measurement of any observable selects a discrete set of states which are the corresponding eigenvectors, the family of possible configurations of a qubit is a continuous set. From that point of view, we can say that the quantum theory is both *digital* and *analog* in its nature, though it is neither digital nor analog, as well as the funding fathers of the theory said that an electron is both a *particle* and a *wave*, although being neither particle nor wave.

The consequence of that duality, from an information theoretical point of view, is the feature commonly known as *quantum parallelism*. That is more apparent if one considers a register of n classical bits and its quantum analogue. In the classical case, a string of n bits can be in one of 2^n different configurations. Each possible configuration is indicated with an integer number $x = 0, 1, \ldots 2^n - 1$, as for example

$$x \equiv 1001 \ldots 10100 . \tag{1.11}$$

In the quantum case, a system of n qubits has a continuous family of possible states:

$$|\psi\rangle = \sum_{x=0}^{2^n-1} c_x |x\rangle , \tag{1.12}$$

where $|x\rangle$ indicates a vector in the computational basis of n qubits, which has an expression of the following kind

$$|x\rangle = |1\rangle|0\rangle|0\rangle|1\rangle \ldots |1\rangle|0\rangle|1\rangle|0\rangle|0\rangle , \tag{1.13}$$

15

or $|x\rangle \in \{|0\rangle, |1\rangle\}^{\otimes^n}$, and lives in the tensor product space $\mathcal{H} \otimes \mathcal{H} \otimes \ldots \otimes \mathcal{H}$. Hence, we can say that the quantum state experiences all the classical states at once. By linearity, the action of a unitary transformation produces the the output state

$$|\psi_{\text{out}}\rangle = U|\psi\rangle = \sum_x c_x U|x\rangle . \tag{1.14}$$

If parallelism in classical computation is realized by implementing one operation at the same time over several registers of bits, in the quantum case the same physical operation can realize several different computations at the same time over the *same* register of qubits. More precisely the number of parallel quantum computations equals the number of orthogonal vectors in the computational space, which is *exponential* in the number of qubits.

To conclude, let us mention that, as in the classical case one can make computation in other basis as the decimal or the hexadecimal system, in the quantum case one can define a qu*d*it as a system which presents d stationary levels, with an associated Hilbert space $\mathcal{H} \cong \mathbb{C}^d$.

1.3   Interference and algorithms

The features of the so-called quantum parallelism might not be of any practical help for the scopes of computation without the phenomenon of quantum *interference*. After the general introduction given above, in this section we discuss a simple but significative example of a quantum algorithm. The first proposal of a *quantum algorithm* to solve a specific problem in an efficient way was formulated by David Deutsch and Richard Jozsa in 1992 [DJ92]. Even though the considered problem was not of a particular interest by itself, that was the first example of a quantum algorithm that allows to solve a problem more efficiently than any known classical algorithm. Other important proposals followed, such as the Grover's and the Shor's algorithm. As we will see, the algorithm takes advantage of a clever utilization of quantum interference.

The problem under consideration is the following, known as the Deutsch's problem. A dichotomic function f is defined over a register of n bits

$$f \quad : \quad x \quad \longrightarrow \quad f(x) \in \{0, 1\}, \tag{1.15}$$

where a state of the register of n bits is indicated with x, with $x = 0, 1, \ldots 2^n - 1$. Moreover, the function is constrained to be either *constant* or *balanced*. The problem is to determine if the function is constant or balanced. The 'classical' way to deterministically solve that kind of problem is to evaluate the function at least $2^n/2 + 1$ times. On the other hand, the 'quantum' approach requires *only a single* evaluation of the function f.

Here, we will describe the case in which the register is composed of only one bit, $x \in \{0, 1\}$. Classically, one needs to evaluate the function twice to determine whether it is constant ($f(0) = f(1)$) or balanced ($f(0) = 1 \oplus f(1)$, where $\oplus$ indicates the sum modulo 2). We will try to put the emphasis on the crucial role played by interference in the *computational speedup* which can be reached with quantum algorithms. For that purpose, we will review the structure of the algorithm and, in order to emphasize its physical interpretation, we will formulate a simple analogy with two relevant physical examples. The first analogy is with the *double-slit* thought experiment, the second one is with a *Mach-Zehnder* interferometer. The latter is a variation on the example discussed in [Ek98] based on the Aharonov-Bohm effect [AB59].

1.3.1 The Deutsch's algorithm

Let us consider a register of n qubits with the computational states $|x\rangle \in \{|0\rangle, |1\rangle\}^{\otimes n}$. The realization of the dichotomic function as a unitary transformation requires, besides the register state $|x\rangle$, an ancillary qubit, denoted $|y\rangle \in \{|0\rangle, |1\rangle\}$, that encodes the output of the function. In other words, a unitary transformation U_f is associated to the function f, in such a way that its action on the computational states is:

$$U_f \; : \; |x\rangle|y\rangle \; \longrightarrow \; U_f|x\rangle|y\rangle = |x\rangle|y \oplus f(x)\rangle \; . \tag{1.16}$$

It is important to notice that, because of the linearity of quantum transformations, the definition in (1.16) allows to compute the action of U_f over a generic state which is a coherent superposition of the computational states:

$$U_f \sum_x c_x |x\rangle|y\rangle = \sum_x c_x U_f |x\rangle|y\rangle = \sum_x c_x |x\rangle|y \oplus f(x)\rangle \; . \tag{1.17}$$

Hence, an initial state without any correlation, such as $|\psi_{\text{in}}\rangle = \sum_x c_x|x\rangle|y\rangle$, is mapped by U_f into a state which presents correlations between the register qubits and the ancillary qubit, such as $|\psi_{\text{out}}\rangle = \sum_x c_x|x\rangle|y \oplus f(x)\rangle$. That is indeed an *entangled* state.

Coming back to the *Deutsch's algorithm*, we consider the case of a single-qubit register, with $|x\rangle \in \{|0\rangle, |1\rangle\}$. The system, composed of one register and one ancillary qubit, is initially prepared in the state

$$|\psi_0\rangle = |0\rangle|1\rangle \; . \tag{1.18}$$

The first step is to apply a Hadamard gate to both the qubits. That unitary transformation is defined in the single-qubit computational basis by the following matrix:

$$H = \frac{1}{\sqrt{2}} \begin{bmatrix} 1 & 1 \\ 1 & -1 \end{bmatrix} \; . \tag{1.19}$$

That yields the following intermediate state:

$$|\psi_1\rangle = H \otimes H|\psi_0\rangle = \left[\frac{|0\rangle + |1\rangle}{\sqrt{2}}\right] \otimes \left[\frac{|0\rangle - |1\rangle}{\sqrt{2}}\right] . \tag{1.20}$$

After that *local change of basis*, we can apply the function of interest, which is realized through the corresponding unitary transformation, to obtain

$$|\psi_2\rangle = U_f|\psi_1\rangle = \left\{\frac{|0\rangle \left[|f(0)\rangle - |\bar{f}(0)\rangle\right]}{2} + \frac{|1\rangle \left[|f(1)\rangle - |\bar{f}(1)\rangle\right]}{2}\right\}, \tag{1.21}$$

where $\bar{f}(x) = 1 \otimes f(x)$ indicates the logical negation. Notice that the function f is defined on the computational states $|0\rangle$ and $|1\rangle$, while in (1.21) it is evaluated on a coherent superposition of them. One can say that the function is evaluated both on $|0\rangle$ and $|1\rangle$ at the 'same time'; the presence of coherent superpositions in the quantum theory is at the heart of what is often called the *quantum parallelism*. At this point, one has to distinguish the two cases. If the function is constant ($f(0) = f(1) = f$), the expression in (1.21) simplifies to

$$|\psi_2\rangle = \left[\frac{|0\rangle + |1\rangle}{\sqrt{2}}\right] \otimes \left[\frac{|f\rangle - |\bar{f}\rangle}{\sqrt{2}}\right] . \tag{1.22}$$
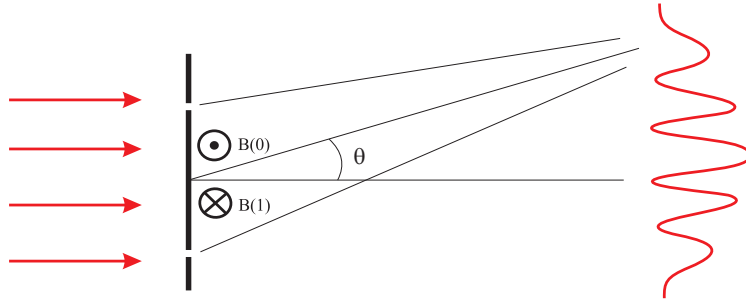
Figure 1.1: The double-slit experiment with a pair of ideal solenoids 'hidden' behind the slits. The magnetic flux carried by the solenoids can assume two possible values, determining a shift in the interference pattern.

Otherwise, if the function is balanced ($f(0) = \bar{f}(1)$), we obtain

$$|\psi_2\rangle = \left[\frac{|0\rangle - |1\rangle}{\sqrt{2}}\right] \otimes \left[\frac{|f(0)\rangle - |f(1)\rangle}{\sqrt{2}}\right]. \tag{1.23}$$

The last step is to apply again a Hadamard transformation on both qubits to obtain (apart of an irrelevant global phase factor):

$$|\psi_3\rangle = H \otimes H|\psi_2\rangle = \begin{cases} |0\rangle \otimes |1\rangle & \text{if } f \text{ is constant} \\ |1\rangle \otimes |1\rangle & \text{if } f \text{ is balanced} \end{cases} \tag{1.24}$$

In conclusion, the output state is $|\psi_3\rangle$, which — in principle with unit probability — has the first qubit in the state $|0\rangle$ if f is a *constant* function, while it is in the state $|1\rangle$ if the function is *balanced* (*non-constant* in the single-bit case). On the other hand, the second qubit ends in the state $|1\rangle$ in both the cases, hence being in principle used as a 'control' qubit to check the presence of possible errors.

We can say that the Deutsch's algorithm computes the function $F(f) = f(0) \oplus f(1)$. The function $F(f)$ describes a 'global' feature of f. Here we have described how the quantum algorithm can compute a *global* property of the function, such as $F(f)$, with *only one* evaluation of the function f, instead of the two evaluations needed in the classical case. That efficiency of the quantum algorithm becomes *exponentially* more relevant increasing the number of qubits in the register, moving from the Deutsch's algorithm to the Deutsch-Jotza's algorithm.

At that point of the discussion, it could be unclear, because hidden in calculations, what is the *physical interpretation* of that kind of algorithm. Often it is commented that *interference* is responsible for the computational speedup, since it is 'sensible' to global features of the function. It can be also argued that the perfect constructive — or destructive — interference which appears in correspondence with a constant or balanced function is responsible for the efficiency of the algorithm. In the following subsections we will try to further motivate that kind of argumentations with the help of two familiar *thought experiments*.

1.3.2 The double-slit experiment

Quoting Richard Feynman, we may say that the double-slit experiment contains all the strangeness, as well as the mystery, of the quantum theory. If that is true, we can argue that it can as well contain the features of quantum mechanics which lead to the *computational efficiency* of *quantum algorithms*.

As it is well known, a particle moving towards a double-slit produces an *interference pattern*. If a monochromatic beam, with wave length λ, impacts on the screen containing the two slits, which are separated by a distance d (we assume that the slits are infinitely narrow), the probability of finding a particle moving along the direction θ (see figure 1.1) is proportional to

$$\chi(\theta) = \frac{1}{2} \left| 1 + e^{ikd\sin\theta} \right|^2 = 1 + \cos(kd\sin\theta) , \qquad (1.25)$$

where $k = 2\pi/\lambda$ is the corresponding wave number. Hence, the principal maximum of probability (or intensity) is at $\theta_{\max} = 0$, while the first point of destructive interference is in correspondence with $kd\sin\theta_{\min} = \pi$.

If the beam is composed of *charged particles*, with an electric charge q, and if an infinite solenoid is situated behind the slits, the interference pattern is *shifted*. If the magnetic flux trapped in the ideal solenoid is Φ, an additional phase shift does appear in (1.25), and the probability of finding a particle at angle θ turns to be proportional to

$$\tilde{\chi}(\theta) = \frac{1}{2} \left| 1 + e^{i(kd\sin\theta+\delta)} \right|^2 = 1 + \cos(kd\sin\theta + \delta) , \qquad (1.26)$$

where the additional phase shift, due to the Aharonov-Bohm effect [AB59], is

$$\delta = \frac{q\Phi}{\hbar}. \qquad (1.27)$$

If the magnetic flux is an *even multiple* of one-half the elementary flux quantum, namely if $\delta = 2n\pi$, the interference pattern is left unchanged. On the other hand, if it is an *odd multiple*, namely if $\delta = (2n+1)\pi$, the pattern is shifted in such a way that the maxima and minima are *interchanged*.

Let us now consider the case in which two parallel lines of flux are situated behind the double-slit (see figure 1.1), with corresponding magnetic flux Φ_0 and Φ_1. Let us also suppose that the modulus of the flux is constrained to be one-forth of the elementary flux, namely

$$|\Phi_0| = |\Phi_1| = \frac{\pi}{2} \frac{\hbar}{|q|} . \qquad (1.28)$$

In that setting, the corresponding shift in the interference pattern is given by the sum of two contributions:

$$\tilde{\chi}(\theta) = 1 + \cos(kd\sin\theta + \delta_0 + \delta_1) , \qquad (1.29)$$

where $\delta_0, \delta_1 = \pm\pi/2$.

Now we can state the *analogy* with the Deutsch's algorithm. One can consider the function 'magnetic flux in the solenoid', that function can assume only two values, and can be estimated on the solenoid labeled as '0' and on the one labeled as '1'. The classical solution of the problem of determining whether the function is constant or not, requires two 'classical' measures of the magnetic flux in each solenoid, or of the corresponding current. On the other hand, we argue that, if the function is constant — i.e. the two fluxes are parallel — the interference maxima are *not shifted*; while if the function is balanced, the positions of the maxima and the minima are *interchanged* in the interference pattern. Assuming that one can consider the evaluation of the interference maxima — the principal maximum is sufficient — as a *single operation*, we obtain the analogy with the Deutsch's algorithm. As in the Deutsch's algorithm one has to perform a change of basis between the computational basis $\{|0\rangle, |1\rangle\}$, in which the function f is realized through the unitary U_f, and the basis $\{\frac{|0\rangle+|1\rangle}{\sqrt{2}}, \frac{|0\rangle-|1\rangle}{\sqrt{2}}\}$, in the double-slit experiment one has to change between the *momentum* basis, in which the incoming
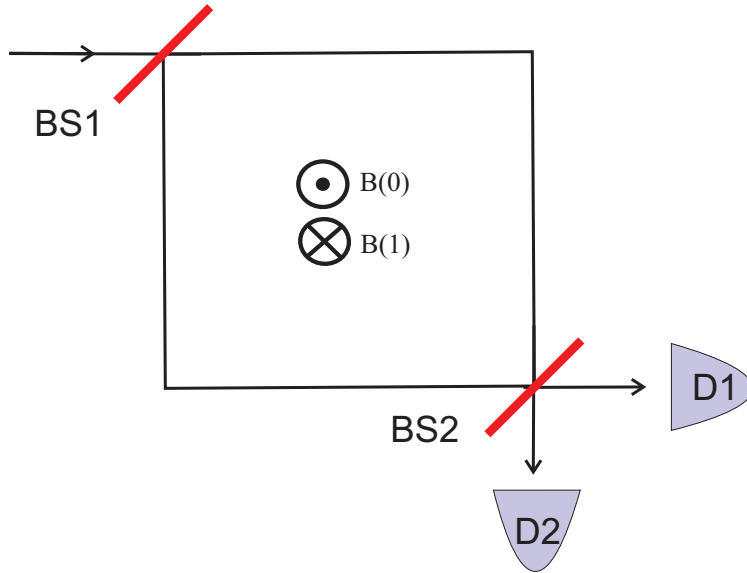
Figure 1.2: The scheme of a Mach-Zehnder interferometer with a pair of lines of magnetic flux trapped in it. The particle flux at the detector is changed depending on the total magnetic flux through the loop.

and the outgoing beams are prepared and measured, and the *position* basis. Where the basis of particle positions is determined by the location of the two slits. Also, it is the particle position that determines — depending on whether the particle pass *above* or *below* the flux lines — the additional phase shift due to the Aharonov-Bohm effect.

Of course, we may say that the analogy is not complete, since the observables that determine the bases have continuous spectrum, as well as the determination of the interference maximum needs a great number of 'spots' detected on the screen, which is something more than a single operation. In the next section, we consider a more direct example, which is a variation of that discussed in [Ek98].

1.3.3 A Mach-Zehnder interferometer

The analogy presented in the previous section is not complete and several differences with the Deutsch's algorithm are present. These differences are mainly related to the fact that it deals with *continuous* variables, instead of *discrete* ones. The interference pattern gives the probability of finding a spot on the screen, which cannot be as sharp as in the discrete-variable case. Hence, in this section we consider another physical example, in which the analogy is with a *Mach-Zehnder interferometer*. An analogous example was discussed in [Ek98]. Also in this example, we are dealing with a beam of charged particle and the Aharonov-Bohm effect will play an important role.

The scheme of the thought experiment is depicted in the figure 1.2. Working in the Heisenberg picture, the input is described by field operator $\hat{a}$ entering in the symmetric beam slipper BS1. The beam splitter acts over the incoming mode in the following way:

$$\text{BS1} \;\; : \;\; \hat{a} \;\; \longrightarrow \;\; \hat{c} = \frac{\hat{a} + i\hat{b}}{\sqrt{2}} \; . \tag{1.30}$$

If a pair of solenoids enters in the interferometric loop, the field operator acquires an additional

phase, which leads to the following operator

$$\hat{c}' = \frac{\hat{a}}{\sqrt{2}} + i\frac{\hat{b}}{\sqrt{2}}e^{i(\delta_0+\delta_1)} \ . \tag{1.31}$$

After the second symmetric beam splitter, BS2, the field operator becomes

$$\hat{d} = \left[\frac{1 - e^{i(\delta_0+\delta_1)}}{2}\right]\hat{a} + i\left[\frac{1 + e^{i(\delta_0+\delta_1)}}{2}\right]\hat{b} \ . \tag{1.32}$$

Finally, the probability of detecting a particle at the detector D1 is given by

$$\chi(\delta_0, \delta_1) = \frac{1}{2}\left[1 + \cos\left(\delta_0 + \delta_1\right)\right] \ . \tag{1.33}$$

As in the previous example, if the fluxes in the solenoids are such that $\delta_0, \delta_1 = \pm\pi/2$, one can easily recognize the analogy with the Deutsch's algorithm. If the function 'magnetic flux of the solenoid' is balanced, there will be a *click* at the detector D1, with probability equal to one. Otherwise, if the function is constant it is the detector D2 that will produce a *click* with unit probability.

1.4   Universal computation

While in the classical case the number of logic gates of one bit are in a *finite number*, in the quantum case the possible one-qubit gates are a *continuous set*. That set is the *unitary group* $U(2)$ for one qubit, or $U(N)$ for $n = \log_2 N$ qubits. Hence, a quantum logic gate can be engineered with in principle arbitrary high, but *finite* accuracy.

In other words, given a gate U, one has to find another unitary V, which is a good approximation for U. For instance, one can consider a *worst-case scenario*, and for a given $\epsilon > 0$, determine a suitable unitary V, such that

$$\sup_\psi |U - V|\psi\rangle| < \epsilon \ . \tag{1.34}$$

A set of gates is said to be *universal* if it has the remarkable property that any quantum gate can be approximated with arbitrary accuracy with a circuit involving only the elements in that set.

It has been shown (see [Di95, Ba95]) that a universal set of gates can be composed by one non-trivial two-qubit gate together with the one-qubit gates. The non-trivial two-qubit gate can be chosen to be the controlled-NOT gate, which is expressed by the following matrix in the two-qubit computational basis:

$$U_{\mathsf{CNOT}} = \begin{bmatrix} 1 & 0 & 0 & 0 \\ 0 & 1 & 0 & 0 \\ 0 & 0 & 0 & 1 \\ 0 & 0 & 1 & 0 \end{bmatrix} \ , \tag{1.35}$$

or the controlled-phase gate, which has the matrix expression

$$U_\chi = \begin{bmatrix} 1 & 0 & 0 & 0 \\ 0 & 1 & 0 & 0 \\ 0 & 0 & 1 & 0 \\ 0 & 0 & 0 & e^{i\chi} \end{bmatrix} \ . \tag{1.36}$$

21

On the other hand, a generic one-qubit transformation can be for instance obtained composing the Hadamard gate, which is defined in the computational basis by the matrix in (1.19), and the so-called $\pi/8$-gate, which has the matrix expression

$$T = \frac{1}{\sqrt{2}} \begin{bmatrix} e^{-i\pi/8} & 0 \\ 0 & e^{i\pi/8} \end{bmatrix} . \tag{1.37}$$

Hence the gates H and T define a *universal set* for the computation over a single qubit, while the gates H, T, and U_{CNOT} are universal for the computation over N-qubits.

1.5 Error correction and prevention

In the discussion of the Deutsch's algorithm, we have assumed a perfect control on the quantum system, from the *state preparation* and the *quantum evolution*, to the *measurement process*. Of course that might not be a reasonable assumption in a realistic description since the presence of *errors* and *noise* is unavoidable in the real world.

We can distinguish two kinds of perturbations with qualitatively different features: the first kind has a purely *quantum* nature, and it is induced by the interaction of the quantum system implementing the logic gate with the environment; the second kind has instead a *classical* nature, and it is caused by the presence of instrumental noise in the 'external parameters' used to *control* the system. The undesired interaction with the environment is the source of the phenomenon known as quantum *decoherence* [BP02]. The effects of this interaction can be modeled by means of suitable 'master equations' (i.e. evolution equations) for the density matrix of the quantum system implementing the logic gate; at least in the Markovian regime, they are negligibly small if the *operational time* of the logic gate is short enough. On the other hand, the classical perturbations stem from an unavoidable noisy component intrinsic in the external driving fields (e.g. laser beams [Wi98]) that can be usually regarded as classical fields; hence, it is essentially due to instrumental instability. In other words, it is caused by the interaction of the classical fields with an environment of classical degrees of freedom.

In order to preserve the efficacy of the quantum algorithm even in the presence of noise, one needs to build a *fault-tolerant* computation (see [Pr98]). Without entering in the details, we only mention that one can individuate two possible strategies in order to protect the quantum algorithm from the action of the noise. The first kind of strategy is based on *error correcting codes* (see [Sh95, Ca95, St96, Go96]) and can be viewed as an *a posteriori* approach. The second kind of *strategy* is to prevent the effects of the noise on the efficacy of the gate taking advantages of the *symmetries* of both the system under consideration and the noise affecting it. Among that kind of *a priori* approaches, we can individuate dynamical schemes, based on the use of *decoherence free subspaces* [ZR97, Li98], or of the *quantum Zeno* and similar effects [Fa05], and geometric scheme, including *topogical* [Ki03, Og99] and *holonomic* computation [ZR99, Pa99].

Chapter 2

The holonomic way

A *quantum algorithm* is nothing more than the *physical evolution* of a quantum system, which can be either free or experimentally driven. In full generality, an algorithm transforms an input state $|\psi(0)\rangle$ into an output state $|\psi(T)\rangle = U|\psi(0)\rangle$ after a certain operational time T. If the system evolves according to the time-dependent Hamiltonian $H(t)$, the output state is given by the solution of the corresponding Schrödinger equation, which is formally expressed by the evolutor

$$U = \mathbf{T} e^{-i \int_0^T H(t)dt} , \qquad (2.1)$$

(here and in the following we put $\hbar = 1$) where $\mathbf{T}$ stands for the time ordered product. In particular situations, the unitary transformation U can be factorized as the product of two unitaries

$$U = V(T) \times \Gamma, \qquad (2.2)$$

where $V(T)$ is often referred to as the *dynamical phase* and Γ as the *geometric phase*. These can be Abelian ($V(T), U \in \mathrm{U}(1)$), or non-Abelian ($V(T), U \in \mathrm{U}(N)$) phases. The appellative *geometric* is justified by the fact that the factor Γ does not depend on any dynamical quantity, such as the instantaneous energy, the operational time T, or the rate of changes of the Hamiltonian. On the other hand, the geometric phase is completely determined by the underlining geometry of the space of quantum states, and is interpreted as a *holonomy* phenomenon.

In this introductory chapter, we will briefly discuss how geometric phases do appear in physics and outline the role that they can play in the framework of *quantum information processing*. There are several ways to present that topic. Historically, geometric phases were discussed in [Be84, Si83] as emerging in the *quantum adiabatic limit*. Soon after, it was recognized that geometric phases can appear in more general conditions, in particular without requiring the adiabatic limit. The adiabatic limit being not needed, it was substituted by the hypothesis of a *cyclic* evolution of the quantum state [AA87]. It was recognized that an earlier investigation in [Pa56], about relative phase of polarized beams of classical light, could be interpreted in the context of geometric phases, also leading to the definition of the geometric phase for *non-cyclic* evolution [SB88]. Here, we will follow a different rute, trying to put the emphasis on how geometric phases arise from *physical* and *mathematical* considerations, starting from the phenomenon of quantum and classical interference, to the analysis of the dynamical equations of a non-relativistic quantum system. The exposition of the topic is oriented to the main subject of the present Dissertation, which is the *robustness* of *holonomic gates* under *parametric noise*. Hence the introduction to quantum holonomies and holonomic computation is far to be complete, we only hope that it might be clear and, as much as possible, self contained.

2.1 Introduction

One of the most important challenges through the realization of quantum information tasks is the implementation of quantum logic gates that are *robust* against unwanted perturbations [NC00, Be04]. As we have also recalled in the previous chapter, two kinds of perturbation with qualitatively different features can be distinguished. We distinguish a *quantum* noise, emerging from the interaction of the system with an environment of quantum degrees of freedom, and a *classical*, or *parametric* noise, which arises from the interaction of the quantum system with an environment of classical degrees of freedom. Being of classical nature, the effects of these perturbations can be evaluated by studying standard (non-autonomous) Schrödinger equations where the parametric noise is taken into account by suitably modeling the noisy components of the classical parameters (e.g. the field amplitude) associated with the external fields.

Among the several strategies for realizing quantum logic gates discussed in the literature, a prominent position is held by *holonomic gates*. The so-called *holonomic computation* was first proposed by Paolo Zanardi and Mario Rasetti in [ZR99] (see also [Pa99]), and relies on the theory of holonomy in *principal fibre bundles* [Na05], a subject which is familiar to theoretical physicists due to the central role played in *gauge theories* [Ma92] and in the well-known phenomenon of Abelian [Be84, Si83] and non-Abelian [WZ84] adiabatic phases. Actually, a holonomic gate can be regarded as a straightforward application of the theory of non-Abelian adiabatic phases to quantum computation.

As we will discuss below, the holonomic approach to quantum computing requires to work in the *adiabatic regime*. Hence, one can argue that longer operational time are needed, leading to a less efficient computation. On the other hand, the major advantage of the *holonomic approach* with respect to *standard dynamical schemes* is that, because of its geometric nature, it is expected to be particulary *robust* in the presence of a certain kind of *parametric noise*. Thus, a longer computational time can be balanced by a stronger robustness.

2.2 A taste of the geometry of quantum mechanics

As it is well known, in quantum mechanics a physical system is described by means of a properly chosen Hilbert space, that we generically indicate as $\mathcal{H}$. A *pure state* of the quantum system can be associated to a non-vanishing vector $|\psi\rangle \in \mathcal{H}_0$, where $\mathcal{H}_0 = \mathcal{H} - \{0\}$. On the other hand, the mathematical information contained in the vector $|\psi\rangle$ is physically redundant, since the probabilistic interpretation requires the normalization of the vector, $\langle\psi|\psi\rangle = 1$, and because two vectors which differ by a numerical phase factor, $|\psi'\rangle = e^{i\alpha}|\psi\rangle$, are physically indistinguishable. In the presentation of quantum algorithm, or in general quantum information processing, one often makes use of the vectors to represent the *pure* states of the system. This representation is justified by the sake of simplicity, but it is obviously not the completely correct way of dealing with quantum states. The faithful way is to consider the equivalence classes of vectors with respect to the relation $\sim$, defined as follows: $|\phi\rangle \sim |\psi\rangle$ if and only if $|\phi\rangle = z|\psi\rangle$ for some non-vanishing complex number $z = |z|e^{i\alpha}$. Thus, when one says that a system is in the state $|\psi\rangle$, the vector has to be consider just as a *representative element* of its equivalence class. The quotient space $\mathcal{H}/\sim$ is the *complex projective space* associated with $\mathcal{H}$, which we will indicate as $\mathcal{H}P$. For a system with n stationary levels, one has $\mathcal{H} \cong \mathbb{C}^n$, and the associated projective space will be denoted as $\mathbb{C}P^{n-1}$. While $\mathbb{C}^n$ is a n-dimensional complex vector space, the projective space is a $(n-1)$-dimensional complex differential manifold, which is also a $2(n-1)$-dimensional real manifold, in particular it is endowed which a

rich structure which yields $\mathbb{C}P^{n-1}$ to be a Kähler manifold (see for instance [CJ04] for a complete discussion). The complex projective space is also called the *space of the rays* associated to $\mathcal{H}$. From the definition, it follows that a ray is nothing more than a one-dimensional subspace of $\mathcal{H}$, hence a way to represent the element of the rays' space is by means of the map

$$|\psi\rangle \;\longrightarrow\; \Pi(|\psi\rangle) = \rho_\psi = \frac{|\psi\rangle\langle\psi|}{\langle\psi|\psi\rangle}\,, \tag{2.3}$$

which associates to each vector the projector on the corresponding one-dimensional subspace, that projector is commonly called the *density operator* or *density matrix*. Obviously, $\Pi(|\psi\rangle) = \Pi(|\phi\rangle)$ if and only if $|\psi\rangle \sim |\phi\rangle$. Even though a pair of equivalent vectors describe the same physical configuration, it is well known that the relative phase plays a fundamental role in the interference phenomena. If the state of the system is splitted into two branches, in such a way that each branch acquires a different, but coherent, phase shift, once the branches are recombined one has $|\psi'\rangle \simeq |\psi\rangle + e^{i\alpha}|\psi\rangle$, and the relative phase α modulates the interference pattern.

The discussion of above concerns the kinematics of *finite-dimensional* quantum mechanics. From a *dynamical point of view*, in the Hilbert space one has to consider the Schrödinger equation

$$i\frac{d}{dt}|\psi(t)\rangle = H(t)|\psi(t)\rangle \tag{2.4}$$

with an initial condition $|\psi_0\rangle$. If the Hamiltonian operator is hermitian, the modulus of the wave function is preserved at each subsequent time $\langle\psi(t)|\psi(t)\rangle = \langle\psi_0|\psi_0\rangle$. Under the action of the map (2.3), the Schrödinger equation projects into the von Neumann equation

$$i\frac{d}{dt}\rho(t) = [H(t), \rho(t)] \tag{2.5}$$

with initial condition $\rho_0 = |\psi_0\rangle\langle\psi_0|$. In that case, the trace of the density operator is preserved $\mathrm{tr}\,(\rho(t)) = \mathrm{tr}\,(\rho(0))$.

Example 1 (A two-level quantum system) *For a two-level system, $\mathcal{H} \cong \mathbb{C}^2$. One can chose a logical basis $\{|0\rangle, |1\rangle\}$ to represent the vectors, namely $|\psi\rangle = a|0\rangle + b|1\rangle$. If $\langle\psi|\psi\rangle = R^2$, we have $|a|^2 + |b|^2 = R^2$, and a representative element for the corresponding equivalence class can be chosen and parameterized as follows*

$$|\psi\rangle = Re^{i\alpha}\left(\cos\frac{\theta}{2}|0\rangle + \sin\frac{\theta}{2}e^{i\phi}|1\rangle\right)\,. \tag{2.6}$$

Notice that the range of parameters can be chosen to be $\phi \in [0, 2\pi[$ and $\theta \in [0, \pi]$. The corresponding rank-one projector is written as

$$\rho_\psi = \frac{|\psi\rangle\langle\psi|}{\langle\psi|\psi\rangle} = \rho_{\psi_{ij}}|i\rangle\langle j| \tag{2.7}$$

where the indexes i and j assume values $\{0, 1\}$, and the matrix representation of the projector is

$$\rho_{\psi_{ij}} \equiv \frac{1}{2}\begin{bmatrix} 1+z & x+iy \\ x-iy & 1-z \end{bmatrix} \tag{2.8}$$

25

where

$$\begin{cases} x &= \sin\theta\cos\phi \\ y &= \sin\theta\sin\phi \\ z &= \cos\theta \end{cases} , \tag{2.9}$$

that explicitly shows that the rays' space $\mathbb{C}P^1$ is a two dimensional sphere, known in this context as the Bloch sphere.

2.2.1 Quantum mechanics on the fibre bundle

The discussion of above suggests how the physical interpretation infers a particular *geometric structure* on the carrier Hilbert space. From a geometrical point of view, we are dealing with a *principal fibre bundle* $\mathcal{H} \xrightarrow{\Pi} \mathcal{H}P$, with the group $\mathbb{R}^+$ which plays the role of the *structure group* as well as of the *typical fibre* (see for instance [Na05], or [CJ04] for a complete discussion). Analogously, indicating with $\mathcal{B} = \{|\psi\rangle \in \mathcal{H} \mid \langle\psi|\psi\rangle = 1\}$ the sphere of unit radius in the Hilbert space, it can be useful, for physical reasons and for the simplicity of the exposition, to divide the projection Π in two steps. We can write $\Pi = \pi \circ \Pi'$, where $\Pi'(|\psi\rangle) = \frac{|\psi\rangle}{\langle\psi|\psi\rangle}$ is a map from $\mathcal{H}$ to $\mathcal{B}$, and $\pi(|\psi\rangle) = |\psi\rangle\langle\psi|$ is a map from $\mathcal{B}$ to $\mathcal{H}P$. Hence we have decomposed

$$\mathcal{H} \xrightarrow{\Pi} \mathcal{H}P = \mathcal{H} \xrightarrow{\Pi'} \mathcal{B} \xrightarrow{\pi} \mathcal{H}P . \tag{2.10}$$

In correspondence with that, the bundle $\mathcal{B} \xrightarrow{\pi} \mathcal{H}P$ is also a principal fibre bundle, with structure group $\mathrm{U}(1)$, which expresses to the *phase ambiguity*. In other words, a pair of normalized vectors, such that $|\psi_2\rangle = e^{i\alpha}|\psi_1\rangle$, belong to the same fibre. The structure group $\mathrm{U}(1)$ acts on the fibre as $|\psi_1\rangle \to e^{i\theta}|\psi_1\rangle$. The relative phase between $|\psi_2\rangle$ and $|\psi_1\rangle$ corresponds to the unique element $u \in \mathrm{U}(1)$ which transforms $|\psi_1\rangle$ in $|\psi_2\rangle$, that is to say, $u|\psi_1\rangle = |\psi_2\rangle$.

2.3 The Pancharatnam connection

Shivaramakrishnan Pancharatnam, in 1956, considered the problem of defining a relative phase between two beams of polarized light with non-parallel polarization. Notice that for a pair of beams with the same polarization, the relative phase is immediately defined, the question arises when one considers pairs of non-parallel polarizations. If the two vectors are non-orthogonal a relative phase can be defined used a prescription introduced by him in [Pa56]. This prescription was physically inspired and motivated by the phenomenon of interference. Let us consider two polarized beams of light, expressed by the complex vectors ψ_1 and ψ_2, which are superimposed coherently giving rise to the vector $\psi = \psi_1 + \psi_2$. The overall square intensity is $I^2 = |\psi_1|^2 + |\psi_2|^2 + 2\Re\{(\psi_1, \psi_2)\}$, and the interference fringes are modulated by $\Delta = \arg(\psi_1, \psi_2)$. Hence, the interference is completely *constructive* when the scalar product (ψ_1, ψ_2) is real, i.e. $\Delta = 0$, and completely *destructive* if the scalar product is purely imaginary. The idea of Pancharatnam was to define the relative phase for non-orthogonal polarizations as

$$\Delta = \arg(\psi_1, \psi_2) . \tag{2.11}$$

On the contrary, in the case the two vectors are mutually orthogonal, the interference pattern disappears and the relative phase cannot be defined. A way to compare two phases, or in other words, to

compare two points belonging to different fibres in the corresponding fibre bundle is called a *connection*.

Example 2 (A two-level quantum system) *For our limited purposes, and from a purely mathematical point of view, a beam of light is completely equivalent to a two-level quantum system. While the states of polarization are defined by points on the Poincaré sphere (or the Poincaré ball if the polarization is non-complete), the pure states of a two-level quantum system are defined by the points on the Bloch sphere (or the Bloch ball if the states are mixed). Let us consider a beam of spin-$1/2$ particles which is splitted in two branches, polarizers and delay plates are disposed along the paths in order to handle the polarization of each beam and their relative phase. As an example, let us consider three different states of polarization:*

$$|\psi_1\rangle = e^{i\chi_1}|0\rangle \tag{2.12}$$

$$|\psi_2\rangle = e^{i\chi_2}\frac{|0\rangle + |1\rangle}{\sqrt{2}} \tag{2.13}$$

$$|\psi_3\rangle = e^{i\chi_3}\frac{|0\rangle + i|1\rangle}{\sqrt{2}} \,. \tag{2.14}$$

Using the definition (2.11), two states with different polarization can always be chosen to be in phase by adjusting the global phase of one with respect to the other. With a phase shifter one can adjust the differences $\chi_i - \chi_j$. For the pair $|\psi_1\rangle$, $|\psi_2\rangle$ the relative phase is

$$\beta_{12} = \arg \langle \psi_1 | \psi_2 \rangle = \chi_2 - \chi_1 \,. \tag{2.15}$$

For the second pair $|\psi_2\rangle$, $|\psi_3\rangle$, one obtains

$$\beta_{23} = \arg \langle \psi_2 | \psi_3 \rangle = \chi_3 - \chi_2 + \pi/4 \,. \tag{2.16}$$

Finally, for the third pair $|\psi_3\rangle$, $|\psi_1\rangle$:

$$\beta_{31} = \arg \langle \psi_3 | \psi_1 \rangle = \chi_1 - \chi_3 \,. \tag{2.17}$$

It follows that the relative phases are constrained to satisfy $\beta_{12} + \beta_{23} + \beta_{31} = \pi/4$. Hence, it is not possible to make them vanish jointly. In other words, if one adjusts the global phases in order to set the scalar products $\langle \psi_1 | \psi_2 \rangle$ and $\langle \psi_2 | \psi_3 \rangle$ to be real-valued, the scalar product $\langle \psi_3 | \psi_1 \rangle$ cannot be real-valued at the same time. The corresponding relative phase is constrained to take the value: $\beta_{31} = \arg \langle \psi_3 | \psi_1 \rangle = \pi/4$.

Let us now consider the Pancharatnam rule from an *infinitesimal* point of view. In order to compare the phases of $|\psi\rangle$ and $|\psi + d\psi\rangle = |\psi\rangle + |d\psi\rangle$ one has to consider the scalar product

$$\langle \psi | \psi + d\psi \rangle = \langle \psi | \psi \rangle + \langle \psi | d\psi \rangle \,. \tag{2.18}$$

The relative phase is given by the argument

$$\beta = \arg \langle \psi | \psi + d\psi \rangle \simeq \frac{\Im \langle \psi | d\psi \rangle}{\langle \psi | \psi \rangle} \,, \tag{2.19}$$

that yields to identify a *one-form* which computes the relative phase of neighbor vectors. The linear form

$$A \equiv \frac{\Im \langle \psi | d\psi \rangle}{\langle \psi | \psi \rangle} \tag{2.20}$$

is called a *connection* one-form (in this framework, it is the Pancharatnam connection). A curve γ on the total space (now the Hilbert space $\mathcal{H}$) is said to be *horizontal* if the connection one-form identically vanishes on it, namely $A|_\gamma = 0$. As a consequence, the vectors along a horizontal curve are *locally in phase* one with the other. A connection one-form can be in general defined on a *principal fibre bundle*. It takes values in the *algebra of the structure group*. Starting from vectors in $\mathcal{H}$, the connection takes value in the complex line, while, in the case one restricts to normalized vectors, i.e $|\psi\rangle \in \mathcal{B}$ (the sphere of unit radius), it is real-valued and reads as follows:

$$A = \Im \langle \psi | d\psi \rangle = -i \langle \psi | d\psi \rangle \ . \tag{2.21}$$

The last equality holds true since

$$1 = \langle \psi + d\psi | \psi + d\psi \rangle = 1 + \langle \psi | d\psi \rangle + \langle d\psi | \psi \rangle \ , \tag{2.22}$$

and $\langle \psi | d\psi \rangle$ is purely imaginary.

Let us consider three vectors: $|\psi_0\rangle$, $|\psi_1\rangle = |\psi_0\rangle + |d\psi_{10}\rangle$, and $|\psi_2\rangle = |\psi_0\rangle + |d\psi_{20}\rangle$. Also we have $|\psi_2\rangle = |\psi_1\rangle + |\psi_{21}\rangle = |\psi_1\rangle + |d\psi_{20}\rangle - |d\psi_{10}\rangle$. The relative phases are:

$$\beta_{10} = \langle \psi_0 | d\psi_{10} \rangle \tag{2.23}$$

$$\beta_{20} = \langle \psi_0 | d\psi_{20} \rangle \ , \tag{2.24}$$

while

$$\beta_{21} = \langle \psi_1 | d\psi_{20} - d\psi_{10} \rangle = \beta_{20} - \beta_{10} + \langle d\psi_{10} | d\psi_{21} \rangle \ . \tag{2.25}$$

The extra term is given by the *differential* of the connection one-form, which is the associated *curvature*, or *field strength*:

$$F = dA = -i \langle d\psi | d\psi \rangle \ . \tag{2.26}$$

Example 3 (A two-level quantum system) *For a two level system, one can parametrize normalized vectors in the following way*

$$|\psi\rangle = e^{i\chi} \left(\cos(\theta/2) |0\rangle + \sin(\theta/2) e^{i\phi} |1\rangle \right) \ , \tag{2.27}$$

and compute a small variation

$$|d\psi\rangle = id\chi |\psi\rangle + e^{i\chi} \left[-\sin(\theta/2) \frac{d\theta}{2} |0\rangle + \left(\cos(\theta/2) \frac{d\theta}{2} + id\phi \sin(\theta/2) \right) e^{i\phi} |1\rangle \right] \ . \tag{2.28}$$

Hence, one obtains:

$$A = -i \langle \psi | d\psi \rangle = d\chi + \frac{1}{2} (1 - \cos\theta) \, d\phi \ . \tag{2.29}$$

Let us consider three vectors: $|\psi_0\rangle$, $|\psi_1\rangle = |\psi_0\rangle + |d\psi_{10}\rangle$, and $|\psi_2\rangle = |\psi_0\rangle + |d\psi_{20}\rangle$. Also we have $|\psi_2\rangle = |\psi_1\rangle + |\psi_{21}\rangle = |\psi_1\rangle + |d\psi_{20}\rangle - |d\psi_{10}\rangle$. The relative phases are:

$$\beta_{10} \quad = \quad d\chi_{10} + \frac{1}{2}\left(1 - \cos\theta_0\right)d\phi_{10} \tag{2.30}$$

$$\beta_{20} \quad = \quad d\chi_{20} + \frac{1}{2}\left(1 - \cos\theta_0\right)d\phi_{20}\,, \tag{2.31}$$

while

$$\beta_{21} = \beta_{20} - \beta_{10} - \frac{1}{2}\sin\theta_1 d\theta_{10}d\phi_{21}\,. \tag{2.32}$$

And the extra term corresponds to the curvature associated to the connection,

$$F = \frac{1}{2}\sin\theta d\theta d\phi = dA\,. \tag{2.33}$$

2.3.1 Observations

To conclude this section, following [SB88], we will show how the relative phase between two non-orthogonal vectors can be calculated as the integral of the connection one-form along a *proper* curve. That result will be used in the following chapters, where we discuss the efficacy of holonomic computation under non-perfect experimental control.

Let us consider a curve $|\psi(s)\rangle \in \mathcal{B}$ (the total space in that case), for $s \in [0, 1]$. The curve projects on the base space $\mathcal{H}P$ in the *shadow* curve $|\psi(s)\rangle\langle\psi(s)|$. By definition, the projected curve is *gauge invariant*, i.e. it is invariant under local phase transformations

$$|\psi'\rangle = e^{i\alpha(s)}|\psi(s)\rangle\,. \tag{2.34}$$

On the other hand, the derivative $|u\rangle = |\dot{\psi}\rangle$ of the (normalized) state vector with respect of the curve parameter is not gauge invariant:

$$|u\rangle \quad \longrightarrow \quad e^{i\alpha(s)}\left(|u\rangle + \dot{\alpha}(s)|\psi(s)\rangle\right)\,, \tag{2.35}$$

where $\dot{\alpha}(s) = \frac{d\alpha(s)}{ds}$. That yields the rule for the connection one-form, that transforms *covariantly* as follows:

$$A \quad \longrightarrow \quad A' = A + \dot{\alpha}(s)ds\,. \tag{2.36}$$

One can consider the *covariant derivative* $|u'\rangle$:

$$|u'\rangle \equiv D(|\psi\rangle) = |u\rangle - \langle\psi|u\rangle|\psi\rangle\,, \tag{2.37}$$

that changes covariantly by construction and represents the horizontal component of the derivative along the curve. The covariant derivative can be exploited to define a gauge invariant *metric* as follows:

$$dl = \sqrt{\langle u'|u'\rangle}ds\,. \tag{2.38}$$

The *geodesic* curves, with respect to that metric, satisfy the following geodesic equation:

$$D^2|\psi\rangle = \left(\frac{d}{ds} - iA\right)|u'\rangle = 0\,. \tag{2.39}$$

Notice that the geodesic curve is defined in the total space, nevertheless, since the metric is gauge invariant by construction, all the curves which have the same *shadow* on the base space are equally

29

solutions of the equation (2.39). Hence we can say that the property of a curve to be a geodesic is determined by its shadow.

Let us consider a pair of vectors $|\psi_1\rangle$ and $|\psi_2\rangle$, and a *geodesic* curve $|\gamma(s)\rangle$ connecting them (with $|\gamma(0)\rangle = |\phi_1\rangle$ and $|\gamma(1)\rangle = |\phi_2\rangle$). An important result, contained in [SB88], is that the relative phase $\beta = \arg\langle\phi_1|\phi_2\rangle$ is given by

$$\beta = \int_\gamma A = \int_\gamma \langle\phi(s)|d\phi(s)\rangle \ . \tag{2.40}$$

To prove that statement, the authors of [SB88] considered a *horizontal geodesic* $\tilde{\gamma}$, namely $|\gamma(s)\rangle = e^{i\alpha(s)}|\tilde{\gamma}(s)\rangle$, with $e^{i\alpha(0)} = 1$. As a consequence, since the connection one-form vanishes along a horizontal curve, it fulfills the equation

$$\frac{d^2}{ds^2}|\tilde{\gamma}(s)\rangle = 0 \ . \tag{2.41}$$

One can consider the relative phase between the initial vector $|\psi_1\rangle$ and the one along the horizontal curve $|\tilde{\gamma}(s)\rangle$: that defines a function

$$g(s) = \Im\langle\psi_1|\tilde{\gamma}(s)\rangle \ . \tag{2.42}$$

The derivative $\dot{g}(0) = \Im\langle\psi_1|\frac{d}{ds}\tilde{\gamma}(s)\rangle$ vanishes since the curve is horizontal. On the other hand, the second derivative identically vanishes for $s \in [0,1]$

$$\ddot{g}(s) = \Im\langle\psi_1|\frac{d^2}{ds^2}|\tilde{\gamma}(s)\rangle = 0 \ , \tag{2.43}$$

because of equation (2.41). Hence the function is constant and, in particular, $g(0) = g(1)$. In other words, the initial vector $|\psi_1\rangle$ is in phase with $|\tilde{\gamma}(1)\rangle$, and one obtains

$$\beta = \arg\langle\psi_1|\psi_2\rangle = \arg\langle\tilde{\gamma}(1)|\psi_2\rangle \ . \tag{2.44}$$

Along the geodesic curve γ, one has that

$$A|_\gamma = A|_{\tilde{\gamma}} + \dot{\alpha}ds \ , \tag{2.45}$$

and finally

$$\int_\gamma A = \alpha(1) \ , \tag{2.46}$$

which proves (2.40).

A corollary of that result is that, given three state vectors $|\psi_1\rangle$, $|\psi_2\rangle$ and $|\psi_3\rangle$, with $\arg\langle\psi_1|\psi_2\rangle = \arg\langle\psi_2|\psi_3\rangle = 0$, the relative phase between ψ_3 and ψ_1 is given by the integral of the Pancharatnam connection along a curve which is piecewise made of three geodesic curves connecting them, hence giving the flux of the curvature through the geodesic triangle.

2.4 Appearance of geometric phases in quantum dynamics

In this section we will show how the Pancharatnam connection, in its quantum interpretation, can *naturally* appear in the study of the dynamics of a non-relativistic quantum system, leading to the emerging of a *geometric phase*.

Initially, we will recall how the connection one-form arises in correspondence of *cyclic* evolutions of a quantum system [AA87]. In that case, the evolutor U is factorized as a product of two terms, namely $U = V(T) \times \Gamma$, where $V(T)$ is called the dynamical phase, and Γ is a unitary transformation which is determined only by the geometry of the quantum system and it is commonly called the *geometric phase*. The same phenomenon arises in the limit of *adiabatic* evolution of the system [Be84, Si83]. That is the regime which is of interest for the applications in view of quantum information tasks [ZR99]. Finally, it is recalled that both the adiabatic and non-adiabatic settings can be discussed in the case of *Abelian* $\mathrm{U}(1)$ and *non-Abelian* $\mathrm{U}(N)$ phase factors [WZ84, An88].

2.4.1 Geometric phase after cyclic evolution

Let us consider a time-dependent Hamiltonian $H(t)$ and a solution of the corresponding Schrödinger equation, indicated as $|\psi(t)\rangle$, in the time window $t \in [0, T]$. The solution of the Schrödinger equation

$$i\frac{d}{dt}|\psi(t)\rangle = H(t)|\psi(t)\rangle \tag{2.47}$$

defines a curve

$$C \; : \; t \in [0, T] \; \longrightarrow \; |\psi(t)\rangle \in \mathcal{H} \; . \tag{2.48}$$

That curve is projected on the space of rays by the map

$$\Pi \; : \; |\psi(t)\rangle \; \longrightarrow \; |\psi(t)\rangle\langle\psi(t)| \tag{2.49}$$

onto the curve $C' = \Pi(C)$. The projected curve is the solution of the corresponding von Neumann equation, with the initial condition $|\psi(0)\rangle\langle\psi(0)|$. Taking a representative $|\phi(t)\rangle$ along the curve, it is related to the solution via a *local gauge* transformation

$$|\psi(t)\rangle = e^{i\chi(t)}|\phi(t)\rangle \; . \tag{2.50}$$

One can rewrite (2.47) as follows:

$$i\frac{d}{dt}\left[e^{i\chi(t)}|\phi(t)\rangle\right] = e^{i\chi(t)}H(t)|\phi(t)\rangle, \tag{2.51}$$

and

$$-\dot{\chi}(t)e^{i\chi(t)}|\phi(t)\rangle + ie^{i\chi(t)}|\dot{\phi}(t)\rangle = e^{i\chi(t)}H(t)|\phi(t)\rangle \; . \tag{2.52}$$

Multiplying by $\langle\psi(t)|$ from the left, we obtain

$$\dot{\chi}(t) = i\langle\phi(t)|\dot{\phi}(t)\rangle - \langle\phi(t)|H(t)|\phi(t)\rangle \; , \tag{2.53}$$

which yields

$$\chi(T) - \chi(0) = \int_0^T i\langle\phi(t)|\dot{\phi}(t)\rangle dt - \int_0^T \langle\phi(t)|H(t)|\phi(t)\rangle dt \; . \tag{2.54}$$

The first term on the right hand side is invariant under time parametrization $t \to t'(t)$, thus it is a function only of the support of the curve $|\phi(t)\rangle$. It can be written as $\int i\langle\phi|d\phi\rangle$, where the same expression defining the Pancharatnam connection can be recognized. The second term in (2.54) is invariant under gauge transformations $|\phi(t)\rangle \to e^{i\alpha}|\phi(t)\rangle$, but it is not invariant under time reparametrization $t \to t'(t)$. That term is the instantaneous expectation value of the energy $E(t)$ computed *along* the solution. Finally, the equation (2.54) reads

$$\chi(T) - \chi(0) = -\int_{\phi(t)} A - \int_{\phi(t)} E(t)dt \; . \tag{2.55}$$

A special case arises when the evolution of the system in the rays space is *cyclic*, i.e. $|\psi(T)\rangle = e^{i\alpha}|\psi(0)\rangle$. Selecting a representative *closed* curve $|\phi(t)\rangle$, with $|\psi(t)\rangle = e^{i\chi(t)}|\phi(t)\rangle$ and $|\phi(T)\rangle = |\phi(0)\rangle = |\psi(0)\rangle$, we obtain

$$\alpha = -\oint_{\phi(t)} A - \oint_{\phi(t)} E(t)dt . \tag{2.56}$$

Notice that, for a closed curve, the quantity $\oint A$ is gauge invariant. The corresponding phase factor $e^{-i\oint A}$ is called the *holonomy*. The holonomy is determined only by the specific expression of the connection one-form, and by the shadow of the closed curve $|\phi(t)\rangle$. Being gauge invariant, the holonomy is a property of the projected loop on the rays' space — the *shadow* of the path — and not of the path itself. Hence, taking a coherent superposition of the initial and the final state

$$|\psi(0)\rangle + |\psi(T)\rangle = (1 + e^{i\alpha})|\psi(0)\rangle , \tag{2.57}$$

one could in principle observe an interference pattern which is made of two contributions: the dynamical phase which is determined by the instantaneous energy as $\int E(t)dt$, and an additional phase shift which is the holonomy $e^{-i\oint A}$. Since the additional factor $e^{-i\oint A}$ depends only on the support of the curve in the rays' space and on the details of the connection one-form, it is called the *geometric phase*.

2.4.2 Adiabatic evolution

In the previous section, we have recalled how a geometric phase arises in correspondence with a cyclic evolution in the space of rays, this being related to the non-trivial geometry of the complex projective space. On the other hand, a cyclic evolution appears in correspondence with a peculiar expression of the system Hamiltonian, of its time dependence and for a certain value of the operational time T. Since the cyclicity of the dynamics appears as a special feature of the solution of the Schrödinger equation, it can only be determined *a posteriori* and, in general, the time dependence of the Hamiltonian does not give any transparent information about it as, for instance, it might not be cyclic, $H(T) \neq H(0)$.

The idea of a cyclic evolution in the rays' space is indeed a rather abstract concept, in the sense that one is not directly dealing with the rays' space when designing, planning or performing any experiment. It would be preferable to have a way to control the system and determine *a priori* if the evolution of the system will be cyclic. That can be done easily if one works in the *adiabatic regime*. With this term, here and in the following, we indicate a physical setting in which the adiabatic approximation of quantum mechanics is reliable.

Since the quantity that can in principle be experimentally controlled is not the state of the system but at most its Hamiltonian, it would be interesting, in view of the applications, to design a strategy that allows to *infer* a cyclic evolution of the state through the instantaneous control of the system Hamiltonian, for instance a cyclic evolution should appear in correspondence with a cyclic Hamiltonian.

Let us consider a time-dependent Hamiltonian with the following instantaneous spectral decomposition

$$H(t) = \sum_n \epsilon_n(t)P_n(t) , \tag{2.58}$$

for $t \in [0, T]$, where $\epsilon_n(t)$ are distinct *instantaneous* eigenvalues and $P_n(t)$ the corresponding eigenprojectors. Here, we are going to consider the case in which all the eigenvalues are not-degenerate at

each $t \in [0, T]$. In that case, each eigenprojector has unit rank, $P_n(t) = |n(t)\rangle\langle n(t)|$, where we have chosen instantaneous representative vectors $|n(t)\rangle$ (with $|n(T)\rangle = |n(0)\rangle$). In the reference frame $\{|n(t)\rangle\}$, one can write a generic solution of the Schrödinger equation as follows:

$$|\psi(t)\rangle = \sum_n a_n(t) e^{-i \int \epsilon_n(t)dt} |n(t)\rangle \, , \tag{2.59}$$

where the dynamical phases are factorized. Omitting to explicitly indicate the time dependence, one can write

$$H|\psi\rangle = \sum_n a_n e^{-i \int \epsilon_n dt} \epsilon_n |n\rangle \, , \tag{2.60}$$

and

$$|\dot{\psi}\rangle = \sum_n \dot{a}_n e^{-i \int \epsilon_n dt} |n\rangle + -i \sum_n a_n \epsilon_n e^{-i \int \epsilon_n dt} |n\rangle + \sum_n a_n e^{-i \int \epsilon_n dt} |\dot{n}(t)\rangle \, . \tag{2.61}$$

Hence, the Schrödinger equation reads:

$$\sum_n \dot{a}_n |n\rangle + \sum_n a_n |\dot{n}\rangle = 0 \, . \tag{2.62}$$

Multiplying on the left by $\langle m|$ we obtain

$$\dot{a}_m = -a_n \langle m|\dot{n}\rangle \, . \tag{2.63}$$

The term on the right hand side can be evaluated by differentiation of the instantaneous eigenvalue equation

$$H|n\rangle = \epsilon_n |n\rangle \, . \tag{2.64}$$

Taking the scalar product with $|m\rangle$ yields

$$\langle m|\dot{H}|n\rangle + \epsilon_m \langle m|\dot{n}\rangle = \dot{\epsilon}_n \langle m|n\rangle + \epsilon_n \langle m|\dot{n}\rangle \, , \tag{2.65}$$

and one obtains, for $m \neq n$,

$$\langle m|\dot{n}\rangle = \frac{\langle m|\dot{H}|n\rangle}{\epsilon_n - \epsilon_m} \, . \tag{2.66}$$

Coming back to the equation (2.63), we have obtained:

$$\dot{a}_n = -a_n \langle n|\dot{n}\rangle - \sum_{m \neq n} a_m \frac{\langle n|\dot{H}|m\rangle}{\epsilon_m - \epsilon_n} e^{i \int (\epsilon_n - \epsilon_m)dt} \, . \tag{2.67}$$

In the adiabatic limit, the instantaneous eigenvectors *decouple* each other

$$\frac{\hbar \left|\langle n|\dot{H}|m\rangle\right|}{(\epsilon_m - \epsilon_n)^2} \longrightarrow 0 \, , \tag{2.68}$$

and we can write

$$\dot{a}_n = -a_n \langle n|\dot{n}\rangle \, , \tag{2.69}$$

whose solution reads:

$$a_n(t) = e^{-\int \langle n|dn\rangle} a_n(0) \, . \tag{2.70}$$

33

As a consequence, if the system is initially in an eigenstate, say $a_n(0) = \delta_{nm}$, it *remains* in the corresponding eigenstate at each subsequent time:

$$H(0)|\psi(0)\rangle = \epsilon(0)|\psi(0)\rangle \longrightarrow H(t)|\psi(t)\rangle = \epsilon(t)|\psi(t)\rangle . \tag{2.71}$$

In particular, if the Hamiltonian is cyclic, $H(T) = H(0)$, the dynamics in the rays' space is also cyclic, and the state vector acquires a geometric and a dynamical phase

$$|\psi(T)\rangle = e^{-\int \langle n|dn\rangle} e^{-i\int \epsilon_n dt} |\psi(0)\rangle. \tag{2.72}$$

Let us consider a quantum system with a finite number of levels, say $\mathcal{H} \cong \mathbb{C}^N$. The system Hamiltonian can always be written as $H = \sum_\alpha h_\alpha \lambda_\alpha$, where the operators $\{\lambda_\alpha\}_{\alpha=1}^{N^2}$ are a basis in the linear space of hermitian operators (a set of generalized Gell-Mann matrices, or the Pauli matrices for $N = 2$), with real coefficients h_α. From that point of view, a Hamiltonian operator is nothing more than an element of a N^2-dimensional real vector space. Hence, a time dependent Hamiltonian, $H(t) = \sum_\alpha h_\alpha(t)\lambda_\alpha$, defines a path in $\mathbb{R}^{N^2}$, and a cyclic Hamiltonian a closed loop. On the other hand, a Hamiltonian operator can be determined by a set of parameters $\{x\}$, which, for instance, correspond to classical fields that determines the interactions and that in principle might be experimentally controlled. In particular, these classical parameters can be subjected to a set of physical constraints. In that case one can write $x \in \mathcal{M}$, where $\mathcal{M}$ is a suitable manifold. From that point of view, the system Hamiltonian can be seen as a function

$$H \; : \; x \in \mathcal{M} \; \longrightarrow \; H[x] . \tag{2.73}$$

In the following, we describe the idea that the quantum system can be controlled through that set of classical parameters that, for this reason, will be also called *control parameters*, as well as we will refer to $\mathcal{M}$ as the *control manifold*.

As the Hamiltonian is a function on $\mathcal{M}$, the same holds for its spectral decomposition

$$H[x] = \epsilon_n[x]P_n[x] . \tag{2.74}$$

In the case of non-degenerate eigenvalues, one can write $P_n[x] = |n[x]\rangle\langle n[x]|$. A closed path over the control manifold

$$\gamma \; : \; t \in [0, T] \; \longrightarrow \; x(t) \in \mathcal{M}, \tag{2.75}$$

with $x(T) = x(0)$, corresponds to a loop $H[x(t)]$ in the space of Hamiltonian. The loop $H[x(t)]$ determines an associated time-dependent Schrödinger equation:

$$i\frac{d}{dt}|\psi\rangle = H[x(t)]|\psi\rangle . \tag{2.76}$$

In the adiabatic limit, if the system is initially in the ray $|n[x(0)]\rangle\langle n[x(0)]|$, it remains into the corresponding instantaneous eigenspace (determined by $|n[x(t)]\rangle\langle n[x(t)]|$) at each subsequent time. Hence, a loop in the Hamiltonian *infers* a loop in the space of rays, and one can write:

$$|\psi(T)\rangle = e^{-\oint_\gamma \langle n|dn\rangle} e^{-i\int_\gamma \epsilon_n dt} |\psi(0)\rangle , \tag{2.77}$$

with $|n[x(0)]\rangle = |\psi(0)\rangle$, and $|n[x(0)]\rangle = |n[x(T)]\rangle$. Hence we can introduce the *adiabatic connection*:

$$A = -i\langle n[x]|dn[x]\rangle = -i\langle n[x]|\partial_\mu n[x]\rangle dx_\mu . \tag{2.78}$$

34

Which can also be expressed by means of its component in the local set of coordinates, namely

$$A_\mu = -i\langle n|\partial_\mu n\rangle \ . \tag{2.79}$$

Notice that, in contrast to the Pancharatnam connection, this one-form is indeed defined on the control manifold, and not on the Hilbert space. In the present case, we are dealing with a fibre bundle with total space corresponding to the family of spaces of degeneracy labeled by the index $n[x]$, while the *base space* is the control manifold $\mathcal{M}$, and the structure group is U(1).

2.4.3   Example: a spin-$1/2$ in a quasi-static magnetic field

Let us consider a spin-$1/2$ in an adiabatically changing magnetic field. The time-dependent Hamiltonian is

$$H(t) = -\frac{1}{2}\mathbf{B}(t)\sigma \tag{2.80}$$

where σ indicates the Pauli matrices. Notice that the Hamiltonian is determined by the value of the instantaneous magnetic field, hence the corresponding control manifold is $\mathcal{M} \cong \mathbb{R}^3$. In the basis $\{|0\rangle, |1\rangle\}$, with $\sigma_z|0\rangle = |0\rangle$ and $\sigma_z|1\rangle = -|1\rangle$, the instantaneous ground state can be written as

$$|\psi_0\rangle = \cos\frac{\vartheta}{2}|0\rangle + e^{i\varphi}\sin\frac{\vartheta}{2}|1\rangle \tag{2.81}$$

where the instantaneous magnetic is written in polar coordinates as

$$\mathbf{B} = |\mathbf{B}|(\sin\vartheta\cos\varphi, \sin\vartheta\sin\varphi, \cos\vartheta) \ . \tag{2.82}$$

The ground state energy $E_0(t) = -\frac{1}{2}|\mathbf{B}(t)|$, and the energy gap with the excited state is $\Omega = |\mathbf{B}(t)|$. With the choice (2.81), the corresponding connection one-form has the following form:

$$A = -i\langle\psi_0|d\psi_0\rangle = \frac{1}{2}d\varphi\,(1 - \cos\vartheta) \ . \tag{2.83}$$

After an *adiabatic* loop γ followed by the magnetic field in the *operational time* T, the ground state acquires a phase factor:

$$e^{i\Phi} = e^{-i\Phi_g} \times e^{-i\Phi_d} \tag{2.84}$$

where $\Phi_d = \int_0^T E_0(t)dt$ gives the dynamical phase, and the geometric phase is expressed by:

$$\Phi_g = \oint_\gamma A = \frac{1}{2}\oint d\varphi\,(1 - \cos\vartheta) = \frac{\omega}{2} \ , \tag{2.85}$$

where ω is the solid angle spanned by the magnetic field.

For non-adiabatic loop, the evolution of the system might be non-cyclic, even in correspondence of a cyclic magnetic field. With the initial condition $|\psi(0)\rangle = |\psi_0\rangle$, one has to solve the corresponding Schrödinger equation in order to obtain the final state $|\psi(T)\rangle$. The relative phase between the final and initial states is defined by $\arg\langle\psi_0|\psi(T)\rangle$. The plot in figure 2.1 shows the *average gate fidelity* (see the appendix B) between the *adiabatic* evolution and the *dynamical* evolution as a function of the operational time T, in correspondence of loops with the same support.
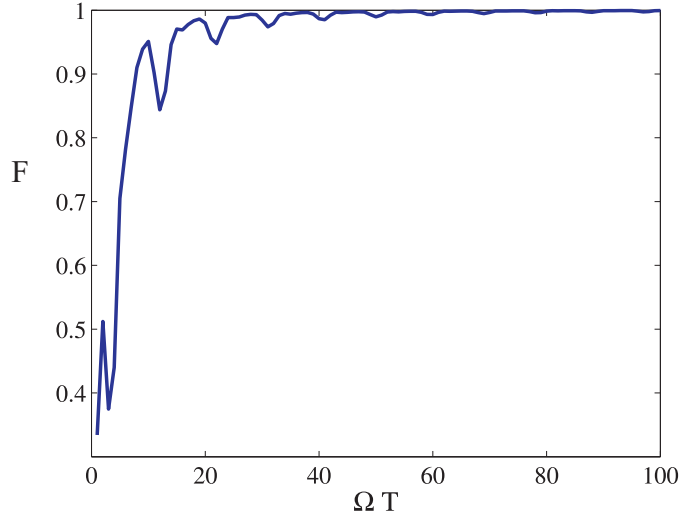
Figure 2.1: Average gate fidelity between the adiabatic and the dynamical transformation for the spin-1/2 in an changing magnetic field, as a function of the adimensional operational time ΩT. The adiabatic dynamics is approached in the limit $\Omega T \gg 1$.

2.4.4 Non-Abelian holonomies

In the previous sections, we have considered the case of Abelian, $U(1)$, phase factors, both for the adiabatic and the non-adiabatic setting. The discussion can be naturally extended to the situation in which multiple eigenvalues are present, and one can observe a non-Abelian , $U(d)$, phase factor. The spectral decomposition (2.74), can present eigenprojectors with rank greater than one. The main difference, from a geometric point of view, is that one is dealing with a principal fibre bundle with structure group $U(d)$.

In order to fix the ideas, let us consider the case of *adiabatic* geometric phases. Let us select a d-dimensional subspace, corresponding to the eigenprojector $P_n[x]$, and the eigenspace $\mathcal{H}_n[x]$. One can consider an initial vector $|\psi_0\rangle \in \mathcal{H}_n[x]$, and an adiabatic loop γ in the control manifold. At the end of the loop, the eigenspace will come back to itself, $\mathcal{H}_n[x(T)] = \mathcal{H}_n[x(0)]$, followed by the final state $|\psi(T)\rangle \in \mathcal{H}_n[x(T)]$. Hence, in general, the system will acquire a non-Abelian phase factor:

$$|\psi(T)\rangle = U|\psi(0)\rangle, \tag{2.86}$$

where $U \in U(d)$, is a *unitary matrix* acting in the d-dimensional eigenspace $\mathcal{H}_n[x(0)]$.

Let us chose a frame in $\mathcal{H}_n[x(0)]$, denoted with $\{|\eta_a[x(0)]\rangle\}$ and let it evolves according to the Schrödinger equation. Hence, the corresponding solutions $\{|\eta_a[x(t)]\rangle\}$, with

$$i\frac{d}{dt}|\eta_a[x(t)]\rangle = H[x(t)]|\eta_a[x(t)]\rangle , \tag{2.87}$$

define an orthonormal basis in $\mathcal{H}_n[x(t)]$ at each time $t \in [0, T]$. Another basis $\{|\phi_a[x(t)]\rangle\}$ in $\mathcal{H}_n[x(t)]$ can be chosen such that $|\eta_a[x(t)]\rangle = U_{ab}[x(t)]|\phi_b[x(t)]\rangle$, and $|\psi_a[x(T)]\rangle = |\psi_a[x(0)]\rangle = |\eta_a[x(0)]\rangle$, corresponding to a time-dependent unitary matrix $U_{ab}[x(t)] \equiv U \in U(d)$. Omitting to indicate explicitly the dependence from $x(t)$, equation (2.87) reads:

$$HU_{ab}|\phi_b\rangle = idU_{ab}|\phi_b\rangle + iU_{ab}d|\phi_b\rangle . \tag{2.88}$$

36

Multiplying from the left by $\langle \eta_c| = \langle \phi_d | U_{cd}{}^*$ one obtains

$$U_{cd}{}^* U_{ab} \langle \phi_d | H | \phi_b \rangle = i U_{cd}{}^* dU_{ab} \langle \phi_d | \phi_b \rangle + i U_{cd}{}^* U_{ab} \langle \phi_d | d\phi_b \rangle \; . \tag{2.89}$$

Since the $|\phi_a\rangle$ are eigenvectors of the instantaneous Hamiltonian, one can write

$$U_{cd}{}^* U_{ab} \epsilon_n \delta_{db} = i U_{cd}{}^* dU_{ab} \delta_{db} - U_{cd}{}^* U_{ab} A_{db} \; , \tag{2.90}$$

where we have defined the *matrix-valued* connection one form

$$A_{db} = -i \langle \phi_d | d\phi_b \rangle \; . \tag{2.91}$$

The expression in (2.90) has a matrix form:

$$\epsilon \mathbb{I} = i\hbar dU U^\dagger - \hbar U A U^\dagger \; . \tag{2.92}$$

Multiplying by $U^\dagger$ from the left and U from the right we obtain

$$\epsilon \mathbb{I} = i U^\dagger dU - A \; . \tag{2.93}$$

The latter is a differential equation for the unitary U, that we can rewrite explicitly as

$$i U^\dagger \frac{dU}{dt} = \epsilon + A \; . \tag{2.94}$$

The formal solution, with initial condition $U(0) = \mathbb{I}$ is

$$U(T) = e^{-i \int_0^T \epsilon(t) dt} \times \mathbf{T} e^{-i \int A} \; . \tag{2.95}$$

Notice that the first factor is the dynamical contribution to the phase inside the degenerate eigenspace, it corresponds to an irrelevant U(1) *global* phase factor. On the other hand, the second factor, as in the Abelian case, is independent of the parametrization of the curve and of the operational time and is interpreted as the geometric contribution, or *non-Abelian holonomy*. The matrix $A_{ab} = -i \langle \phi_a | d\phi_b \rangle$, or the operator $A_{ab} = -i \langle \phi_a | d\phi_b \rangle | \phi_a \rangle \langle \phi_b |$ is the corresponding non-Abelian connection *one-form*. Since the instantaneous degenerate space is determined by a point on the control manifold, we can write the connection as a one-form over $\mathcal{M}$, with component expression $A = A_\mu dx_\mu$, where

$$A_\mu \equiv -i \langle \phi_a | \partial_\mu \phi_b \rangle \; . \tag{2.96}$$

Neglecting the dynamical part (for example, putting $\epsilon_n = 0$), we obtain a holonomic non-Abelian gate, which has the following expression

$$\Gamma = \mathbf{P} e^{-i \int A} \; . \tag{2.97}$$

Since the holonomy is independent of the particular parametrization of the loop $x(t)$, we have substituted the time-ordering with the path-ordering symbol $\mathbf{P}$.

37

2.5 Universal computation with the holonomic group

The observation of non-Abelian holonomies naturally leads to the *application* of geometric phases for the scopes of *quantum computing* or, in general, for *quantum information processing*. Since a quantum algorithm is realized as a unitary evolution of a quantum system, one can argue that the geometric phases can be regarded as a *special class* of unitary transformations. In the present section, we recall how geometric phases can be exploited in order to realize universal quantum computation.

Let us consider a quantum system, together with a family of isodegenerate Hamiltonian functions

$$H \quad : \quad x \in \mathcal{M} \quad \longrightarrow \quad H[x] , \tag{2.98}$$

with a point-wise spectral decomposition

$$H[x] = \sum_k \epsilon_k[x] P_k[x] . \tag{2.99}$$

The corresponding Hilbert space factorizes as a direct sum of (sub)spaces

$$\mathcal{H} = \oplus_k \mathcal{H}_k[x] , \tag{2.100}$$

each corresponding to a different eigenenergy. A loop on the control manifold

$$\gamma \quad : \quad t \in [0,T] \quad \longrightarrow \quad \gamma(t) \in \mathcal{M} , \tag{2.101}$$

with starting point $x_0 = \gamma(0) = \gamma(T)$, is said to be adiabatic if

$$\dot{\gamma}/\gamma \ll \inf_{h \neq k} |\epsilon_h[\gamma] - \epsilon_k[\gamma]| , \tag{2.102}$$

If the control parameters evolve in time along an adiabatic loop, the overall unitary transformation factorizes in the following way:

$$U(T) = \oplus_k e^{-i\phi_k(T)} \Gamma_k(\gamma) P_k[x_0] , \tag{2.103}$$

where $\phi_k(T) = \int_0^T \epsilon_k[\gamma(t)] dt$ are the dynamical contributions to the phase, and

$$\Gamma_k(\gamma) = \mathbf{P} e^{-i \int_\gamma A_k} \tag{2.104}$$

are the holonomies associated to each subspace. Thus, the dynamics in each degenerate subspace $\mathcal{H}_k[x_0]$ at the initial point x_0 are decoupled. In each of the subspace, the adiabatic connection is in general matrix valued, and takes values in the Lie algebra $\mathrm{u}(d_k)$, where d_k is the dimension of the corresponding subspace. For the scope of geometric quantum computation, one needs to pick up one degenerate subspace, say $\mathcal{H}_k$ of dimension $d = d_k$, that will play the role of a *computational space*. By itself, this subspace hasn't any tensor product structure, nevertheless it is mathematically equivalent to — and can be used to *simulate* — a register of N qubits, with $N = \log_2 d$. From that point of view, one can notice that the dimension of the degenerate subspace grows *exponentially* with the number of qubits. Neglecting the dynamical phase, the holonomy can be exploited in order to produce a quantum gate in a *completely* geometric fashion. Furthermore, the quantum gate is determined through the control of the classical parameters x.

After the introduction of adiabatic geometric phases, it should be clear that in correspondence to a given *adiabatic* loop in the control manifold one obtains an unitary gate which is the corresponding holonomy. On the other hand, one cannot in principle avoid that, for a given loop, the holonomy is *trivial*, i.e. it is a numerical phase factor in the computational space, or that different holonomies obtained by different loops do *commute* each other. Changing the loop in the parameter space corresponds to change the obtained holonomic gate, also in this case we cannot in principle avoid the situation in which all the loop give rise to the same gate — or the same *subgroup* of gates — hence not allowing to take advantage of the full computational potentialities of the system. In other words, there is need to identifies the conditions under which an universal quantum computation is possible using only holonomic transformations in the selected computational subspace. That kind of problem was proposed and solved by Paolo Zanardi and Mario Rasetti in [ZR99]. In the following we will give a short survey of their results.

Two *ingredients* enter in the definition of the holonomic transformation: the selected *loop* γ over the control manifold, and the explicit expression of the *connection* one form. First of all, one has to notice that the set of loops over the manifold with fixed starting point x_0 is endowed with a law of composition. Since the adiabatic holonomy does not depend on the operational time, we can put

$$\gamma \;:\; s \in [0,1] \;\longrightarrow\; \gamma(s) \in \mathcal{M} \;. \tag{2.105}$$

Hence, one can notice that two loops can be composed in the following way

$$\gamma_2 \cdot \gamma_1(t) = \theta(1/2 - t)\gamma(2t) + \theta(t - 1/2)\gamma(2t - 1) \tag{2.106}$$

(where θ is the *heavy-side* function). In correspondence with that, an inner product can be defined on holonomies as follows

$$\Gamma(\gamma_2)\Gamma(\gamma_1) = \Gamma(\gamma_2 \cdot \gamma_1) \;. \tag{2.107}$$

Notice that the trivial loop $\gamma_0(t) = x_0$ corresponds to the trivial holonomy $\Gamma(\gamma_0) = \mathbb{I}$, and the inverse holonomy corresponds to the loop preformed in the opposite way $\Gamma^{-1}(\gamma) = \Gamma(\gamma')$, where we have defined $\gamma'(t) = \gamma(1 - t)$. Hence, the set of the corresponding holonomies is a group, called the *holonomy group* associated to the adiabatic connection. That group is denoted $\mathrm{hol}(A)$.

The holonomy group $\mathrm{hol}(A)$ is in general a *proper* subgroup of the whole unitary group $\mathrm{U}(d)$ acting in the d-dimensional subspace chosen as computational subspace. In order to obtain universal holonomic computation, one has to require that the holonomy (sub)group is *not* a proper subgroup, i.e. $\mathrm{hol}(A) = \mathrm{U}(d)$. If that condition holds true, it is possible to approach any unitary transformation with *arbitrary* high accuracy, with a *finite* sequence of holonomic transformations which corresponds to a sequence of loops. In that case, the connection one-form A is said to be *irreducible*. Hence, the universality of holonomic computation is equivalent to the irreducibility of the corresponding connection one-form.

The irreducibility of the connection can be determined studying the associated *curvature*, or field strength, $F = dA$. Its component expression, in a local set of coordinates $\{x_\mu\}$ on $\mathcal{M}$, reads

$$F_{\mu\nu} = \partial_\nu A_\mu - \partial_\mu A_\nu - [A_\mu, A_\nu] \;. \tag{2.108}$$

The important result, for our purpose, is that the connection is irreducible *if and only if* the components of the curvature *span* the whole Lie algebra $\mathrm{u}(d)$ of the unitary group [Na05]. As was discussed in [ZR99], irreducibility can be proven to be the *generic case* (in the sense that the set of irreducible
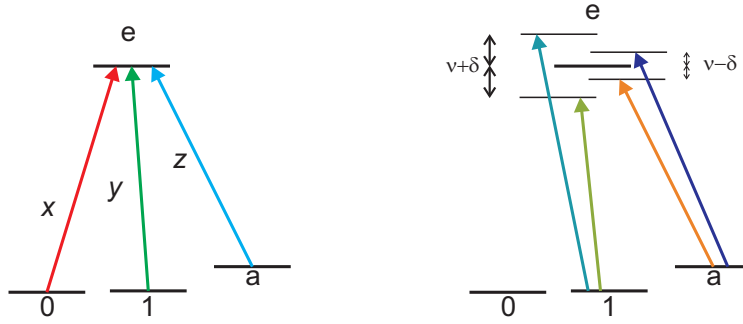
Figure 2.2: On the left: structure of the levels for a single ion with the coupling fields. On the right: blue and red de-tuned laser fields related to the realization of the two-qubit geometric gate.

connections is an open subset which is dense in the set of all possible connection one-forms). On the other hand, that result leaves the problem of explicitly identify a physically reliable Hamiltonian over a suitable manifold of control parameters with an associated irreducible connection one-form.

To conclude, one can notice that the approach we have outlined in this section take in consideration a system of d-levels *as a whole*, without taking in account (and even without requiring it), that a system of $N = \log_2 d$ qubits has a precise *tensor product* structure. Also from that point of view, as the name says, the holonomic approach can be interpreted as a *global* approach to quantum computation. On the other hand, as also recalled in the chapter 1, in contrast to this *top-down* approach, one can take a *bottom-up* point of view and obtain any N-qubit gate as the composition of simple one-qubit and two-qubits gates.

In the next section, we will discuss the proposal that was presented in [Du01] that involves a physically reliable Hamiltonian and exploit the bottom-up point of view.

2.6 Physical realizations

The first experimentally feasible proposal for the realization of an all-holonomic computation was given by Luming Duan, Ignacio Cirac and Peter Zoller in [Du01]. A possible physical system is an array of ions in a Pauli trap, which can be manipulated with appropriate laser beams. The same physical setting has been discussed in order to realize standard *dynamical* scheme for quantum computing [Ci95, So99, Mo99, Ci00], and the single and multi-qubit operations have been experimentally demonstrated [Mo95, Ro99]. Even if other models have been proposed in the literature [Fa00], the model of Duan *et al.* is probably the one most extensively studied also with reference to different physical systems, as Josephson junctions [Fa03] and semiconductor quantum dots [So03], and can be regarded as a *reference point* for the subject.

2.6.1 Geometric manipulation of trapped ions

All the ions are assumed to have the same structure of electronic levels (see the scheme on the left hand side of figure 2.2). For the jth ion, it is composed of two degenerate stable or metastable state $|0\rangle_j$ and $|1\rangle_j$ which, as the notation suggests, identify the computational space of the jth qubit $\mathcal{H}_0^j = \mathrm{span}\{|0\rangle_j, |1\rangle_j\}$; an excited state $|e\rangle_j$ and an ancillary low-energy state $|a\rangle_j$. In such a way, one-qubit degrees of freedom are attached to each ion. In order to obtain universal computation, the
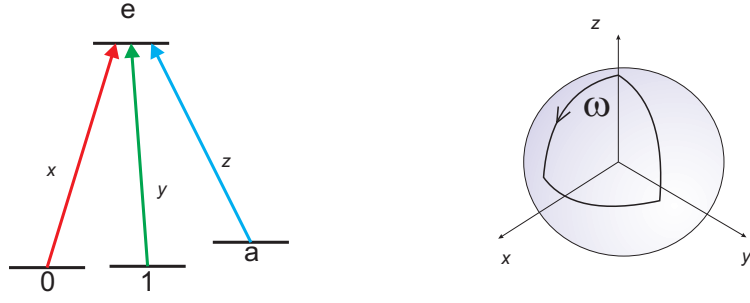
Figure 2.3: The level scheme and the control manifold for the (second) single-qubit geometric gate.

ability to realize a pair of non-commuting single-qubit unitary gates and one nontrivial two-qubit transformation is required.

The gates that can be generated in a complete geometric fashion can be chosen in the following way:

1. The first one-qubit gate is

$$U_1^j = e^{i\Phi_1 |1\rangle_j \langle 1|} , \qquad (2.109)$$

which is a single-qubit *phase* gate, that has the matrix expression

$$U_1^j \equiv \begin{bmatrix} 1 & 0 \\ 0 & e^{i\Phi_1} \end{bmatrix} \qquad (2.110)$$

in the computational basis.

2. The second one-qubit gate is

$$U_2^j = e^{i\Phi_2 \sigma_y^j} , \qquad (2.111)$$

where $\sigma_y^j = i\left(|1\rangle_j\langle 0| - |0\rangle_j\langle 1|\right)$ is the Pauli matrix in the computational basis. The corresponding matrix expression of the gate is:

$$U_2^j = \cos\Phi_2 \mathbb{I}^j + i\sin\Phi_2 \sigma_y^j \equiv \begin{bmatrix} \cos\Phi_2 & \sin\Phi_2 \\ -\sin\Phi_2 & \cos\Phi_2 \end{bmatrix} . \qquad (2.112)$$

3. The two-qubit gate, acting on the jth and kth qubit, is

$$U_3^{jk} = e^{i\Phi_3 |11\rangle_{jk}\langle 11|} . \qquad (2.113)$$

Its matrix expression in the computational basis of the pair of qubits j and k (the two-qubit computational states are $\{|00\rangle_{jk}, |01\rangle_{jk}, |10\rangle_{jk}, |11\rangle_{jk}\}$) is

$$U_3^{jk} \equiv \begin{bmatrix} 1 & 0 & 0 & 0 \\ 0 & 1 & 0 & 0 \\ 0 & 0 & 1 & 0 \\ 0 & 0 & 0 & e^{i\Phi_3} \end{bmatrix} . \qquad (2.114)$$

The arguments Φ_1, Φ_2 and Φ_3 are adjustable parameters depending on the chosen loop in the parameter manifold.

In order to realize the single-qubit gates, an ion in the trap is addressed with three laser beams corresponding to the three possible transition from the low-energy levels to the excited level. The degenerate levels are supposed to have different angular momentum in such a way that the corresponding transitions can be addressed with laser beams which differ in polarization. In the rotating frame, the interaction picture Hamiltonian reads as follows:

$$H = (\Omega_0 |0\rangle\langle e| + \Omega_1 |1\rangle\langle e| + \Omega_a |a\rangle\langle e| + \text{h.c.}) \tag{2.115}$$

where Ω_0, Ω_1 and Ω_a are the three, in general complex, Rabi frequencies, and h.c. denotes the Hermitian conjugate, and we have omitted the index labeling the ions.

The first one-qubit gate

To generate the holonomic gate U_1 one has to set $\Omega_0 = 0$. In such a way, the $|0\rangle$ level is completely decoupled. Also, we choose the following parametrization: $\Omega_1 = -\Omega \sin(\vartheta/2)e^{i\varphi}$ and $\Omega_a = \Omega \cos(\vartheta/2)$. The common factor Ω gives the total "intensity" of the interaction $\Omega^2 = \Omega_1^2 + \Omega_a^2$. Its value is relevant in order to validate the adiabatic approximation, while it is the relative amplitude between Ω_1 and Ω_a that determines the dynamics in the adiabatic limit. Hence, the manifold of control parameters is a two-dimensional sphere. With that parametrization, the system presents a dark state, i.e. a state with zero energy:

$$|\psi\rangle = \cos\frac{\vartheta}{2}|1\rangle + \sin\frac{\vartheta}{2}e^{i\varphi}|a\rangle \; . \tag{2.116}$$

The initial configuration of the system has to be chosen in correspondence with the point $\vartheta = 0$ (the North pole), in which the state $|\psi\rangle = |1\rangle$ has zero energy. The connection one-form is written as

$$A_1 = -i\langle\psi|d\psi\rangle = \sin^2\frac{\theta}{2}d\varphi = \frac{1}{2}(1 - \cos\vartheta)\,d\varphi \; . \tag{2.117}$$

After an adiabatic loop in the parameter space, the acquired geometric phase equals one-half of the solid angle spanned by the loop. For a given loop, which identifies a solid angle ω_1, we obtain the holonomic gate $e^{i\frac{\omega_1}{2}|1\rangle\langle 1|}$.

The second one-qubit gate

In the following chapters, we will consider the following holonomic gate as a case study. In order to realize the one-qubit gate U_2, we need to constraint the three Rabi frequency to be real-valued, furthermore, the parameters are constrained to take values on a two-sphere. It is thus convenient to introduce polar coordinates. Putting $x = \Omega_0$, $y = \Omega_1$, and $z = \Omega_a$, we write the following parametrization:

$$\begin{cases} x &= \Omega \sin\vartheta \cos\varphi \\ y &= \Omega \sin\vartheta \sin\varphi \\ z &= \Omega \cos\vartheta \end{cases} . \tag{2.118}$$

In that case, the spectrum of (2.115) is threefold:

$$\sigma = \{0, \pm\Omega\} \; , \tag{2.119}$$

42

with the null eigenvalue which is doubly degenerate. The two degenerate eigenstates with vanishing energy can be chosen as follows:

$$
\begin{aligned}
|\psi_0\rangle &= \cos\vartheta\left(\cos\varphi|0\rangle + \sin\varphi|1\rangle\right) - \sin\vartheta|a\rangle \,, \\
|\psi_1\rangle &= -\sin\varphi|0\rangle + \cos\varphi|1\rangle \,.
\end{aligned}
\tag{2.120}
$$

Hence, while the eigenenergy is fixed, the corresponding eigenspace is a function of the control parameters, i.e. a function on the two-sphere.

The corresponding connection one-form is matrix-valued and reads as follows:

$$
A_2 = -i\langle\psi_\alpha|d\psi_\beta\rangle = -\cos\vartheta\, d\varphi\, \sigma_y^{\alpha\beta} \,,
\tag{2.121}
$$

where $\sigma_y^{\alpha\beta}$ are the components of the Pauli matrix. After an *adiabatic loop* in the parameter space, which spans a *solid angle* ω_2 (see the figure 2.3), one obtains the non-Abelian holonomy

$$
U_2 = e^{-i\omega_2\sigma_y} \,.
\tag{2.122}
$$

The two-qubit gate

The realization of the two-qubit gate requires to exploit the interactions between two ions. Ions interact between themselves via the Coulomb force. For small deviations from the equilibrium position, this interaction can be modeled by a set of collectives modes which describe the vibrational degrees of freedom of the array of ions.

In order to realize the two-qubit gate U_3, one vibrational mode with frequency ν is selected, typically it corresponds to the vibrational motion of the center of mass of the chain. Both the jth and the kth ions are addressed with the same combination of laser fields. While the $|0\rangle$ levels are decoupled ($\Omega_0 = 0$), the $|1\rangle$ and $|a\rangle$ levels are independently coupled to the excited state with a laser field composed of two beams, a blue and red de-tuned components. More precisely, the de-tuning for the transition $|1\rangle \leftrightarrow |e\rangle$ is chosen to be $\pm(\nu + \delta)$, where δ is an additional shift, and $\pm(\nu - \delta')$ for the other transition, where δ' can be chosen to be $\delta' = -\delta$ (see the scheme depicted in figure 2.2). In this way, only the second order transitions are resonant. In the Lamb-Dicke regime ($\eta \ll 1$), the system Hamiltonian reads:

$$
H = \frac{\eta^2}{\delta}\left(-|\Omega_1|^2\sigma_{j1}^{\phi_1}\sigma_{k1}^{\phi_1} + |\Omega_a|^2\sigma_{ja}^{\phi_a}\sigma_{ka}^{\phi_a}\right)
\tag{2.123}
$$

where

$$
\sigma_{j\mu}^{\phi_\mu} = e^{i\phi_\mu}|e\rangle\langle\mu| + \text{h.c.} \,,
\tag{2.124}
$$

with $\mu = 1, a$. One can take the parametrization $|\Omega_1|^2 = |\Omega|^2\sin(\vartheta/2)$ and $|\Omega_a|^2 = |\Omega|^2\cos(\vartheta/2)$ and $\phi_1 - \phi_a = \varphi$. Starting from the point $\vartheta = 0$, the vector $|11\rangle$ adiabatically follows $|\psi\rangle = \cos(\vartheta/2)|11\rangle + e^{i\varphi}\sin(\vartheta/2)|aa\rangle$, while the vectors $|00\rangle, |01\rangle$ and $|10\rangle$ are decoupled. Also in this case, if the loop spans a solid angle ω_3, the corresponding gate is $U_3 = e^{i\frac{\omega_3}{2}|11\rangle\langle11|}$.

2.7 The argument of robustness of geometric phases

In the adiabatic case, the geometric phase acquired in correspondence of a closed loop γ on the control manifold is given by the integral of the adiabatic connection:

$$
\Phi = \oint_\gamma A \,.
\tag{2.125}
$$

43

In the examples discussed above, one can invoke the (Abelian) Stokes' theorem and write:

$$\Phi = \int_S F \ , \tag{2.126}$$

where S is a surface with *boundary* γ, and F is the curvature field associated to A.

In the presence of parametric noise, the loop is changed to the *noisy loop* γ_n:

$$\gamma \ \longrightarrow \ \gamma_n \ . \tag{2.127}$$

As a consequence, in correspondence of a noisy adiabatic path, one obtains a noisy geometric phase:

$$\Phi_n = \int_{\gamma_n} A \ , \tag{2.128}$$

which can be also written as the integral of the curvature over the surface S_n spanned by the noisy path:

$$\Phi_n = \int_{S_n} F \ . \tag{2.129}$$

It is worth noticing that the quantity in (2.129) is a stochastic variable, defined as a stochastic integral. The *fluctuations* in Φ_n are determined by the fluctuations in the noisy loop and by the fact that in general the noisy path might *not* be closed. The non-closure of the path makes the integral in (2.128) no more gauge invariant. Following [SB88] and [DP03], one can "close" the loop following a *geodesic* rule. Obviously, that approach makes sense only for small perturbations.

Corresponding with the noisy path, one has a holonomic transformation, or geometric phase

$$\Gamma_n = \exp\left(-i\Phi_n\right) \ , \tag{2.130}$$

which is itself a stochastic variable. The geometric phase is *fault-tolerant*, with respect to parametric noise, if the integral in (2.129) is stable with respect to the fluctuation induced by the noise affecting the loop in the parameter manifold. Hence the issue is to determine in which conditions, regarding the noise and the system, the stochastic integral in (2.129) [or in (2.128)] has negligible fluctuations.

2.7.1   Berry phase in a fluctuating magnetic field

Following Gabriele De Chiara and Massimo Palma in [DP03], in this section we describe the argument in *favor* of the robustness of the geometric phase with respect to parametric noise. Obviously the robustness is not an absolute property of geometric phase, the claim is that it can be more robust than its dynamical counterpart.

The system under consideration is a spin-$1/2$ degree of freedom in the presence of a *noisy adiabatic* magnetic field. With reference to the example discussed in the section 2.4.3, here we consider a noisy magnetic field and the corresponding Schrödinger equation:

$$i\frac{d}{dt}|\psi\rangle = -\frac{1}{2}\mathbf{B}(t)\sigma|\psi\rangle \ . \tag{2.131}$$

In the presence of parametric noise, the magnetic field is the sum of two parts:

$$\mathbf{B}(t) = \mathbf{B}_0(t) + \mathbf{K}(t) \ , \tag{2.132}$$

where $\mathbf{B}_0(t)$ identifies and ideal (noiseless) closed loop experienced by the magnetic field during an operational time T, and $\mathbf{K}(t)$ is a noisy contribution to the magnetic field which can be modeled as a

stochastic process with vanishing mean value. For instance, we will take in consideration a stationary Ornstein-Uhlenbeck process (see for instance [Ga83]) with amplitude ε and band-width Γ, along each of the three components of $\mathbf{K}(t)$. In particular, the two-times correlation function has the following form:

$$C(|t - s|) = \langle K_j(t), K_l(s)\rangle_{\mathrm{noise}} = \delta_{jl}\varepsilon^2 e^{-\Gamma|t-s|} , \qquad (2.133)$$

where K_j indicates the jth components of the field.

In the discussion below we explicitly require that the noise is adiabatic, hence generating an adiabatic sample path. This condition can be stated by requiring that the band-width of the noise is sufficiently *narrow*, in our case that condition reads $\Gamma \ll |\mathbf{B}|$. That ensures that the high frequencies give a sufficiently small contribution.

If, in correspondence of the ideal loop γ, the instantaneous magnetic field is written in polar coordinates as

$$\mathbf{B}_0(t) = |\mathbf{B}_0(t)| \left(\sin\vartheta_0(t)\cos\varphi_0(t), \sin\vartheta_0(t)\sin\varphi_0(t), \cos\vartheta_0(t)\right) , \qquad (2.134)$$

the noisy magnetic field, which follows the noisy path γ_{n} has an analogous expression

$$\mathbf{B}(t) = |\mathbf{B}(t) + \mathbf{K}(t)| \left(\sin\vartheta(t)\cos\varphi(t), \sin\vartheta(t)\sin\varphi(t), \cos\vartheta(t)\right) . \qquad (2.135)$$

For small amplitude of the noise, the angular variables can be expressed by their first-order Taylor expansion:

$$\begin{aligned}
\vartheta(t) &\simeq \vartheta_0(t) + \delta\vartheta(t) \\
\varphi(t) &\simeq \varphi_0(t) + \delta\varphi(t) .
\end{aligned} \qquad (2.136)$$

Without noise, the geometric phase is $\Phi = \int_\gamma A$, and the dynamical phase is denoted Φ_d. In the presence of noise, the adiabatic connection

$$A = \frac{1}{2}\left(1 - \cos\vartheta\right)d\varphi \qquad (2.137)$$

has to be evaluated along the noisy loop. One can write a first-order perturbative expansion for the integral of the connection of the following kind:

$$\Phi_{\mathrm{n}} = \int_{\gamma_{\mathrm{n}}} A \simeq \int_\gamma A + \delta\Phi . \qquad (2.138)$$

Using the expression in (2.136), one has:

$$\delta\Phi = \int_0^T \frac{(1 - \cos\vartheta_0(t))}{2} d\delta\varphi(t) + \int_0^T \frac{\sin\vartheta_0(t)}{2}\delta\vartheta(t)d\varphi_0(t) + \int_0^T \frac{\sin\vartheta_0(t)}{2}\delta\vartheta(t)d\delta\varphi(t) . \qquad (2.139)$$

Hence, we have written the perturbative term in (2.138) as a stochastic integral, in which one can distinguish three contributions:

- A term which is of the first order in the amplitude of the noise, and is determined by the component of the noise along the angle φ:

$$\delta\Phi_1 = \frac{1}{2}\int_0^T (1 - \cos\vartheta_0(t)) \, d\delta\varphi(t) . \qquad (2.140)$$

45

- A second term of the first order in the noise amplitude, determined by the component of the noise along the angle ϑ:

$$\delta\Phi_2 = \frac{1}{2} \int_0^T \sin\vartheta_0(t)\delta\vartheta(t)d\varphi_0(t) . \tag{2.141}$$

- A term of the second order in the amplitude of the noise, which is determined by the correlations between the noise components along the angle ϑ and φ:

$$\delta\Phi_3 = \frac{1}{2} \int_0^T \sin\vartheta_0(t)\delta\vartheta(t)d\delta\varphi(t) . \tag{2.142}$$

The philosophy adopted in [DP03] was to neglect the second-order term, hence writing

$$\Phi_n \simeq \Phi + \delta\Phi_1 + \delta\Phi_2 . \tag{2.143}$$

At this point, they did several assumption. They consider an ideal loop in which $\vartheta_0(t) = \vartheta_0$ is constant, they put $\varphi(t) = 2\pi\frac{t}{T}$, and choice the unperturbed magnetic field with constant modulus, $|\mathbf{B}_0(t)| = B$. They neglect the term $\delta\Phi_1$ by noticing that it is responsible of the fact that the noisy path might be in general non-closed, making use of the discussion in [SB88] about geometric phases in the non-cyclic setting (see also the section 2.3.1 in this chapter). The remaining term $\delta\Phi_2$ was finally written in the following way:

$$\delta\Phi_2 = \int \frac{1}{2}\sin\vartheta_0\delta\vartheta(t)d\varphi_0(t) = \int_0^T \frac{1}{2}\left(\frac{B_{03}}{B^3}\mathbf{B}_0 \cdot \mathbf{K} - \frac{K_3}{B}\right)\frac{2\pi dt}{T} , \tag{2.144}$$

where B_{0j} and K_j indicate the jth component of the fields, and we have omitted the time dependence. Finally, the geometric phase in the presence of the noise is given by the following stochastic integral:

$$\Phi_n = \Phi + \frac{\pi}{T}\int_0^T\left(\frac{B_{03}}{B^3}\mathbf{B}_0 \cdot \mathbf{K} - \frac{K_3}{B}\right)dt . \tag{2.145}$$

They computed the mean value and the variance σ_Φ of that stochastic integral. While the mean value is zero, the mean square has the following expression (in the limit $\Gamma T \gg 1$):

$$\sigma_\Phi^2 = 2\frac{\varepsilon^2}{B}\left[(\pi\cos\vartheta_0\sin\vartheta_0)^2 + \left(\pi\sin^2\vartheta_0\right)^2\right]\frac{1}{\Gamma T} . \tag{2.146}$$

Notice that the quantity $N = \Gamma T$ can be interpreted as the average *number of statistically independent fluctuations* made by the noise component during the operational time T. That quantity turns to be a crucial parameter for the description of noisy geometric phase. In particular, we can see from the expression in (2.146) that the variance of the geometric phase vanishes (at the first order in the noise amplitude) in the limit $N \to \infty$. In other words, the geometric phase is stable if the noise is allowed to experience *sufficiently many* adiabatic oscillation during the operational time.

The expression in (2.146) has to be compared with the variance of the corresponding dynamical phase. Notice that the dynamical phase is written as a stochastic integral of the following form:

$$\Phi_d = \int_0^T |\mathbf{B}(t)| \simeq BT + \int_0^T \frac{\mathbf{B}_0 \cdot \mathbf{K}}{B}dt . \tag{2.147}$$

The mean value of the dynamical phase vanishes, while its mean square has the following form:

$$\sigma_d^2 = \frac{\varepsilon^2}{B}\int_0^T dt \int_0^T ds \left[\sin^2\vartheta\cos(\varphi_0(t) - \varphi_0(s)) + \cos^2\vartheta_0\right]e^{-\Gamma|t-s|} , \tag{2.148}$$

46

that, as can be easily checked, in the limit $\Gamma T \gg 1$ scales linearly with the operational time T.

The *total phase* acquired at the end of the adiabatic loop is the sum of the dynamical and the geometric contribution. The overall variance is not the sum of the variances because the two phases are not independent, since both are determined by the stochastic process **K**. Nevertheless, since the variance of the geometric phase scales as T^{-1}, while the one of the dynamical phase scales as T, the main contribution to the fluctuations of the phase comes from the dynamical part in the limit of long operational time.

2.8 Strategies for fault-tolerant holonomic gates

It is clear that the first-order analysis reviewed in the previous section suggests a possible *strategy* in order to obtain a *fault-tolerant* quantum computation in the context of the holonomic approach.

The argument of robustness of the holonomic gates states that the fluctuations in the geometric phase become *negligible* (at first order in the noise amplitude) increasing the parameter N, which expresses the average number of statistically independent oscillations of the noise. Hence, for a *given* noise, identified by its *amplitude* and its *band width* (or its *correlation time*), one can reduces the fluctuations of the noise by increasing the operational time T. Hence the cost of a longer operational time is compensated by a more robust computation.

The first-order analysis suggest to take the limit $T \to \infty$ in order to ideally obtain vanishing fluctuations in the holonomic gate. More realistically, one has to consider a feasible operational time which results from a *balance* between different physical and computational aspects.

The main idea of the present Thesis, that will be discussed in details in the chapters 4 and 5 is to refine that strategy taking into account the effects of the noise on the geometric phase at the second order in the perturbative expansion. One can indeed argue that, if for longer operational time the first-order contribution to the variance of the geometric phase is negligible, one has to consider the terms of the second order. The dependence of the second order correction from the operational time — or the number of noise fluctuations N — will hence determine the optimal strategy in order to achieve a robust holonomic gate.

Chapter 3

Robustness of non-adiabatic holonomic gates

This chapter is mainly based on the paper [Lu07'], in which we have studied the behavior of a non-Abelian and *non-adiabatic* holonomic gate in presence of parametric noise. That kind of gate was presented in a recent paper [Fl06] in the context of the non-Abelian one-qubit gate which was part of the proposal for a fully holonomic computation in [Du01] (also recalled in the previous chapter, section 2.6). The main result, contained in [Lu07'] and reviewed in this chapter, is that for non-Abelian *fast* gates, the adiabatic condition might not be reached in the presence of noise, hence the standard argument of robustness of holonomic gates cannot be applied. On the other hand, a different kind of mechanism which leads to an effect of cancelation of the noise can be observed. That kind of effect is completely dynamical and is not related to the geometric features of the holonomic transformation.

3.1 Introduction

Since the very beginning, holonomic gates were considered to be intrinsically robust against classical noise [Pa01], thanks to the geometric features of holonomy in Hilbert bundles. As we will briefly recall below, three main ingredients are needed in order to realize such holonomic gates.

The first ingredient is a suitable physical system described by a quantum Hamiltonian depending on some set of parameters, these parameters being associated with the external (classical) driving fields that are assumed to be experimentally controllable functions of time; the unavoidable instrumental instability (stochastic noise) affecting the fields is the source of the kind of classical noise, that has been mentioned above.

The second ingredient consists in selecting a suitable eigenspace of the given Hamiltonian — an eigenspace depending smoothly on the external parameters, hence actually an iso-degenerate family of eigenspaces; and in fixing in the parameter space an 'initial point' and a loop through this point. To such a loop corresponds an excursion of the parameter-dependent Hamiltonian (hence, of its eigenprojectors) and a certain *ideal unitary transformation* in the *encoding eigenspace*, namely, that particular relevant eigenspace fixed by the initial (and final) point of the loop in the parameter space. This ideal transformation is determined by *Kato's adiabatic evolutor* associated with the given Hamiltonian and with the chosen loop in the parameter space, and it has a simple geometric interpretation as a holonomy phenomenon (geometric phase). The ideal unitary transformation plays a central role in Kato's

formulation of the adiabatic theorem [Ka51] applied to our context. Indeed, the external parameters are controllable functions of time and, in the *adiabatic limit*, the *real evolution over the operational time* determined by the given physical Hamiltonian becomes *cyclic* in the encoding eigenspace and (apart from an irrelevant overall 'dynamical phase factor') *coalesces in this subspace with the ideal unitary transformation*. We stress that the ideal unitary transformation should be thought, in our context, as an *ideal quantum gate* whose behavior can be, in general, only approached by a *non-ideal quantum gate* corresponding to the real evolution over a suitably large, but finite, operational time.

Accordingly, the third ingredient is the choice of a suitable operational time — which will be called *balanced working time*, in the following — for the real quantum gate. This time span must be short enough to achieve a fast quantum computation and to avoid the ravages of decoherence, but long enough to justify the adiabatic approximation (i.e. to approach the behavior of the ideal quantum gate) which is at the root of the appearing of geometric phases [1]. Hence, a balanced working time is determined by a touchy trade-off between two competing and not necessarily compatible demands. On the other hand, the drawback of a longer operational time of a holonomic gate with respect to standard dynamical gates can be balanced by the robustness that can be achieved in the holonomic setting, leading to less computational time spent in error correction. Also from that point of view, one has to determine a balanced working time taking in account the computational time and the resistance to noise.

The problem of robustness of holonomic gates against parametric noise has been studied both in the Abelian [DP03] and in the non-Abelian case [So04]. In these papers, the effects of random perturbations of the control parameters are considered. It is worth noticing, however, that such effects are evaluated with the adiabatic limit already being performed, thus essentially confirming quantitatively the standard qualitative *geometric argument* usually adopted to support the robustness of holonomic gates, argument which was recalled in the previous chapter (see the section 2.7). We emphasize that, on the other hand, the operational time (in particular, the balanced working time) of a quantum gate is obviously always finite; hence, in principle, the mentioned geometric argument can be applied only with a certain degree of approximation in concrete devices. A critical analysis of this simple, but somewhat subtle, issue was the main contribution of the paper [Lu07'].

As holonomic gates are generally considered to be *a priori* robust against parametric noise, attention has mainly focused on the study of decoherence effects [Ca03, Ca04, Fu05, Pa06] and on the possibility of partially suppressing them [Wu05]. These investigations show that for certain physical systems, and for certain models and regimes of the coupling with the environment, one is able to estimate the typical time-scale within which the effects of decoherence can be neglected. Hence one can determine, in principle, a balanced working time for these systems. At this point, according to what has been observed above, one should actually *check* whether this balanced working time guarantees a suitable robustness of the quantum gate against parametric noise, namely, whether the effects of this kind of noise on the fidelity of the non-ideal quantum gate with respect to the ideal one can be neglected or not.

Recently, a new ingredient has been proposed for the implementation of a holonomic quantum gate [Fl06] (see also [Tr06, Fl06']). Indeed, some authors have observed — for the model of a ion-trap

---

[1]We recall that geometric phases arise also in the context of (non-adiabatic) cyclic evolutions [AA87, An88], but only *adiabatic* phases are relevant for our purposes.

geometric quantum gate proposed by Duan *et al.* [Du01], model which is also central in the present Dissertation — the existence of an *optimal working time*, namely, of a specific operational time for which the non-ideal (i.e. finite-time) gate behaves *exactly* as the ideal (i.e. adiabatic) gate; they show, furthermore, that over the optimal working time the effects of the environment are negligible. Thus, such a optimal working time turns out to be also a balanced working time. Again we stress that, anyway, the fact that the non-ideal gate behaves, in correspondence to the optimal working time, as the ideal one cannot be used to rule out the influence of parametric noise on the base of the standard geometric argument. Indeed, one should not expect that, perturbing the loop in the parameter space, the non-ideal gate will still mimic the behavior of the ideal one. Hence, once again, one cannot apply, in principle, the standard geometric argument to support the robustness of this kind of holonomic gate against parametric noise.

In the present chapter, we will try to illustrate this assertion by means of quantitative arguments, focusing on the ion-trap model proposed by Duan *et al.* [Du01].

3.2 Adiabatic versus finite time gates

The main aim of this section is to review critically the standard argument that is commonly used in the literature in order to support the robustness of holonomic gates against noise. As already stressed in the introduction, non-ideal holonomic gates — i.e., holonomy-based devices that can be concretely realized in a laboratory — must necessarily have a finite working time which should be short enough in order to avoid the perturbing effects of decoherence. This issue has been carefully analyzed in a recent paper [Fl06], where it is shown explicitly, on the base of a concrete model of adiabatic holonomic gate, that decoherence effects can prevent the possibility of achieving a faithful holonomic gate when the adiabatic limit is approached. This result is coherent with theoretical speculations (see [SL05, SL05+]) on the failure of the adiabatic theorem in presence of dissipative terms in the master equation governing the dynamics of the physical system implementing the quantum gate.

In [Fl06, Fl06'] it has been also shown that there may exist *specific* operational times ('optimal working times') for non-ideal holonomic gates allowing to obtain a high fidelity together with a good robustness against decoherence. It is then worth studying the robustness of non-ideal holonomic gates against instrumental noise.

Even though there are several approach to the adiabatic theorem (see for instance [BF28, Me62]), as a first step we will consider the Kato's proof of the adiabatic theorem [Ka51]. This proof was originally formulated in order to go beyond some limitations imposed by previous proofs [BF28], such as the requirement of a Hamiltonian with *non-degenerate* eigenvalues. However, the most remarkable idea in Kato's proof is the introduction of an *ideal evolution operator* — that we may call the 'Kato evolutor' — reproducing the typical adiabatic behavior of a quantum system; one can then prove that, under suitable hypotheses, in the proper limit the *real* evolution of the quantum system *coalesces* with the ideal adiabatic evolution.

In the standard construction of holonomic gates, a quantum system is considered with a Hamiltonian which depends on points $\mathbf{r}$ on a suitable manifold $\mathcal{M}$. For the sake of simplicity, here we consider the case in which the family of Hamiltonian functions $H(\mathbf{r})$ is isodegenerate with a pure discrete spectrum. A local set of coordinates $\{x^\mu\}$ on $\mathcal{M}$ plays the role of parameters that are supposed to be experimentally controllable. The control parameters are allowed to perform a cyclic evolution

in the operational time T

$$\gamma \mid t \in [0, T] \longrightarrow \mathbf{r}(t), \tag{3.1}$$

with $\mathbf{r}(T) = \mathbf{r}(0)$.

As usual, we define $s \equiv t/T$, in terms of this parameter the Schrödinger equation reads as follows:

$$\psi_T'(s) = -iTH(\mathbf{r}(s))\psi_T(s), \quad s \in [0, 1], \tag{3.2}$$

where we have re-defined $\mathbf{r}(s) \equiv \mathbf{r}(sT)$. Here and in the following $X'(s) \equiv dX(s)/ds$.

In view of the case study that will be considered below, we restrict our discussion to the special case in which the distinct eigenvalues of $H(\mathbf{r}(s))$ are a finite set and do not depend on time. In these hypotheses, the time dependent Hamiltonian has a spectral decomposition

$$H(\mathbf{r}(s)) = \sum_{l=0}^{n-1} \lambda_l P_l(s). \tag{3.3}$$

Where λ_l are all distinct eigenvalues and $P_l(s)$ are the corresponding instantaneous eigenprojectors, we also assume that the eigenprojectors are at least piecewise twice continuously differentiable for $s \in [0, 1]$. In the following we pick up one eigenprojectors, say P_0, that corresponds to the computational subspace that will be introduced below. In order to neglect an overall phase factor the dynamical contribution to the adiabatic transformation and to simplify the notation we set $\lambda_0 = 0$ and rename $P(s) \equiv P_0(s)$.

The solution of the Schrödinger equation (3.2) reads

$$\psi_T(s) = V_\tau(s)\psi_T(0). \tag{3.4}$$

$V_T(s)$ is the unitary operator which describes the dynamical transformation that obeys:

$$V_T'(s) = -iTH(\mathbf{r}(s))V_T(s), \tag{3.5}$$

with the initial condition $V_T(0) = \mathbb{I}$.

On the other hand, the adiabatic transformation is defined as a solution of the equation

$$U'(s) = iA(s)U(s), \tag{3.6}$$

where

$$iA(s) = [P'(s), P(s)] = P'(s)P(s) - P(s)P'(s). \tag{3.7}$$

The solution of (3.6) is completely determined once the initial condition is given. The solution $U(s)$, with the initial condition $U(0) = \mathbb{I}$, is unitary and has the property

$$P(s)U(s) = U(s)P(0). \tag{3.8}$$

This last relation indicates that $U(s)$ transforms isometrically the eigenprojector at initial time $P(0)$ onto the instantaneous eigenprojector $P(s)$. In order to look closely at the computational space, we consider the operator

$$W(s) \equiv U(s)P(0), \tag{3.9}$$

since $W(s)P(0) = U(s)P(0)$, $U(s)$ is equivalent to $W(s)$ when restricted on functions of the eigenprojector $P(0)$. It is easy to see that $W(s)$ obeys the equation

$$W'(s) = P'(s)W(s). \tag{3.10}$$

The adiabatic theorem states that the dynamical transformation, restricted to the eigenspace with eigenprojector $P(0)$, asymptotically approaches the adiabatic transformation. Since we are interested in the final transformation, defining $W \equiv W(1)$ and $V_T \equiv V_T(1)$, the following relation holds [Ka51]:

$$[V_T - W] P(0) = iV_T \sum_{l \neq 0} \frac{\Delta_l(T)}{\lambda_l T} ,$$ (3.11)

where

$$\Delta_l(T) = \left[V_T^\dagger(s) P_l(s) W'(s) \right]_0^1 - \int_0^1 d\sigma V_T^\dagger(\sigma) \left(P_l(\sigma) W'(\sigma) \right)'$$ (3.12)

It is easy to show [Ka51] that the operators $\Delta_l(T)$ are bounded uniformly with respect to T, i.e. there exists a positive number $M \in \mathbb{R}$ such that

$$\| V_T \Delta_l(T) \| \leq M,$$ (3.13)

where $\| \cdot \|$ indicates a suitable operator norm. Hence

$$\| [V_T - W] P(0) \| \leq M \sum_{l \neq 0} \frac{1}{|\lambda_l T|} .$$ (3.14)

Notice that $\Delta_l(T)$ depend on the gate operational time T through the unitary operator $V_T(s)$. Thus we can expect, before the asymptotic limit, an oscillatory behavior of a suitably defined gate fidelity as a function of T. The fidelity revivals described in [Fl06] are a particular case of this general oscillatory behavior at finite operational time.

Equation (3.10) defines a notion of parallel transport which corresponds to the adiabatic transformation. Let us choose a basis $\{\psi_\alpha(s)\}$ in the instantaneous subspace

$$P(s) = \sum_\alpha |\psi_\alpha(s)\rangle\langle\psi_\alpha(s)|.$$ (3.15)

The adiabatic connection is defined as follows [WZ84]:

$$A \equiv A_{\alpha\beta}(s) = \langle\psi_\beta(s)| \frac{d}{ds} \psi_\alpha(s)\rangle$$ (3.16)

The adiabatic transformation at the end of a loop in the parameter manifold can be written as $W = W_{\alpha\beta} |\psi_\beta(1)\rangle\langle\psi_\alpha(1)|$ and is obtained as the integral of the connection one-form ha s follows:

$$W = \mathbf{P} \exp -i \int_\gamma Ads ,$$ (3.17)

where $\mathbf{P}$ stands for the path ordered product. In a local chart $Ads = A_\mu dx^\mu$. By means of the (in general non-Abelian) Stokes' theorem, the holonomy is determined by the curvature tensor, whose component expression is

$$F_{\mu\nu} = \partial_\nu A_\mu - \partial_\mu A_\nu - [A_\mu, A_\nu] .$$ (3.18)

In most of the applications for quantum information tasks, the path ordered integral in (3.17) reduces to a simple exponential and the Abelian version of the Stokes' theorem can be applied:

$$W = \exp\left(-i \int_C F_{\mu\nu} dx^\mu \wedge dx^\nu \right) ,$$ (3.19)

where C is a region whose boundary is the loop γ. The usual argument in favor of the robustness of holonomic gates follows directly from expression (3.19). Since the integral of the curvature is supposed to depend weakly on the details of the loop, the adiabatic transformation is considered to be robust against a certain kind of *local* perturbations in the loop γ which weakly affect the integral in (3.19).

To conclude this section, we emphasizes that what is really needed in order to obtain a transformation with a geometrical character is a cyclic evolution of the eigenspace $(P(1) = P(0))$. The adiabatic theorem ensures that this cyclic evolution appears in correspondence with a loop in the parameters manifold in the adiabatic limit (hence in correspondence of a cyclic Hamiltonian). Only in this limit the argument of robustness of holonomic gate can be applied.

3.3 A case study

It was observed in [Fl06], that in particular situations the holonomic transformation appearing in the adiabatic limit can be mimed by a non-adiabatic holonomic transformation. That corresponds to a cyclic evolution attained in correspondence of an operational time T far before the adiabatic regime is reached.

That kind of situation was observed in [Fl06] with respect of one of the non-Abelian one-qubit holonomic gates which is part of the proposal for a fully geometric computation in [Du01] (see also the chapter 2 of the present Dissertation). We recall that the system under consideration is made of a single ion in a Pauli trap, which presents the following structure of stationary levels:

- A doubly degenerate low-energy level, which identifies a two-dimensional subspace which is used for encoding information. A computational basis $\{|0\rangle, |1\rangle\}$ is selected. These levels define the computational space of one qubit.

- A high-energy level, denoted $|e\rangle$.

- An ancillary, quasi degenerate level, which is denoted as $|a\rangle$.

All the transitions between the low-energy levels and the high-energy level are considered to be singularly addressed with resonant laser fields. A schematic picture is depicted in figure 3.1(a). The corresponding Hamiltonian, in the interaction picture and in the rotating frame, can be written as follows:

$$H = \Omega \left[x|0\rangle\langle e| + y|1\rangle\langle e| + z|a\rangle\langle e| + \text{h.c.} \right] . \tag{3.20}$$

In general, the Rabi's frequencies $\Omega x, \Omega y, \Omega z$ can take complex values, nevertheless, here we are interested in the case they are real-valued. The Hamiltonian in (3.20) is indeed a family of Hamiltonian functions depending on the real parameters x, y, z. Its spectrum is $\sigma = \{0, \pm\Omega\sqrt{x^2 + y^2 + z^2}\}$, with the vanishing eigenenergy which is doubly degenerate. The form of the spectrum suggests to introduce the constraint $x^2 + y^2 + z^2 = 1$ on the amplitude of the laser fields. With that constraint, one is dealing with a family of Hamiltonian functions which is defined on a two-dimensional sphere. Hence the control manifold is $\mathcal{S}^2$. Notice that, while the eigenenergies are constant functions on the two-sphere, the corresponding eigenprojectors depends on the values of the control parameters. Introducing polar coordinates, one can write an instantaneous eigenprojector $P(\vartheta, \varphi)$ corresponding to the doubly degenerate *dark* states. One can choose a corresponding basis in the degenerate space in
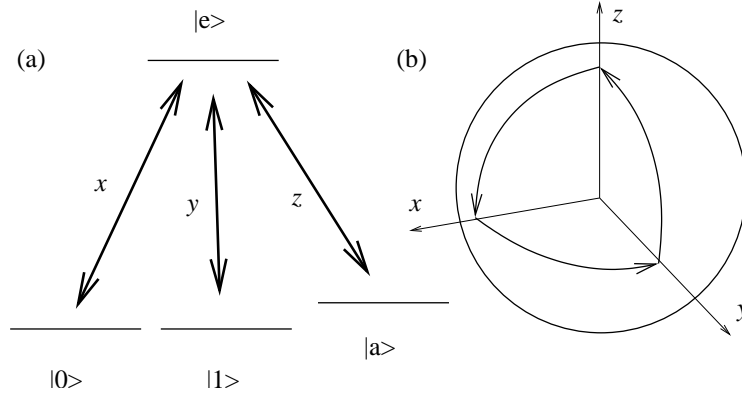
Figure 3.1: Structure of the atomic levels and resonant lasers (a); unperturbed loop (3.25) in the parameter manifold (b).

the following way:

$$\begin{cases} |\psi_0\rangle &= \cos\vartheta\,(\cos\varphi|0\rangle + \sin\varphi|1\rangle) - \sin\vartheta|a\rangle\,, \\ |\psi_1\rangle &= -\sin\varphi|0\rangle + \cos\varphi|1\rangle\,. \end{cases} \tag{3.21}$$

Notice that, for $\vartheta = 0, \pi$ (at the north and south pole), the computational space is uncoupled and the dark states corresponds to the computational basis, namely $|\psi_0\rangle = |0\rangle$ and $|\psi_1\rangle = |1\rangle$. These points can be used as starting points for the system evolution.

As one can check immediately, the connection one-form has the following, matrix valued form:

$$A \equiv A_{\alpha\beta} = -i\langle\psi_\alpha|d\psi_\beta\rangle = -\cos\vartheta\sigma_{y_{\alpha\beta}}, \tag{3.22}$$

where σ_y is the Pauli matrix in the computational basis $\{|0\rangle, |1\rangle\}$. Hence, after an adiabatic excursion of the control parameters along a closed path on the control manifold, one obtains the transformation in the computational space

$$|\psi_{\mathrm{in}}\rangle \longrightarrow |\psi_{\mathrm{out}}\rangle = W|\psi_{\mathrm{in}}\rangle \tag{3.23}$$

with

$$W = \exp\left(-i\omega\sigma_y\right) \tag{3.24}$$

where ω is the solid angle spanned by the loop in the parameters' spaces.

Here we consider the closed path in the parameter manifold that was studied in [Fl06]. For $s \in [0, 1]$ we take (see figure 3.1(b)):

$$\begin{aligned} \vartheta(s) &= \begin{cases} 3s\pi/2 & s \in [0, 1/3] \\ \pi/2 & s \in [1/3, 2/3] \\ 3\pi/2\,(1-s) & s \in [2/3, 1] \end{cases} \\ \varphi(s) &= \begin{cases} 0 & s \in [0, 1/3] \\ 3\pi/2\,(s - \frac{1}{3}) & s \in [1/3, 2/3] \\ \pi/2 & s \in [2/3, 1] \end{cases} \end{aligned} \tag{3.25}$$

The solid angle related to the loop (3.25) is $\omega = \pi/2$, hence the corresponding holonomic gate is $W = -i\sigma_y$. As was observed in [Fl06], the remarkable property of this path is that it presents perfect revivals of the gate fidelity at finite operational time. The same behavior was predicted for all the

55

loops constructed by moving from the north pole to the equator through a meridian and back to the north pole through another meridian with piecewise constant velocity. In the case of the loop (3.25) there is a perfect revival of fidelity in correspondence of the operational times:

$$T_k^* = \frac{3\pi}{2\Omega}\sqrt{16k^2 - 1}, \ \ k = 1, 2, \ldots \tag{3.26}$$

In the following we are mostly concerned with the first optimal operational time $T^* = T_1^*$.

To conclude this section we notice that a geometric phase appears in correspondence to a non adiabatic *cyclic* dynamics [AA87, An88]. In particular, for our case study, it happens that, in correspondence to an optimal operational time, the evolution becomes cyclic and the acquired geometric phase is equal to the adiabatic holonomy.

3.4 Models of parametric noise and perturbation

In order to study the robustness of non ideal holonomic gates, we consider the response of the system under parametric noise in the ideal loop (3.25). In order to quantify the robustness of the gate, the noisy finite time evolution of the system is solved with numerical methods and the average gate fidelity (see the appendix B) is calculated. In the following, several models of noise are taken into account: in section 3.4.1 we consider the response of the system under a monochromatic perturbation of the three Rabi frequencies in (3.20); in section 3.4.2 we discuss the response of the system under a telegraphic perturbation in the three Rabi frequencies. An additional model was also discussed in [Lu07'], leading to analogous results.

3.4.1 Monochromatic perturbation

In this section we consider the behavior of the system in the presence of a small random perturbation in the control parameters. As a first approach to the problem of the robustness of the non-adiabatic holonomic gate, we consider a simple monochromatic perturbation instead of a more realistic model for the parametric noise. That kind of perturbation can be viewed as a small *probe* function used to test the stability of the gate. A generic noisy path can be written as follows:

$$\mathbf{r}_{\mathrm{n}}(t) = \mathbf{r}(t) + \epsilon(t), \ \ t \in [0, T], \tag{3.27}$$

where the vector $\mathbf{r}(t)$ describes the unperturbed loop and $\epsilon(t)$ is a three component vector including the perturbation of the path. We have chosen a monochromatic perturbation at frequency η and considered a noisy path obtained from (2.118) and (3.25):

$$\begin{cases} x_{\mathrm{n}}(s; \eta, \epsilon_\eta, T, \phi_1) &= x(s) + \epsilon_\eta e^{i\eta T s + i\phi_1} \\ y_{\mathrm{n}}(s; \eta, \epsilon_\eta, T, \phi_2) &= y(s) + \epsilon_\eta e^{i\eta T s + i\phi_2} \\ z_{\mathrm{n}}(s; \eta, \epsilon_\eta, T, \phi_3) &= z(s) + \epsilon_\eta e^{i\eta T s + i\phi_3} \end{cases} , \tag{3.28}$$

where $\mathbf{r}_{\mathrm{n}}(s) \equiv (x_{\mathrm{n}}(s), y_{\mathrm{n}}(s), z_{\mathrm{n}}(s))$, $\phi \equiv (\phi_1, \phi_2, \phi_3)$ are random initial phases uniformly distributed in $[0, 2\pi)$ and ϵ_η is the strength of the noise (chosen to be equal for the three component). Notice that this model of noise acts on both the amplitude and the de-tuning of the lasers. Strictly speaking, it does not preserve the control manifold, since it is incompatible with the constraint of real valued Rabi's frequencies in the Hamiltonian (3.20). From (3.28), it is clear that at finite operational time the perturbation does *not* reduces to a geometric perturbation of the loop in the parameters space
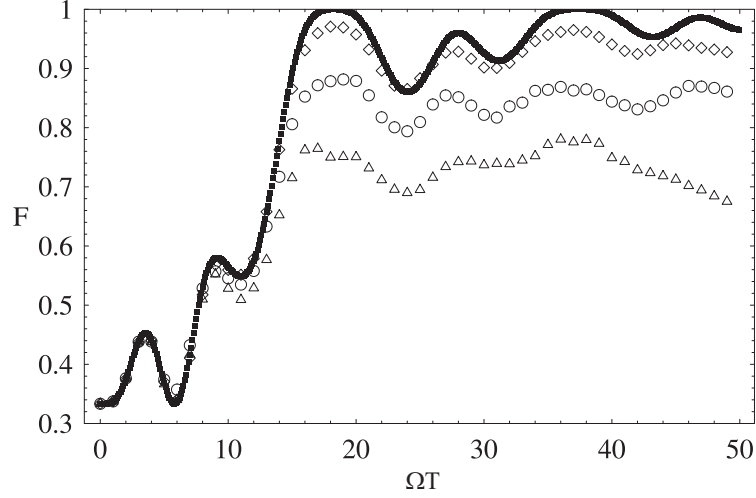
Figure 3.2: Average gate fidelity as a function of the adimensional operational time ΩT for several noise frequencies for the model in section 3.4.1. Black boxes: $\epsilon_\eta = 0$; circles: $\epsilon_\eta = 0.1\Omega, \eta = 0.1\Omega$; triangles: $\epsilon_\eta = 0.1\Omega, \eta = 0.2\Omega$; squares: $\epsilon_\eta = 0.1\Omega, \eta = 0.3\Omega$.

since the perturbed path itself depends on the operational time. In the presence of the noise, different values of the operational time T correspond to different loops in the parameters manifold.

For given values of η, ϵ_η, T and ϕ, we consider the solution of the Schrödinger equation

$$V'_T(s; \eta, \epsilon_\eta, \phi) = -iTH(\mathbf{r}_n(s))V_T(s; \eta, \epsilon_\eta, \phi), \quad s \in [0, 1]. \tag{3.29}$$

where, in presence of noise, the re-scaled Hamiltonian $H(\mathbf{r}_n(s))$ depends on T too. Since we are mainly interested in the transformation emerging at the end of the loop, we set $V_T(\eta, \epsilon_\eta, \phi) \equiv V_T(1; \eta, \epsilon_\eta, \phi)$.

Notice that, for all practical purposes, taking the average on the random phases corresponds to the action of the completely positive map

$$\rho \longrightarrow \mathcal{E}(\rho) = \frac{1}{(2\pi)^3} \int d\phi V_T(\eta, \epsilon_\eta, \phi)\rho V_T(\eta, \epsilon_\eta, \phi)^\dagger . \tag{3.30}$$

This completely positive map has to be compared with the ideal adiabatic unitary dynamics. To do that, we have evaluated the average gate fidelity by means of the formula in [Ni02] (see equation B.7 in the appendix B).

For several values of η, ϵ_η and ϕ, equation (3.29) is numerically solved using the relation:

$$V_T(\eta, \epsilon_\eta, \phi) = \lim_{N \to \infty} \overset{\leftarrow}{\prod}_{k=0...N} \exp\left[-i\tau H(\mathbf{r}_n(k/N))\frac{1}{N}\right] , \tag{3.31}$$

where $\overset{\leftarrow}{\prod}$ stands for the path ordered product. The effective completely positive map (3.30) is evaluated taking the average over 50 or more choices of the initial phases ϕ. Figure 3.2 shows the estimated average gate fidelity plotted as a function of the adimensional operational time ΩT, for several values of the noise amplitude and frequency. The unperturbed dynamics corresponds to $\epsilon_\eta = 0$ and can be compared with the analytical results in [Fl06], it exhibits perfect revivals of the average gate fidelity at finite time, in particular the first optimal operational time is at $\Omega T_1^* \simeq 18.25$. The numerical results show that the pattern of the gate fidelity as a function of the operational time can be completely different in presence of noise.
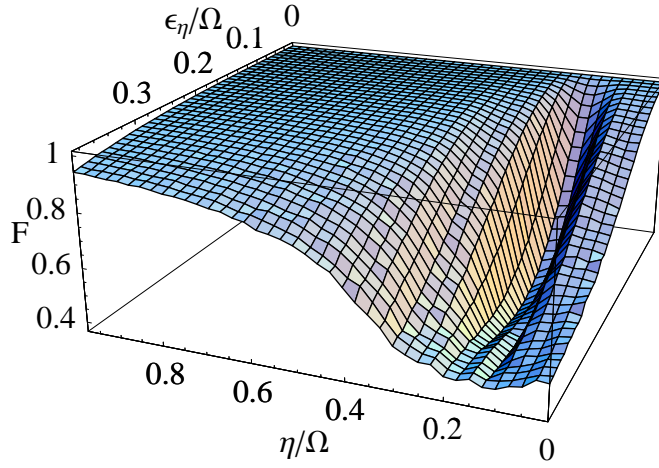
Figure 3.3: Average gate fidelity at the first optimal operational time as a function of adimensional noise frequency (η/Ω) and amplitude (ϵ_η/Ω) for the model in section 3.4.1.

The average gate fidelity at the first optimal operational time T_1^* in the presence of parametric noise is plotted in the figure 3.3 as a function of both amplitude and frequency of the noise. This plot suggests that the gate can indeed present high fidelity also for rather large noise amplitude ($\epsilon_\eta = 0.4\Omega$). It is worth to notice that this is true unless the perturbation frequency is in a particular range approximatively about $\eta \simeq 0.15\Omega$. The presence of a typical frequency scale in the pattern of the fidelity is a feature that will be reencountered in the other models of noise considered below.

We have also studied, with the same methods, the response of the system in presence of analogous perturbations which have different symmetries. We have considered the case in which only the real part of (3.28) is taken; in this case the perturbation acts only in the amplitude of the coupling but not in the de-tuning. The corresponding average gate fidelity at the first optimal operational time is plotted in figure 3.4. We have also analyzed the case of a perturbation which is square wave shaped; in this case a *probe* function is identified by its half period and initial phase. Also in this case, the corresponding pattern of the average gate fidelity is exactly analogous to the one shown in figure 3.3 and 3.4. That leads to the conclusion that the pattern of fidelity is largely independent of the details of the chosen probe function and a rather general behavior as function of the typical frequency is observed.

Analogous results are also found for other loops of the same kind, such as the loop with the angle φ varying from 0 to $\pi/4$ in (3.25) which is related to the Hadamard gate.

3.4.2 Telegraphic noise

In this section, we consider a more realistic model for a noisy perturbation. Here we study the robustness of the non-adiabatic holonomic gate in attained correspondence of the first optimal operational time T^* in the presence of a telegraphic noise acting on the control parameters.

Taking in consideration the ideal loop (3.25), here we study the noisy paths of the following kind:

$$\begin{cases} x_{\mathrm{n}}(s; \tau_{\mathrm{step}}, \epsilon, T) &= x(s) + \xi_1(s, \tau_{\mathrm{step}}, T) \\ y_{\mathrm{n}}(s; \tau_{\mathrm{step}}, \epsilon, T) &= y(s) + \xi_2(s, \tau_{\mathrm{step}}, T) \\ z_{\mathrm{n}}(s; \tau_{\mathrm{step}}, \epsilon, T) &= z(s) + \xi_3(s, \tau_{\mathrm{step}}, \tau) \end{cases} \quad , \tag{3.32}$$
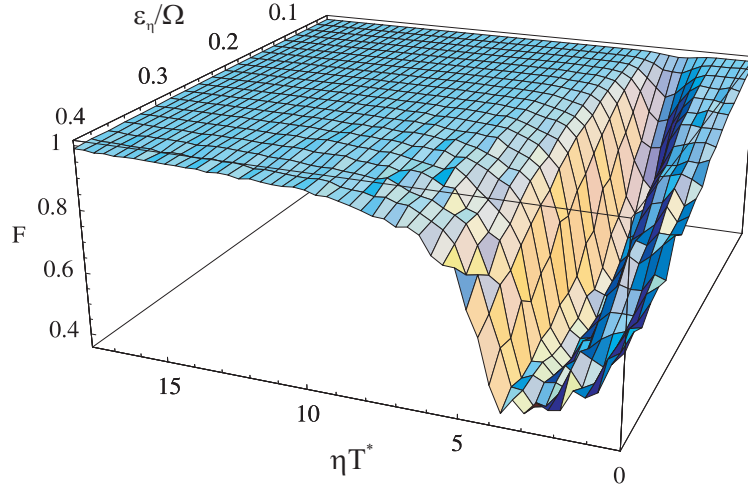
Figure 3.4: Average gate fidelity as a function of both the average number of independent fluctuation of the noise $N = \eta T^*$ and the amplitude of the noise ε for a monochromatic perturbation (section 3.4.1), that affects only the amplitude of the fields, in correspondence with the first optimal operational time ΩT.

where $\xi_i(s, \tau_{\text{step}}, T) \in [-\epsilon, \epsilon]$ are three real random variables, uniformly distributed in the chosen interval, which are piecewise constant for $(j-1)\tau_{\text{step}} \le sT \le j\tau_{\text{step}}$.

Hence, the model of noise considered here is characterized by two parameters: its amplitude ϵ, and the typical time τ_{step}. The corresponding two-times correlation function presents an exponential decay $C(t, s) \simeq e^{-\Gamma|t-s|}$ for $|t - s| \le \tau_{\text{step}}$, where the correlation time is of the order of typical time of the noise mode, namely $\tau = \Gamma^{-1} \simeq \tau_{\text{step}}$.

It is interesting to compare the behavior of the gate at the first optimal operational time to the case of longer operational time in presence of noise. It is possible to see [Fl06, Fl06'] that the fidelity oscillations shown in figure 3.2 in absence of noise are strongly suppressed if $k \ge 3$ in equation (3.26) (we are near the adiabatic regime). A good approximation of the adiabatic regime can be already obtained for the fourth optimal operational time.

In order to study the behavior of the gate at finite operational time, we have evaluated the average gate fidelity for a fixed value of the noise amplitude $\epsilon = 0.1\Omega$ as a function of the noise typical frequency $(\Omega\tau_{\text{step}})^{-1}$ in correspondence of the first four optimal working times (the forth operational time corresponds to $\Omega T_4^* \simeq 75.21$) in the same range of values for the ratio $(\Omega\tau_{\text{step}})^{-1}$ between the noise typical frequency and the system typical frequency. The results are shown in figure 3.5. The data plotted in this figure lead us to formulate two kind of considerations: first of all we notice again the unexpected result that the non-adiabatic optimal working times (the first, for instance) appears to be more robust than longer operational times (the forth optimal operational time, for instance); secondly, we observe the same qualitative behavior of the pattern of fidelity for all the optimal operational times under study, that suggests the presence of a common mechanism which account for the cancelation of the effects of the noise.

In apparent contrast to the intuition related to the usual argument of robustness of holonomic gates we notice that, in the same range of frequencies of the non adiabatic case (and, therefore, for a larger number of fluctuations), F reaches lower values. Moreover, the adiabatic gate needs higher values of the frequency of noise for recovering the ideal behavior. We conclude that the (approximately)
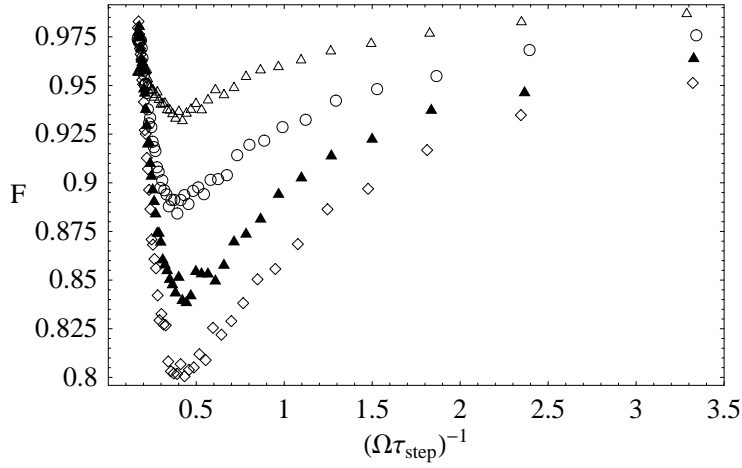
Figure 3.5: Average gate fidelity as a function of the noise typical frequency for the noise model in section 3.4.2 for the first four optimal operational times. Triangles, circles, full triangles and squares correspond respectively to the first, second, third and fourth optimal operational time. $\epsilon = 0.1\Omega$.

adiabatic (purely geometric) NOT transformation is more sensitive to parametric noise than the non-adiabatic one.

The average gate fidelity ia also plotted in figure 3.6 as a function of both the operational time and the number of fluctuations of the noise (hence for different values of the parameter τ_{step}) for a fixed value of the noise amplitude.

We have also analyzed the case of a noise which include de-tuning by considering complex random variables $\xi_i(s, \tau_{\text{step}}, T)$. The result are completely analogous and the introduction of a noise in the de-tuning does not introduce new elements in the pattern of fidelity.

3.5 Analysis of the results

The aim of this section is to furnish a physical explanation for the observed behavior of the average gate fidelity. Due to the fact that all the models of noise induce the same qualitative behavior of the fidelity, in the following we are going to consider in more details the model presented in section 3.4.2.

As already recalled, the relevant parameter for the geometrical cancelation usually related to holonomic gates in the adiabatic regime is the number of fluctuations of the noise during the gate operational time (denoted N). This effect is related only to the swept solid angle and is independent of the chosen operational time. If the number of cycles of the noise is large enough, the fluctuations in the solid angle spanned by the loop are expected to become negligible. To be more specific. let us suppose that, after a noisy loop, the swept solid angle is ω and the mean square over the realizations of the noise is $\langle \Delta\omega^2 \rangle$. In figure 3.7 the mean square is plotted as a function of the number of cycles of the noise; since, in the adiabatic limit, the gate depends only on the swept solid angle, the fluctuations of the gate are expected to have the same behavior as the fluctuations in the solid angle.

As already explained in the previous section, figure 3.5 shows the average gate fidelity as a function of the adimensional typical noise frequency $(\Omega\tau_{\text{step}})^{-1}$ for several values of the evolution time which correspond to the first four optimal operational times. The plot shows an analogous behavior of the fidelity as a function of the typical noise frequency *independently* of the particular value of the operational time; moreover, the minimum of the fidelity is reached in correspondence of
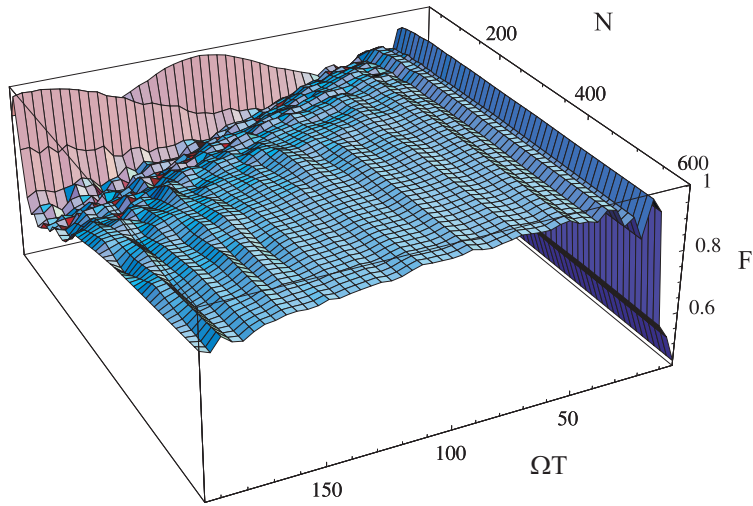
Figure 3.6: Average gate fidelity as a function of both the average number of independent fluctuation of the noise N and the operational time ΩT, for the telegraphic noise with real components discussed in the section 3.4.2. The amplitude of the noise is $\epsilon = 0.1\Omega$
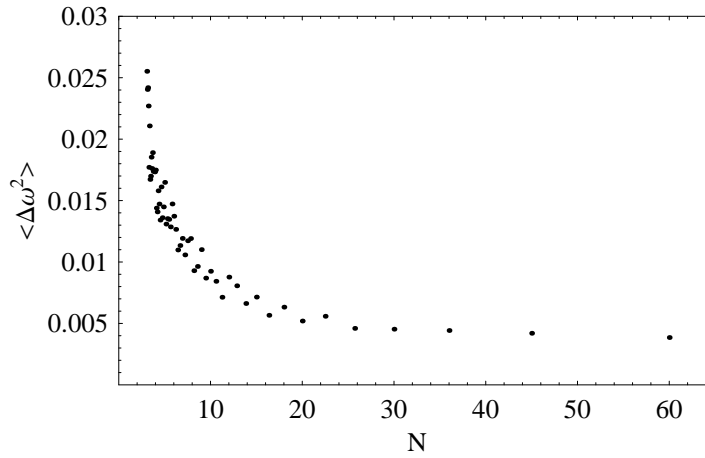
Figure 3.7: Fluctuations in the solid angle spanned by a noisy loop as a function of the number of perturbations of the noise N, for the noise model in section 3.4.2. $\epsilon = 0.1\Omega$.
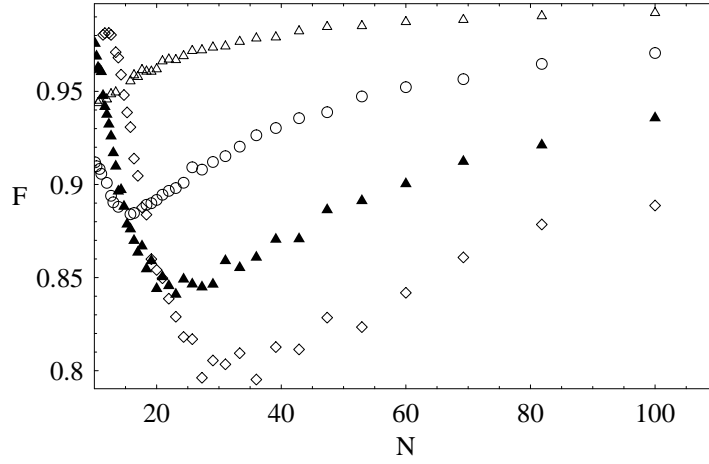
Figure 3.8: Average gate fidelity as a function of the number of fluctuations of the noise N for the noise model in section 3.4.2 for the first four optimal operational times. Triangles, circles, full triangles and squares correspond respectively to the first, second, third and fourth optimal operational time. $\epsilon = 0.1\Omega$. Compare with figure 3.5 and 3.7.

$(\Omega\tau_{\text{step}})^{-1} \simeq 0.5$ for all the considered values of the operational time. In order to cast some light on the nature of the cancelation effect, the same data are plotted in figure 3.8 as functions of the number of fluctuations of the noise (notice that $N = \Omega T (\Omega\tau_{\text{step}})^{-1}$). A direct comparison of figures 3.5 and 3.8 suggests that the relevant quantity which accounts for the mechanism of cancelation of the effects of the noise is its typical frequency $(\Omega\tau_{\text{step}})^{-1}$ and *not only* the number of fluctuations N. On the other hand, the fluctuations of the solid angle around the ideal value $(\pi/2)$ start to be negligible for $N > 20$; a comparison with the curve for the fourth optimal working point (squares in figure 3.8) suggests that the recovery of the fidelity for long cyclic evolution times is given also by geometric cancelation.

For non adiabatic evolution times one can imagine the existence of a different mechanism which accounts for the observed cancelation of the noise effects for sufficiently fast noise which is related to a *dynamical* instead of geometrical cancelation. A dynamical effect could not be directly related to the swept solid angle: in this case the relevant parameter is expected to be the typical time of the noise τ_{step} and a dynamical cancelation of the noise should appear if its typical frequency is sufficiently large compared to the system frequency, namely $(\Omega\tau_{\text{step}})^{-1} \gg 1$. Of course this condition implies, for fixed operational time T, that $N \gg 1$ (the usual condition for geometric cancelation); nevertheless, as figure 3.5 shows, a cancelation of the noise effects appears on a frequency scale $(\Omega\tau_{\text{step}})^{-1} \simeq 1$ *independently* of the chosen value of the operational time, thus suggesting a dynamical mechanism for the noise cancelation at least for the first four optimal operational times.

The fact that in the non adiabatic regime the robustness has a dynamical origin can also explain why the minimum value of the fidelity tends to decrease for increasing values of T^*: if the geometric cancelation is not present, the noise is less effective in disturbing the system when the evolution time is short.

3.6 Final comments

In this chapter we have considered the influence of parametric noise on the efficacy of a non-adiabatic holonomic gate which is expected to be robust in the ideal (adiabatic) case. Two models of parametric noise or disturbance have been discussed in the case of finite operational time. The average gate fidelities for all the models of noise considered here present an analogous qualitative behavior. For each of the three models the non-ideal gate presents a breakdown of the average gate fidelity for small frequencies of the noise (compared to the system Bohr frequency), while a high value of the fidelity is reached for noise with higher frequencies. This can lead to say that the presence of a "resonant frequency" for the breakdown of F is a rather general feature in the presence of parametric perturbations.

We want to stress again that the usual argument in favor of the robustness of holonomic quantum computation is based on the purely geometric nature of the holonomy group that describes the adiabatic transformations. Since the dynamics has a *completely* geometric character *only* in the adiabatic limit, the robustness of adiabatic gates is, in this sense, just a consequence of the adiabatic theorem. Despite these considerations, our calculations show that, at least in certain situations, the first optimal operational time can be preferable to longer operational times with regards to the robustness of the corresponding gate against parametric noise.

Nevertheless, our results lead to the conclusion that the observed revivals of the fidelity for sufficiently fast noises is mainly due to *dynamical* instead of geometrical effects. Our conclusion is that, in the range of operational times considered here, the observed cancelation effects are mainly related to a dynamical average over fast oscillations of the noise $(\Omega\tau_{\text{step}})^{-1} \gg 1$ and there is no relevant connection with the 'geometric' robustness of the swept solid angle which plays a crucial role for the usual argument in favor of robustness of the holonomic computation in the adiabatic regime.

In other words, not only the loop in the parameter space is non-adiabatic in correspondence of the optimal working giving rise to a non-adiabatic holonomy, but also the noise fluctuations cannot be adiabatic since the operational time is not long enough. In that setting, one can observe an effect of cancelation which correspond to an opposite situation with respect to the usual adiabatic-noise setting. The transformation is indeed robust if the noise is much faster than the the typical system time-scale. While in the adiabatic case the geometric cancelation happens when the noise is adiabatic with respect to the system dynamics, in the non-adiabatic case the dynamical cancelation appears when the system internal dynamics is adiabatic with respect of the fluctuations of the noise.

Chapter 4

Robustness of geometric phases: A toy-model

In the chapter 2, we have presented the *holonomic approach* to quantum computation and the argumentation that is commonly used to state its *robustness* with respect to *parametric noise*. In the chapter 3, we have studied the robustness of a non-adiabatic holonomic gate, described its behavior and compared it to the standard argument which can be applied only to adiabatic gates.

The aim of the present chapter is to consider the standard argument in favor of the robustness of holonomic gates in the presence of parametric noise and analyze it in *further details*. It is important to notice that the robustness argument of holonomic computation is *neither* strictly related to any peculiar properties of quantum mechanics, *nor* to any details of the physical system under consideration. The only ingredient which enters in the argument of robustness of holonomic gates is the *geometric nature* of the holonomic transformation. That geometric behavior physically appears in the adiabatic limit, in which the dynamical transformation is described by a holonomy.

For that reason, in this chapter we discuss a simple *toy-model* which represents the simplest physical set in which a holonomy phenomenon can appear. That simple model is a system composed of a semiclassical charged particle which is constrained to move in a plane in the presence of a transverse stationary *magnetic field*. It is worth noticing that that is essentially equivalent to the case of a particle confined in a box which is moved around a line of magnetic flux, example that was originally discussed in [Be84]. Using that model, we can easily study the robustness of the holonomic transformation and obtain general indications about the robustness of holonomic computation in the more interesting situations.

4.1   Geometric phase in the simplest setting

The *standard argument* in favor of the robustness of holonomic gates under parametric noise is a simple *geometric* argumentation which, by itself, has *nothing to do* with quantum mechanics and with the peculiar features of the physical system which implements the holonomic computation. For these reasons, in this section we will concentrate on *the simplest example* in which the geometric argument can be applied, namely a system composed of a *semiclassical* particle moving in a static magnetic field. The interest here is on the *statistical* properties of the area of the surface spanned by a noisy loop. The fact that it is physically related to the phase acquired by the particle gives us a physical motivation to study this system but, by itself, that does *not* play any particular role in our context.

So, let us consider a semiclassical particle endowed with an electric charge q which is constrained to move in the plane, in the presence of a transverse static magnetic field. Let us also suppose that the position of the particle can be experimentally *controlled*, and the particle is constrained to move along a given closed loop:

$$\gamma \ : \ s \in [0,1] \ \longrightarrow \ \gamma(s) \tag{4.1}$$

with $\gamma(1) = \gamma(0)$. We consider a situation in which the particle is allowed to move along the path in the *operational time* T. Hence, in the time interval $t \in [0,T]$, the position of the particle a time t is given by $\gamma(t/T)$.

Also, we suppose that the particle is in an *internal* stationary level, with corresponding energy E_0. If initially the particle is in the state $|\psi_0\rangle$, at the end of the loop it will be in

$$|\psi\rangle = e^{-i\Phi}e^{-iE_0 T}|\psi_0\rangle \ . \tag{4.2}$$

Where the acquired phase factor is the product of two terms: the *dynamical* part $e^{-iE_0 T}$, and the *geometric* part $e^{i\Phi}$. The latter is given by the flux of the magnetic field through the surface spanned by the loop:

$$\Phi = q \int_S B dS = qB\mathcal{S} \ , \tag{4.3}$$

where S is the surface spanned by the loop, and $\mathcal{S}$ is its oriented area. Equivalently, it can be written by means of the line integral of the gauge potential:

$$\Phi = q \oint_\gamma A \ . \tag{4.4}$$

In order to focalize on geometric aspects, one has to neglect the dynamical contribution to the overall phase factor. That can be obtained, for instance, working in a gauge with a vanishing ground state energy, namely $E_0 = 0$.

One can notice that that simple toy-model is essentially equivalent to the system originally considered by Michael Berry in [Be84], where he described the geometric phase acquired by a charged particle confined in a box which is adiabatically moved around a line of magnetic flux. The holonomy transformation induced at the end of the loop is mainly independent of the details of the path, but depends on a global quantity which is the integral in (4.4). In other words, if we consider a perturbed path

$$\gamma_n(t) = \gamma(t/T) + \epsilon(t) \ , \tag{4.5}$$

the argument of the geometric phase changes in

$$\Phi \ \longrightarrow \ \Phi_n = \int_{\gamma_n} A \ . \tag{4.6}$$

The acquired phase factor will remain unchanged *if* the perturbation *preserves* the integral:

$$\int_{\gamma_n} A = \oint_\gamma A \ . \tag{4.7}$$

By virtue of the Stokes' theorem, one can write

$$\int_{\gamma_n} A = B\mathcal{S}_n \tag{4.8}$$

where $\mathcal{S}_n$ indicates the oriented area of the surface S_n spanned by the *noisy path*. Thus, if one is dealing with a perturbation which *preserves* the area of the surface spanned by the loop — i.e. $\mathcal{S}_n = \mathcal{S}$ — the holonomy associated to the loop remains unchanged.

It is worth noticing, however, that in the presence of the noise, the path might not be closed, leading to a *gauge not-invariant* integral in (4.8). What is needed is a rule to define the geometric phase for a non-closed loop or, in other words, one needs a rule to close the path. Taking inspiration by the work of Pancharatnam [Pa56] about phases in classical optics, one can for instance use the *geodesic* rule to close the open loop (see [SB88, DP03] and the chapter 2). Obviously, that kind of approach can be meaningful only locally, that is to say, only for small amplitude of the noise.

On the other hand, one can argue that the fact that the path is non-closed gives rise to an *additional source of error* in the corresponding geometric phase, the error depending essentially on the chosen rule used to close the loop. For non-pathological potentials and for a small amplitude of the perturbation, the error in the evaluation of the integral along the open path is expected to be proportional to the *square* of the amplitude of the noise and, in particular, to be *independent* of the number of fluctuations of the noise during the time evolution.

Let us now consider the following situation. The particle is externally driven in order to follow the given loop γ. Nevertheless, the experimental control on the particle position is not perfect. As an physical example, one can imagine that the particle is immersed in a classical fluid. That yields an additional component in the particle position that can be treated as a Brownian motion which is superimposed to the unperturbed loop.

A perturbation in the loop can be modeled as a stochastic process $\epsilon(t)$, which can be characterized by its correlation functions. For the case of a Markov process, one can consider the two-times correlation function

$$C(t, s) = \langle \epsilon(t)\epsilon(s) \rangle \tag{4.9}$$

and the corresponding correlation time τ. In the case of a stationary process with exponentially decaying correlation function:

$$C(t, s) \simeq e^{-K|t-s|}, \tag{4.10}$$

the correlation time is defined as the inverse of the real part of K, namely $\tau \equiv \Re(K)^{-1}$. If the noisy loop is *drawn* by the particle in an operational time T, the ratio $N = T/\tau$ can be interpreted as the *average number of statistically independent fluctuations* of the noise during the operational time. In this setting, the heuristic argument of robustness of holonomic gates says that if $N \gg 1$ — i.e. if the correlation function of the noise decays *fast enough* compared with the operational time — the changes in the area of the surface spanned by the loop are negligible, that is to say: $\mathcal{S}_n \simeq \mathcal{S}$. In order to develop the analysis of the phase acquired in the noisy case, one needs to be more specific, hence considering suitable models for the noise and selecting a specific loop.

4.2 Geometric phase in the presence of parametric noise

In this section, we will discuss the behavior of the simple geometric evolution of our toy-model in the presence of several kinds of parametric perturbations and noises.

The setting is the following. The dynamics of the particle in the operational time T is associated with the unperturbed loop

$$\gamma(t/T) = (x(t), y(t)) \ . \tag{4.11}$$

To fix the ideas and for the sake of simplicity, here we select two different sample loops:

- The first sample loop has the shape of a *square*, namely:

$$
\begin{aligned}
t \in [0, T_a] \quad &\longrightarrow \quad
\begin{cases}
x(t) &= x_0 + t/T_a \\
y(t) &= y_0
\end{cases} \\
t \in [T_a, 2T_a] \quad &\longrightarrow \quad
\begin{cases}
x(t) &= x_0 + 1 \\
y(t) &= y_0 + (t - T_a)/T_a
\end{cases} \\
t \in [2T_a, 3T_a] \quad &\longrightarrow \quad
\begin{cases}
x(t) &= x_0 + 1 - (t - 2T_a)/T_a \\
y(t) &= y_0 + 1
\end{cases} \\
t \in [3T_a, 4T_a] \quad &\longrightarrow \quad
\begin{cases}
x(t) &= x_0 \\
y(t) &= y_0 + 1 - (t - 3T_a)/T_a \ ,
\end{cases}
\end{aligned}
\tag{4.12}
$$

where $T = 4T_a$ is the operational time corresponding to the *whole loop*.

- The second loop has the shape of *circle*, namely:

$$
t \in [0, T] \longrightarrow
\begin{cases}
x(t) &= x_0 + \frac{1}{\pi} \cos\left(2\pi t/T\right) \\
y(t) &= y_0 + \frac{1}{\pi} \sin\left(2\pi t/T\right) \ .
\end{cases}
\tag{4.13}
$$

Notice that, in both cases, the loops span a surface with oriented area $\mathcal{S} = 1$. Hence the corresponding phase, acquired by the charged particle, is equal to e^{iqB}. One can consider a noise with components

$$
\epsilon(t) \equiv (\epsilon_x(t), \epsilon_y(t)) \ ,
\tag{4.14}
$$

to which the following noisy path is associated:

$$
\gamma_n(t) = \gamma(t) + \epsilon(t) = (x(t) + \epsilon_x(t), y(t) + \epsilon_y(t)) \ .
\tag{4.15}
$$

The noisy phase (4.6) can be expanded in the following way:

$$
\begin{aligned}
\Phi_n = \int_{\gamma_n} y dx &= \int_0^T (y(t) + \epsilon_y(t))(dx(t) + d\epsilon_x(t)) \\
&= \oint_\gamma y dx + \int_0^T \epsilon_y(t) dx(t) + \int_0^T y(t) d\epsilon_x(t) + \int_0^T \epsilon_y(t) d\epsilon_x(t) \ .
\end{aligned}
\tag{4.16}
$$

One can recognized the unperturbed integral:

$$
\Phi_0 = \oint_\gamma y dx \ ,
\tag{4.17}
$$

two perturbative contributions of the *first order* in the noise amplitude:

$$
\Phi_1 = \int_0^T \epsilon_y(t) dx(t) \ ,
\tag{4.18}
$$

and

$$
\Phi_2 = \int_0^T y(t) d\epsilon_x(t) \ ,
\tag{4.19}
$$

and one term which is of the *second order* in the noise amplitude:

$$\Phi_3 = \int_0^T \epsilon_y(t) d\epsilon_x(t) . \qquad (4.20)$$

Each of these perturbative terms, a well as the whole perturbed phase, are defined as stochastic integral.

The section is now divided in three subsections: in the first subsection we consider a monochromatic perturbation acting on the coordinates of the charged particle; in the second one we analytically examine the behavior of the considered toy-model in the presence of a more realistic source of noise which is modeled by a continuous stochastic process (a Ornstein-Uhlenbeck process, see for instance [Ga83]); finally in the third subsection, we present some numerical calculations corresponding to two different models for the noisy component, a Ornstein-Uhlenbeck process and a telegraphic noise. All the calculations, both analytical and numerical, are done in the asymmetric gauge

$$A \equiv -B \, y \, dx . \qquad (4.21)$$

4.2.1 A monochromatic perturbation

Prior to consider a more realistic model of perturbation, in this section we describe the behavior of the geometric phase in the presence of a simple, monochromatic perturbation. The following discussion can look rather academic, nevertheless, it will turn to be useful to understand the main features appearing in correspondence with the slightly more elaborated and probably more realistic situations that will be described in the following sections.

Let us take in consideration the sample unperturbed path which has the shape of a square, performed with piecewise constant velocity. The operational time, needed by the particle to move along the loop, is indicated with T, while the time needed to move along one of the segments of the loop is $T_a = T/4$.

For the sake of simplicity, we consider a perturbed path in which the perturbation acts only on one of the segments that compose the loop. With reference to the square-shaped loop defined in (4.12), we take in consideration the following perturbed loop:

$$\gamma_n(t) = \begin{cases} \gamma(t/T) & \text{for} \quad t \in [0, T_a] \\ \gamma(t/T) + \epsilon(t) & \text{for} \quad t \in [T_a, 4T_a] . \end{cases} \qquad (4.22)$$

Hence, the perturbation is *turned on* only in correspondence of the first segment of the squared loop.

The monochromatic perturbation is written in the following form:

$$\begin{cases} \epsilon_x(t) & = & \varepsilon \cos(\eta t + \phi_x) \\ \epsilon_y(t) & = & \varepsilon \cos(\eta t + \phi_y) , \end{cases} \qquad (4.23)$$

where ϕ_x and ϕ_y are random initial phases. Since that perturbation has *long range correlations*, it is not a good model of noise. On the other hand, the perturbation in (4.23) can be intended as a *probe function*, useful to test the efficacy of the geometric transformation in the presence of disturbance in the classical control parameters. These probe functions have a statistical nature only since the phase

factors ϕ_x and ϕ_y are random variables. We take these random phases to be statistically independent and uniformly distributed in $[-\pi, \pi[$. As a result, the integral in (4.16) is itself a stochastic variable. The perturbation (4.23) is identified by two parameters, the amplitude ε and the characteristic frequency η. In the following, we compute the mean and variance of the stochastic integral in (4.16) in the presence of the perturbation (4.23) as functions of ε and η.

At this point, we distinguish to cases: the first one corresponds to a very peculiar situation in which the perturbation is *transverse* to the segment, i.e. only the $\epsilon_y(t)$ component is present; the second case is the generic one, in which both the transverse $\epsilon_y(t)$ and the parallel component $\epsilon_x(t)$ of the noise are present.

Transverse monochromatic perturbation

In order to obtain a transverse perturbation, one has to put $\epsilon_x(t) = 0$ in (4.23). Hence the expression in (4.16) reduces to

$$\Phi = \oint_\gamma y\,dx + \int_0^T \epsilon_y(t)\,dx(t) \ . \tag{4.24}$$

With the monochromatic perturbation $\epsilon_y(t) = \varepsilon \cos(\eta t + \phi)$. Taking the average over the realizations of the perturbation — i.e. over the choice of the random initial phase ϕ — one obtains that the mean value is left unchanged, namely:

$$\langle \Phi \rangle = \Phi_0 = \oint_\gamma y\,dx \ . \tag{4.25}$$

On the other hand, the variance is given by:

$$\langle \Delta\Phi^2 \rangle = \langle (\Phi - \Phi_0)^2 \rangle = \langle \Phi_1^2 \rangle \ , \tag{4.26}$$

where

$$\Phi_1 = \int_0^{T_a} \epsilon_y(t)\,dx(t) = \varepsilon \int_0^{T_a} \cos(\eta t + \phi)\dot{x}(t)\,dt = \varepsilon \int_0^{T_a} \cos(\eta t + \phi)\frac{dt}{T} \ . \tag{4.27}$$

Hence,

$$\Phi_1 = \frac{\varepsilon}{T_a} \int_0^{T_a} \cos(\eta t + \phi)\,dt = \frac{\varepsilon}{\eta T_a} (\sin(\eta T_a + \phi) - \sin(\phi)), \tag{4.28}$$

and

$$\Phi_1^2 = \frac{\varepsilon^2}{(\eta T_a)^2} \left[\sin^2(\eta T_a + \phi) + \sin^2(\phi) - 2\sin(\eta T_a + \phi)\sin(\phi) \right] \ . \tag{4.29}$$

Taking the average over ϕ, one obtains:

$$\langle \Delta\Phi^2 \rangle = \langle \Phi_1^2 \rangle = \frac{\varepsilon^2}{(\eta T_a)^2} (1 - \cos(\eta T_a)) \ . \tag{4.30}$$

The variance $\langle \Delta\Phi^2 \rangle$ is a measure of the fluctuations in the perturbed flux of the magnetic field. Analogously, one can compute directly the variance of the phase, which reads:

$$\langle \Delta(e^{i\Phi})^2 \rangle = \langle |e^{i\Phi} - e^{i\Phi_0}|^2 \rangle = 2(1 - \langle \cos \Delta\Phi \rangle) \simeq \langle \Delta\Phi^2 \rangle \ , \tag{4.31}$$

and

$$\langle e^{i\Phi} \rangle = e^{i\Phi_0} \ . \tag{4.32}$$

70

One can formulate two observations from the result expressed in (4.30). The first observation is that the amplitude of the fluctuations in the perturbed integral scales as $\varepsilon(\eta T_a)^{-1}$. That can be interpreted as a simple application of the *Riemann-Lebesgue lemma*. The consequence which is relevant for quantum computation is that, for given amplitude and frequency of the perturbation, the variance of the surface spanned by the perturbed loop can be made negligible increasing the operational time T_a. The result of this simple situation is in *agreement* with the *standard argument* of robustness of holonomic gates, since the fluctuations decrease with increasing $N = \eta T_a$. Notice that that behavior corresponds to the fact that the noise has only a transverse component. The second observation is that, if one considers only closed perturbed path, one has to select the allowed frequencies which satisfy $\nu T_a = 2k\pi$, for $k \in \mathbb{Z}$, and equation (4.30) simplifies:

$$\langle \Delta \Phi^2 \rangle = \frac{\varepsilon^2}{(\eta T_a)^2}. \tag{4.33}$$

In other words, the term proportional to $\cos(\eta T_a)$ in (4.30) corresponds to the fact that in the presence of the perturbation the path might not be closed.

Generic monochromatic perturbation

It is more interesting to consider the case in which a perturbation is present both along the x and y components:

$$\begin{cases} \epsilon_x(t) &= \varepsilon \cos(\eta t + \phi_x) \\ \epsilon_y(t) &= \varepsilon \cos(\eta t + \phi_y) . \end{cases} \tag{4.34}$$

In this case, one has to consider all the terms contained in (4.16), which read as follows:

$$\Phi_1 = \int_0^{T_a} \epsilon_y(t) dx(t) = -\frac{\varepsilon}{T_a} \int \cos(\eta t + \phi_y) dt \tag{4.35}$$

$$\Phi_2 = \int_0^{T_a} y(t) d\epsilon_x(t) = -\varepsilon(y_0 + 1)\eta \int \sin(\eta t + \phi_x) dt \tag{4.36}$$

$$\Phi_3 = \int_0^{T_a} \epsilon_y(t) d\epsilon_x(t) = -\varepsilon^2 \eta \int \cos(\eta t + \phi_y) \sin(\eta t + \phi_x) dt . \tag{4.37}$$

It is immediate to distinguish between Φ_1 and Φ_2, which are corrections of the first order in the amplitude of the noise, and Φ_3 which is a correction of the second order. In analogy to what has been done in [DP03], one could *neglect* the higher order correction. Nevertheless we will keep the second-order term during all the calculations and show that its contribution *can be relevant*. Indeed, the description of the consequence of that second order term in the overall integral along the noisy path is the main contribution of the present chapter.

Taking the average over the random initial phases, one obtains:

$$\begin{array}{rclcl} \langle \epsilon_x(t) \rangle &=& \langle \epsilon_y(t) \rangle &=& 0 \\ \langle \epsilon_x^2(t) \rangle &=& \langle \epsilon_y^2(t) \rangle &=& \frac{\epsilon^2}{2} , \end{array} \tag{4.38}$$

and

$$\begin{array}{rclcl} \langle \epsilon_x(t)\epsilon_x(s) \rangle &=& \langle \epsilon_y(t)\epsilon_y(s) \rangle &=& \frac{\epsilon^2}{2} \cos(\eta(t-s)) \\ && \langle \epsilon_x(t)\epsilon_y(t) \rangle &=& 0 . \end{array} \tag{4.39}$$

71

From which it follows that:

$$\langle \Phi_1 \rangle = \langle \Phi_2 \rangle = \langle \Phi_3 \rangle = 0 \ . \tag{4.40}$$

Hence, the mean value of the perturbed integral remains unchanged $\langle \Phi \rangle = \Phi_0$. Its variance reads as follows:

$$\langle \Delta \Phi^2 \rangle = \langle \Phi_1^2 \rangle + \langle \Phi_2^2 \rangle + \langle \Phi_3^2 \rangle - 2\langle \Phi_1 \Phi_2 \rangle - 2\langle \Phi_2 \Phi_3 \rangle - 2\langle \Phi_3 \Phi_1 \rangle \ . \tag{4.41}$$

As we will show below, only the *diagonal* terms do contribute, while the *off-diagonal* terms do vanish. About the diagonal terms, they give the following contributions:

- For the first perturbative term, as in the previous example, we obtain:

$$\Phi_1 = -\frac{\varepsilon}{T_a} \int_0^{T_a} \cos(\eta t + \phi) dt \tag{4.42}$$

that yields

$$\langle \Phi_1^2 \rangle = \frac{\varepsilon^2}{(\eta T_a)^2} \left(1 - \cos(\eta T_a) \right) . \tag{4.43}$$

- For the second term, we have:

$$\Phi_2 = (y_0 + 1) \left(\epsilon_x(T_a) - \epsilon_x(0) \right) = (y_0 + 1) \Delta \epsilon_x \ . \tag{4.44}$$

If $\epsilon_x(T_a)$ and $\epsilon_x(0)$ are statistically independent one obtains:

$$\langle \Phi_2^2 \rangle = 2(y_0 + 1)^2 \langle \epsilon_x^2 \rangle \ . \tag{4.45}$$

However, for the monochromatic perturbation, they are not statistically independent and so we have:

$$\langle \Phi_2^2 \rangle = (y_0 + 1)^2 \varepsilon^2 \left(1 - \cos \eta T_a \right) \ . \tag{4.46}$$

- The last, second-order, term is:

$$\Phi_3 = -\varepsilon^2 \eta \int_0^{T_a} \cos(\eta t + \phi_y) \sin(\eta t + \phi_x) dt \ . \tag{4.47}$$

Its mean square reads

$$\langle \Phi_3^2 \rangle = \eta^2 \varepsilon^4 \int_0^{T_a} dt \int_0^{T_a} ds \langle \cos(\eta t + \phi_y) \sin(\eta t + \phi_x) \cos(\eta s + \phi_y) \sin(\eta s + \phi_x) \rangle \ . \tag{4.48}$$

This expression can be simplified, since

$$\begin{aligned}
\langle \cos(\eta t + \phi_y) \sin(\eta t + \phi_x) \cos(\eta s + \phi_y) \sin(\eta s + \phi_x) \rangle &= \\
\langle \cos(\eta t + \phi_y) \cos(\eta s + \phi_y) \rangle \langle \sin(\eta t + \phi_x) \sin(\eta s + \phi_x) \rangle &= \\
\langle \cos(\eta t + \phi_y) \cos(\eta s + \phi_y) \rangle^2 \ ,
\end{aligned} \tag{4.49}$$

and

$$\langle \cos(\eta t + \phi) \cos(\eta s + \phi) \rangle = \frac{1}{2} \cos(\eta(t - s)) \ , \tag{4.50}$$

72

to obtain:

$$\langle \Phi_3^2 \rangle = \frac{\eta^2 \varepsilon^4}{4} \int_0^{T_a} dt \int_0^{T_a} ds \cos \left(\eta(t-s) \right)^2 = \frac{\epsilon^4}{8} (\eta T_a)^2 \ . \tag{4.51}$$

It is important to notice that the last term is of the forth order in the noise amplitude, but it also depends quadratically on the operational time T_a through the number of cycles of the perturbation $N = \eta T_a$.

- It remains to show that the off-diagonal terms vanishes. For the statical independence of ϵ_x and ϵ_y, one obtains:

$$\langle \Phi_1 \Phi_2 \rangle = \frac{y_0 + 1}{T_a} \int dt \langle \Delta \epsilon_x \epsilon_y(t) \rangle = 0 \tag{4.52}$$

$$\langle \Phi_2 \Phi_3 \rangle = \frac{y_0 + 1}{T_a} \int dt \int ds \langle \epsilon_y(t) \epsilon_y(s) \dot{\epsilon}_x(s) \rangle = 0 \tag{4.53}$$

$$\langle \Phi_3 \Phi_1 \rangle = \int dt \langle \Delta \epsilon_x \epsilon_y(t) \dot{\epsilon}_x(t) \rangle = 0 \ . \tag{4.54}$$

To summarize, we get the following expression for the mean square of the integral along the perturbed path:

$$\langle \Delta \Phi^2 \rangle = \frac{\varepsilon^2}{2} \left[\frac{1}{(\eta T_a)^2} \left(1 - \cos(\eta T_a) \right) + (y_0 + 1)^2 \left(1 - \cos \eta T_a \right) + \right] + \frac{\varepsilon^4}{8} (\eta T_a)^2 \ . \tag{4.55}$$

Let us *emphasize* what is the main result of this section, i.e. the form of the second-order contribution Φ_3, which is not in agreement with the heuristic argument in favor of the robustness of holonomic gates. The important fact is that the fluctuations of the second order increase with increasing number of cycles of the noise. Though that contribution is of higher order in the noise amplitude, even for $\varepsilon^2 \ll \varepsilon$, it can become relevant for sufficiently high values of N or, in other words, for fixed noise frequency and long operational time T.

4.2.2 Noise as a random process

In the previous section, we have considered the behavior of the geometric phase in the presence of a monochromatic perturbation in the loop. The statistical properties of the perturbed integral were obtained taking the average over the choice of the initial phases. In this section, we are going to work with a more realistic model for the noise affecting the control parameters.

Contrary to what was done in the previous section, here we will consider a model for the noise which is described by a stationary random process, characterized by an *exponential decay* of the two-times correlation function. *Also we assume that the relation (A.4) holds true.*

We consider the same unperturbed loop used in the section 4.2.1, the particle is moving with piecewise constant velocity in an operational time T. Each segment of the loop is ran in a time $T_a = T/4$. The noise, acting along both the direction x and y, gives rise to a noisy loop:

$$\gamma \ \longrightarrow \ \gamma_n = \gamma(t/T) + \epsilon(t) \ . \tag{4.56}$$

Let us recall that the noisy phase

$$\Phi = - \int_{\gamma_n} y \, dx \ , \tag{4.57}$$

73

can be expanded as:

$$\begin{aligned}
\Phi &= -\int [y(t) + \epsilon_y(t)] \, d\,[x(t) + \epsilon_x(t)] \\
&= -\int y(t)dx(t) - \int y(t)d\epsilon_x(t) - \int \epsilon_y(t)dx(t) - \int \epsilon_y(t)d\epsilon_x(t) \ ,
\end{aligned}$$

We can distinguish the three contributions:

$$\Phi_1 = -\int_0^T y(t)d\epsilon_x(t) \tag{4.58}$$

$$\Phi_2 = -\int_0^T \epsilon_y(t)dx(t) \tag{4.59}$$

$$\Phi_3 = -\int_0^T \epsilon_y(t)d\epsilon_x(t) \ . \tag{4.60}$$

For the noise component along the x and the y directions, we put (see also the discussion in the appendix A):

$$\langle \epsilon_{x,y}(t) \rangle = 0 \tag{4.61}$$

$$\langle \epsilon_{x,y}(t)\epsilon_{x,y}(s) \rangle = \varepsilon^2 C(t,s) \tag{4.62}$$

$$\langle \dot\epsilon_{x,y}(t)\dot\epsilon_{x,y}(s) \rangle = \varepsilon^2 K(t,s) \tag{4.63}$$

$$\langle \epsilon_x(t)\epsilon_y(s) \rangle = 0 \ , \tag{4.64}$$

with the two-times correlation function:

$$C(t,s) = e^{-\Gamma|t-s|} \ . \tag{4.65}$$

It is instructive to consider the integration only along the first segment [as in (4.22)]. In this case, we write the perturbative terms in (4.58,4.59,4.60) as follows:

$$\Phi_1 \equiv -\int_0^T y_0\dot\epsilon_x(t)dt \tag{4.66}$$

$$\Phi_2 \equiv -\frac{1}{T}\int_0^T \epsilon_y(t)dt \tag{4.67}$$

$$\Phi_3 \equiv -\int_0^T \epsilon_y(t)\dot\epsilon_x(t)dt \ . \tag{4.68}$$

It is immediate to show that:

$$\langle \Phi \rangle = \Phi_0 \ , \tag{4.69}$$

and

$$\langle \Delta\Phi^2 \rangle = \langle (\Phi - \Phi_0)^2 \rangle = \langle \Phi_1^2 \rangle + \langle \Phi_2^2 \rangle + \langle \Phi_3^2 \rangle \ , \tag{4.70}$$

and we obtain:

$$\langle \Phi_1^2 \rangle = y_0^2 \langle (\epsilon_x(T_a) - \epsilon_x(0))^2 \rangle \tag{4.71}$$

$$\langle \Phi_2^2 \rangle = \varepsilon^2 \frac{y_0^2}{T_a^2} \int_0^{T_a} dt \int_0^{T_a} ds\, C(s,t) \tag{4.72}$$

$$\langle \Phi_3^2 \rangle = \varepsilon^4 \int_0^{T_a} dt \int_0^T ds\, C(s,t)K(s,t) \ . \tag{4.73}$$

74

To evaluate these integrals, we assume the following expressions for the correlations functions:

$$C(t-s) = e^{-\Gamma|t-s|} \tag{4.74}$$

$$K(t-s) = \Gamma\left[2\delta(t-s) - \Gamma\right]e^{-k|t-s|} . \tag{4.75}$$

Using the relations in (A.22, A.23, A.24, A.25), in the limit $e^{-\Gamma T_a} \ll 1$, one obtains the following expressions:

$$\langle \Phi_1^2 \rangle = 2\varepsilon^2 y_0^2 \tag{4.76}$$

$$\langle \Phi_2^2 \rangle = \varepsilon^2 y_0^2 \left(\frac{1}{\Gamma T_a} - \frac{2}{(\Gamma T_a)^2} \right) \tag{4.77}$$

$$\langle \Phi_3^2 \rangle = \varepsilon^4 \left(\Gamma T_a + \frac{1}{2} \right) . \tag{4.78}$$

Notice that the three contributions to the total mean square of the noisy integral have different interpretations and behavior:

- The contribution of Φ_1 is related to the fact that the noise in general does not preserve the initial and the final point of the path, if one requires that $\epsilon(T) = \epsilon(0)$ this term vanishes while in the general case it gives a contribution of order ε^2 and is independent of the operational time T.

- The contribution of Φ_2 is related to the fluctuations of the noise in a direction which is transverse to the unperturbed loop, this contribution is of order ε^2 but it depends on the average number of statistical independent fluctuations of the noise during the operational time, denoted $N = \Gamma T$; in particular the mean square of Φ_2 goes to zero in the limit $N \to \infty$.

- The contribution of Φ_3 is related to the combination of noise along orthogonal direction. The term $\langle \Phi_3^2 \rangle$ is of higher order (proportional to ε^4), nevertheless, it is *unbounded* as function of $N = \Gamma T$. We have that for fixed ε the mean square diverges in the limit $N \to \infty$.

Let us now consider the case in which the noise is *turned on* during all the operational time T, namely

$$\gamma_{\mathrm{n}}(t) = \gamma(t/T) + \epsilon(t) \text{ for } t \in [0, T] . \tag{4.79}$$

In analogy to what we have obtained for the one-segment contribution, for the complete loop we have:

$$\Phi_1 = -\int_0^{T_a} y_0 d\epsilon_x(t) - \int_{T_a}^{2T_a} \frac{4(t - T/4)(y_1 - y_0)}{T} d\epsilon_x(t) \tag{4.80}$$

$$-\int_{2T_a}^{3T_a} y_1 d\epsilon_x(t) - \int_{3T_a}^{T} \frac{4(t - 3T/4)(y_0 - y_1)}{T} d\epsilon_x(t)$$

$$\Phi_2 = -\int_0^{T_a} \frac{4(x_1 - x_0)}{T} \epsilon_y(t) dt - \int_{3T_a}^{T} \frac{4(x_0 - x_1)}{T} \epsilon_y(t) dt \tag{4.81}$$

$$\Phi_3 = -\int_0^{T} \epsilon_y(t) d\epsilon_x(t) . \tag{4.82}$$

It is immediate to recognize that the off-diagonal terms $\langle \Phi_h \Phi_k \rangle$, for $h \neq k$, do vanish.

One can neglect the correlation terms between the addends of Φ_1 and Φ_2, which are negligible if the correlation time of the noise decays sufficiently fast with respect to the operational time T. Hence we can write:

$$\langle \Phi_1^2 \rangle = \varepsilon^2 \int_0^{T_a} dt \int_0^{T_a} ds \left[(y_0^2 + y_1^2) K(t-s) + \frac{32(y_1 - y_0)^2}{T^2} ts K(t-s) \right]$$

$$\langle \Phi_2^2 \rangle = 32\varepsilon^2 \int_0^{T_a} dt \int_0^{T_a} ds \frac{(x_1 - x_0)^2}{T^2} C(t-s)$$

$$\langle \Phi_3^2 \rangle = \varepsilon^4 \int_0^T ds \int_0^T dt C(t-s) K(t-s) .$$

Using the relations in (A.22, A.23, A.24, A.25, A.26) we obtain, in the limit $e^{-\Gamma T} \ll 1$:

$$\langle \Phi_1^2 \rangle = 2\varepsilon^2 \left[(y_0^2 + y_1^2) + \frac{16(y_1 - y_0)^2}{T^2} \left(\frac{T^2}{16} - \frac{2}{\Gamma^2} \right) \right] \tag{4.83}$$

$$\langle \Phi_2^2 \rangle = 2\varepsilon^2 \left[\frac{16(x_1 - x_0)^2}{T^2} \frac{2}{\Gamma} \left(\frac{T}{4} - \frac{1}{\Gamma} \right) \right] \tag{4.84}$$

$$\langle \Phi_3^2 \rangle = \varepsilon^4 \left[\Gamma T + \frac{1}{2} \right] . \tag{4.85}$$

Finally, we have found the following general expression for the mean square of the noisy integral (in the limit $e^{-\Gamma T} \ll 1$):

$$\langle \Delta \Phi^2 \rangle = \varepsilon^2 \left(a + b \frac{1}{(\Gamma T)} + c \frac{1}{(\Gamma T)^2} \right) + \epsilon^4 \left(d(\Gamma T) + e \right) . \tag{4.86}$$

That result shows that the terms of order ε^2 and ε^4 in the mean square of the geometric phase give contributions of different nature to the mean square of the noisy integral. While the corrections of order ε^2 are bounded from above, the term of order ε^4 is unbounded. Putting $N = \Gamma T$, for fixed value of ε, one obtains that the lower-order correction decreases with increasing N, while the higher-order terms grows linearly with the number of fluctuations of the noise N.

4.2.3 Comments and interpretations

Let us notice that the leading term at the second order, which is proportional to $\epsilon^4 N$ in (4.86) and (4.78), comes from a stochastic integral of the kind

$$S = \int_0^T \alpha(t) d\beta(t) , \tag{4.87}$$

where both $\alpha(t)$ and $\beta(t)$ are stochastic processes with two-times correlation function $C(t,s) = e^{-\Gamma |t-s|}$. The stochastic integral can be defined as the root mean square limit (see for instance [Ga83]) of the sum

$$S = \sum_{j=0}^{\mathcal{N}-1} \alpha(t_j)(\beta(t_j + \delta t) - \beta(t_j)) \tag{4.88}$$

where $\delta t = T/\mathcal{N}$. The variance of the integral (4.87) is the limit of

$$\Delta S^2 = \sum_i \sum_j \langle \alpha(t_i)\alpha(t_j) \rangle \langle (\beta(t_i + \delta t) - \beta(t_i))(\beta(t_j + \delta t) - \beta(t_j)) \rangle , \tag{4.89}$$

where the average of α and β factorizes for the statistical independence of the processes. We have

$$\Delta \mathcal{S}^2 = \sum_{ij} \langle \alpha(t_i)\alpha(t_j) \rangle \left\{ \langle \beta(t_{i+1})\beta(t_{j+1}) \rangle + \langle \beta(t_i)\beta(t_j) \rangle - \langle \beta(t_{i+1}t)\beta(t_j) \rangle - \langle \beta(t_{j+1})\beta(t_j) \rangle \right\} .$$

(4.90)

Evaluating the two-times correlation functions, one obtains:

$$\Delta \mathcal{S}^2 = \sum_{ij} \langle \alpha(t_i)\alpha(t_j) \rangle \left\{ 2e^{-\Gamma|i-j|\delta t} - e^{-\Gamma|i-j+1|\delta t} - e^{-\Gamma|j-i+1|\delta t} \right\} .$$

(4.91)

The term in curled brackets is

$$\begin{cases} 2(1 - e^{-\Gamma\delta t}) \simeq 2\Gamma\delta t & \text{for} \quad |i-j| = 0 \\ -(1 - e^{-\Gamma\delta t})^2 \simeq -\Gamma^2(\delta t)^2 & \text{for} \quad |i-j| = 1 \\ e^{-\Gamma|i-j|\delta t}(2 - e^{\Gamma\delta t} - e^{-\Gamma\delta t}) \simeq e^{-\Gamma|i-j|\delta t}\Gamma^2(\delta t)^2 & \text{for} \quad |i-j| > 1 \end{cases}$$

(4.92)

and $\langle \alpha(t_i)\alpha(t_j) \rangle = e^{-\gamma|i-j|\delta t}$.

Taking the limit $\delta t \to 0$, only the terms with $|i-j| = 0$ do not vanish, leading to

$$\Delta \mathcal{S} = \sum_j 2\Gamma\delta t \simeq \int_0^T 2\Gamma dt = 2\epsilon^4\Gamma T = 2\epsilon^4 N ,$$

(4.93)

where $N = \Gamma T$ is, as before, the *average number of statistical independent fluctuations*.

Interpretation

In the previous section, we have obtained the following kind expression (for $N \gg 1$) for the variance of the geometric phase up to the second order in the amplitude of the noise:

$$\sigma^2 \simeq a\frac{\varepsilon^2}{N} + b\varepsilon^4 + c\varepsilon^4 N .$$

(4.94)

The terms appearing in (4.94) have a simple interpretation:

- The first-order term gives a contribution to the variance proportional to

$$\sigma_1 = \frac{\varepsilon}{\sqrt{N}} .$$

(4.95)

  That corresponds to the fluctuations which are transverse to the loop. Each transverse fluctuation gives a contribution to the area (the stochastic integral) which is proportional to ε. If the noise experience N statistically independent fluctuations during the operational time, the contribution of each fluctuation to the area of the surface is proportional to ε/N. Since the N fluctuations are in average statistically independent, one has a total variance:

$$\sigma_1 = \frac{\varepsilon}{N}\sqrt{N} = \frac{\varepsilon}{\sqrt{N}} .$$

(4.96)

- The constant second-order term is related to the fact that the noisy loop is in general non closed, hence yielding an additional fluctuation in the stochastic integral which is proportional to the square of the amplitude of the noise. That contributes to the total variance with a term:

$$\sigma_2 = \varepsilon^2 .$$

(4.97)

77

- Finally, the second-order term which is proportional to N is interpreted as follows. A generic oscillation of the noise with amplitude ε contributes to the area of the noisy surface with a term proportional to ε^2. Since N is the average number of statistically independent fluctuations, one has a contribution to the total variance proportional to

$$\sigma_3 = \varepsilon^2 \sqrt{N} \; . \tag{4.98}$$

Analogously, for a monochromatic perturbation (as the one discussed in section 4.2.1), the fluctuations are not statistically independent, hence one has to sum N coherent fluctuations, giving rise to the term $\sigma_3' = \varepsilon^2 N$ [see equation (4.55)].

The three terms have different origins and can be considered to be mutually independent, hence they have to be summed in quadrature, yielding the expression in (4.94).

4.2.4 Numerical evaluations

In this section, we present several results form *numerical calculations* involving few different settings. In particular, we consider two models for the noise affecting the control parameters.

4.2.5 Telegraphic noise

The simplest model is a telegraphic noise. Here we consider a telegraphic noise with correlation time τ (see the appendix A) which perturbs a given loop. We consider the two sample loops introduced above, the first one is a loop which has the shape of a square [as in (4.12)], while the second one is a circular loop [as in (4.13)].

For each loop, which is drawn in the operational time T, we have numerically computed the average $\langle \Phi \rangle$, and the normalized root mean square

$$\Delta \Phi / \Phi = \frac{\sqrt{\langle \Delta \Phi^2 \rangle}}{\langle \Phi \rangle} \tag{4.99}$$

of the noisy integral. We have considered a fixed value of the noise amplitude $\varepsilon = 0.1$, which corresponds to the 10 per cent of the linear dimension of the loop. The results are plotted as a function of the average number of statistically independent fluctuations of the noise, namely $N = T/\tau$. For the square-shaped loop, the mean value and the normalized root mean square are plotted in figure 4.1. For the circle-shaped loop, they are showed in figure 4.2.

4.2.6 Ornstein-Uhlenbeck process

One could notice that the telegraphic noise produces a sample path which is *discontinuous*. A *continuous* sample path is for instance produced by the Ornstein-Uhlenbeck model. In order to visualize the effects of this kind of noise on a given loop, we have plotted some examples of noisy paths for several values of N and of the noise amplitude. For a square-shaped loop, the sample paths are plotted in figure 4.3, while the same is plotted in figure 4.4 for the circle-shaped loop.

For the Ornstein-Uhlenbeck model of noise, the mean value $\langle \Phi \rangle$, and the normalized root mean square $\Delta \Phi / \langle \Phi \rangle$ are plotted in figure 4.5 for the square-shaped loop, and in figure 4.6 for a circular shaped loop for a noise amplitude $\varepsilon = 0.1$.
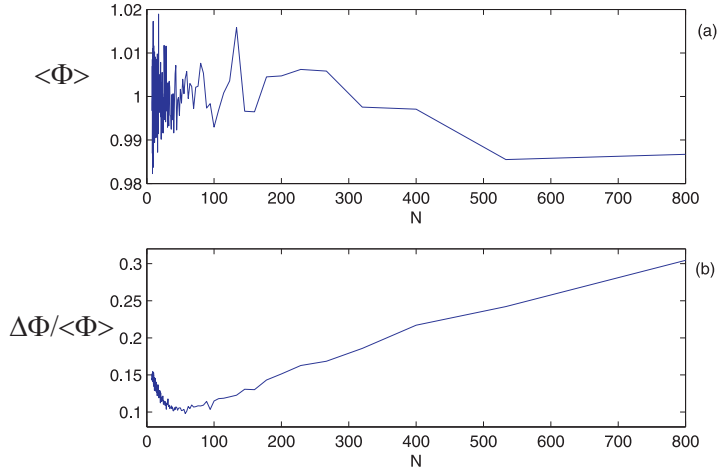
Figure 4.1: (a) For a telegraphic noise, the plot shows the mean value of the integral for the noisy loop related to a square-shaped unperturbed loop as a function of the average number N of fluctuations of the noise. (b) Rescaled root mean square of the integral along the noisy loop as a function of the average number N of fluctuations of the noise. $\varepsilon = 0.1$.
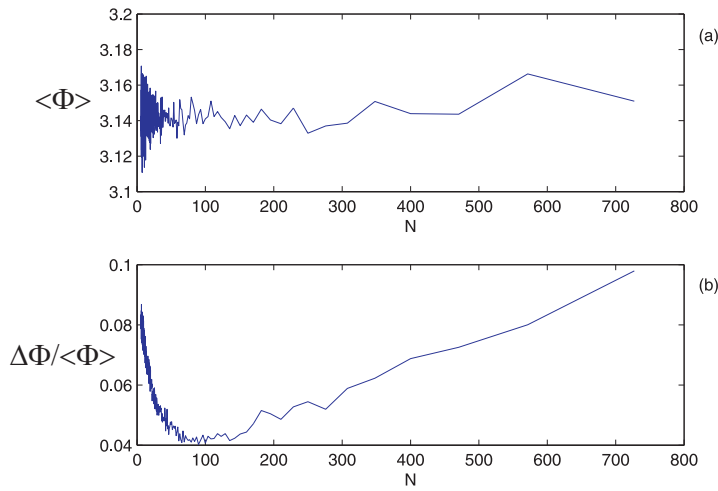
Figure 4.2: (a) For a telegraphic noise, the plot shows the mean value of the integral for the noisy loop related to a circle-shaped unperturbed loop as a function of the average number N of fluctuations of the noise. (b) Rescaled root mean square of the integral along the noisy loop related to a circle-shaped unperturbed loop as a function of the average number N of fluctuations of the noise. $\varepsilon = 0.1$.
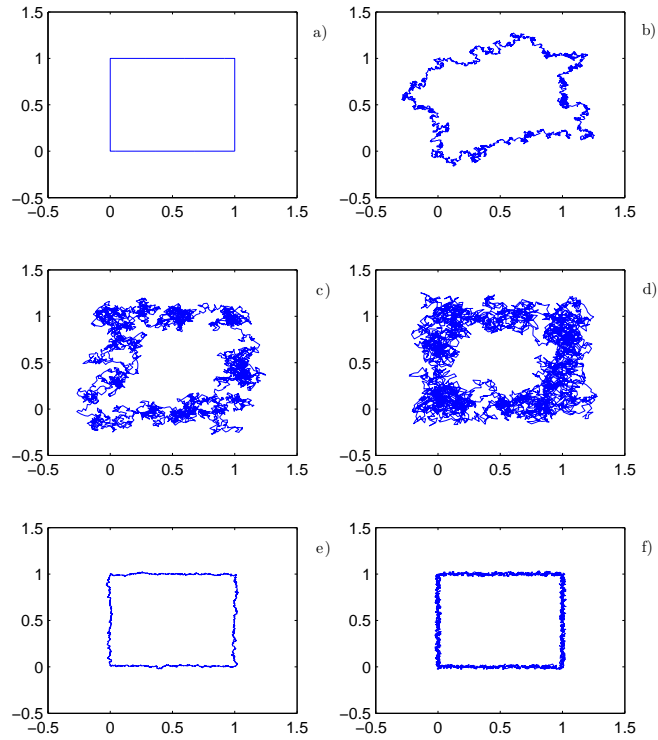
Figure 4.3: Unperturbed square-shaped loop (a), and noisy paths for a Ornstein-Uhlenbeck model of noise, with $\varepsilon = 0.1$ and $N = 10$ (b), $N = 100$ (c), and $N = 200$ (d), and with $\varepsilon = 0.01$ and $N = 100$ (e), and $N = 1000$ (f).
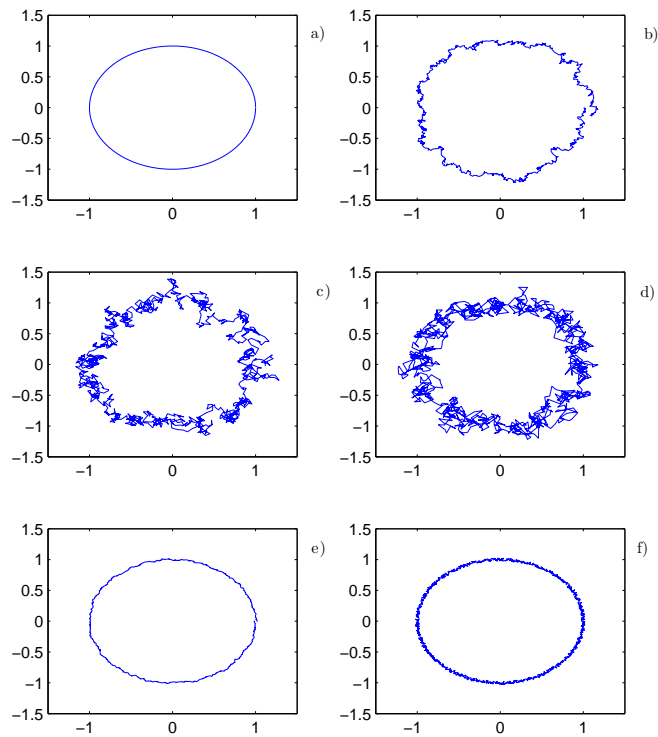
Figure 4.4: Unperturbed circle-shaped loop (a), and noisy paths for a Ornstein-Uhlenbeck model of noise, with $\varepsilon = 0.1$ and $N = 10$ (b), $N = 100$ (c), and $N = 200$ (d), and with $\varepsilon = 0.01$ and $N = 100$ (e), and $N = 1000$ (f).
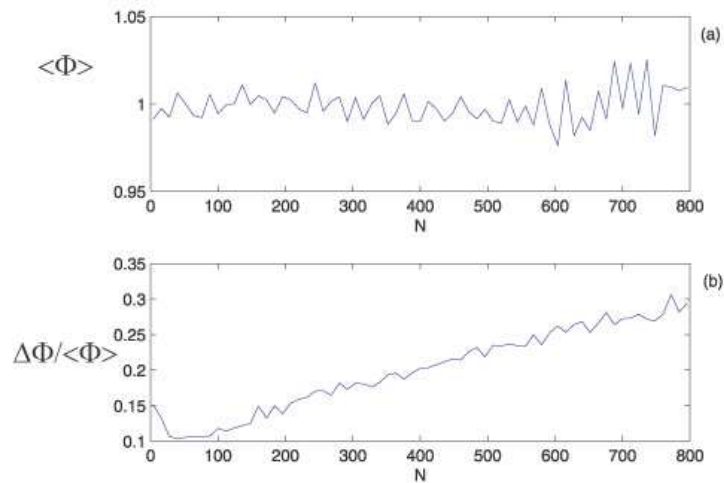
Figure 4.5: (a) Mean value of the integral for the noisy loop related to a square-shaped unperturbed loop as a function of the average number N of fluctuations of the noise, for a noise modeled by a Ornstein-Uhlenbeck process. (b) Rescaled root mean square of the integral along the noisy loop related to a square-shaped unperturbed loop as a function of the average number N of fluctuations of the noise, for a noise modeled by a Ornstein-Uhlenbeck process. $\varepsilon = 0.1$.
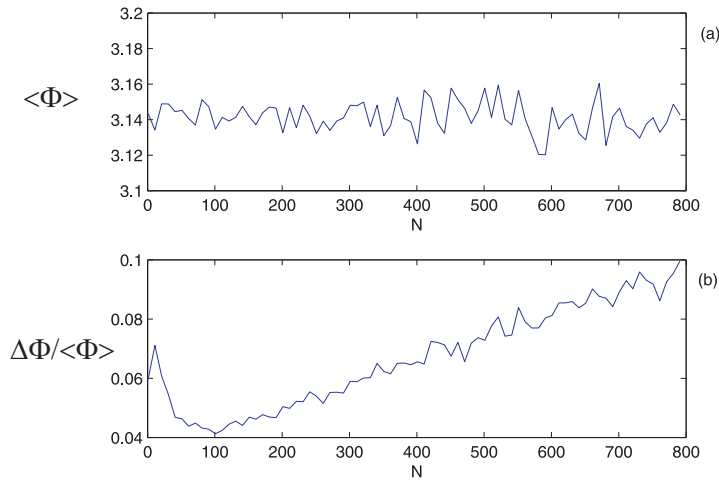
Figure 4.6: (a) Mean value of the integral for the noisy loop related to a circle-shaped unperturbed loop as a function of the average number N of fluctuations of the noise, for a noise modeled by a Ornstein-Uhlenbeck process. (b) Rescaled root mean square of the integral along the noisy loop related to a circle-shaped unperturbed loop as a function of the average number N of fluctuations of the noise, for a noise modeled by a Ornstein-Uhlenbeck process. $\varepsilon = 0.1$.

The variance of the noisy integral increases with increasing N because of the contribution of the term which is of second order in ε. Decreasing the value of ε, the second order effects becomes relevant only for higher value of the average number of fluctuations of the noise N. The mean value and the normalized root mean square are plotted in figure 4.7 for the square-shaped loop, and in figure 4.8 for the circular-shaped one, for a smaller noise amplitude $\varepsilon = 0.01$ of about 1 per cent of the linear dimension of the loops. These plots can be compared with their homologous for a larger noise amplitude $\varepsilon = 0.1$. The second order effects are still present, but become relevant for larger values of N.

At least qualitatively, the numerical results presented here are in agreement with the analytic results and are qualitatively independent of the details of the chosen unperturbed loop and noise model.

4.3 Final comments

In this chapter we have made use of a *simple model* in order to study the *stability* of the *geometric phase*. The appearance of geometric phases is not strictly related to any dynamical quantity determining the specific physical system, but it is mainly a consequence of general geometric features. For that reason, we argue that the simple toy-model can be used to describe the *general behavior* of geometric phases in the presence of *parametric noise*.

The principal result presented in this chapter is the form of the mean square of the geometric phase at the second order in the noise amplitude. We can indeed write the following kind of expression of the mean square as a function of the average number of statistically independent fluctuations of the noise N:

$$\sigma^2 \simeq a \frac{\varepsilon^2}{N} + \varepsilon^4 \left(b + cN \right) \ . \tag{4.100}$$
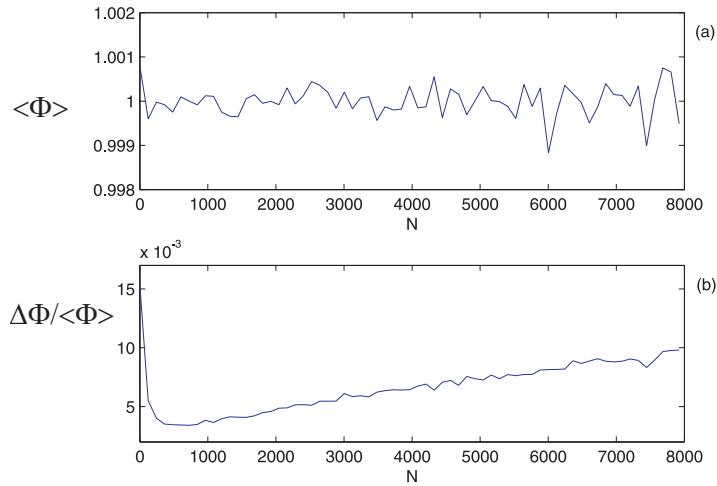
Figure 4.7: (a) The mean value of the integral for the noisy loop related to a square-shaped unperturbed loop as a function of the average number N of fluctuations of the noise, for a noise modeled by a Ornstein-Uhlenbeck process. (b) Rescaled root mean square of the integral along the noisy loop related to a square-shaped unperturbed loop as a function of the average number N of fluctuations of the noise, for a noise modeled by a Ornstein-Uhlenbeck process. $\varepsilon = 0.01$.
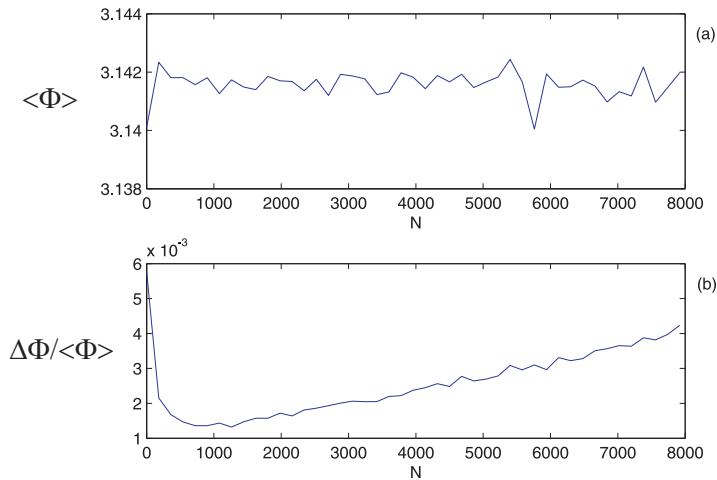
Figure 4.8: (a) The mean value of the integral for the noisy loop related to a circle-shaped unperturbed loop as a function of the average number N of fluctuations of the noise, for a noise modeled by a Ornstein-Uhlenbeck process. (b) Rescaled root mean square of the integral along the noisy loop related to a circle-shaped unperturbed loop as a function of the average number N of fluctuations of the noise, for a noise modeled by a Ornstein-Uhlenbeck process. $\varepsilon = 0.01$.

Besides of the first-order contribution (proportional to ε^2 in the mean square), one can notice two terms which are of higher order. The constant term is related to the fact that the noisy path is in general non-closed, giving rise to an additional uncertainty due to the lost of the gauge invariance. The important term, from our point of view, is the one which is proportional to N. Even if $\varepsilon^4 \ll \varepsilon^2$, that term can become relevant for $N \gg 1$. That observation leads to a *refinement* of the *argument of robustness of the geometric phase* (see section 2.7.1) and of the corresponding *strategy* to obtain *robust holonomic gates* (see the section 2.8). Taking into account the perturbative contributions at the second order, one has to find the *optimal* value of the *operational time* which minimizes the variance in (4.100). The usual argument, based on the first-order term, suggests that the optimal strategy is to approach the limit $T \to \infty$. On the other hand, the second-order analysis states that it is useless to increase the operational time above a certain threshold, and suggests to reach a finite value of the optimal operational time, $T = T_{\mathrm{opt}}$.

Chapter 5

Robustness of geometric phases: A case study

In the previous chapter we presented a discussion about the *argument of robustness* of holonomic computation based a toy-model that, probably, is the simplest physical example in which geometric phases appear. Moreover, the argument of robustness of holonomic gates is *purely geometric* and, as a matter of fact, as nothing to do with quantum mechanics. In the following, we consider the fact that the geometric behavior can appear in *quantum mechanics* in the *adiabatic limit*, giving rise to holonomies, or geometric phases.

We take in consideration a representative example that is considered in literature and discuss the behavior of the corresponding geometric phase in the presence of parametric noise. The case study is one of the *single-qubit holonomic gates* presented in [Du01] (also reviewed in the chapter 2). In particular, we consider *numerical solutions* of the corresponding Schrödinger equation in comparison with the ideal gate which is expected in the adiabatic limit and in the absence of noise. The *second-order effects* that appeared in the discussion of the toy-model in the previous chapter will play a role also in the case study analyzed here. It is worth noticing that the standard argument of robustness refers to the behavior of the noisy geometric phase at the *first order* in the amplitude of the noise. Hence, once the first-order term becomes negligible, the leading contribution corresponds to the *second-order* terms. At this point, the study of the second-order terms becomes *relevant*.

5.1   Single-qubit holonomic gate

As a case study, in this section we consider one of the single-qubit holonomic gates proposed in [Du01]. That gate is reviewed in chapter 2 and it is also central in the discussion of non-adiabatic gate in chapter 3. The system under consideration is a single trapped ion with a structure of stationary or metastable states as depicted in the figure (5.1). Transitions between the levels are driven by resonant lasers fields, hence the system is described, in the rotating frame, by the following Hamiltonian:

$$H = \frac{\Omega}{2} \left(x|0\rangle\langle e| + y|1\rangle\langle e| + z|a\rangle\langle e| + \text{h.c.} \right) . \tag{5.1}$$

In order to obtain the geometric gate, one has to chose the control parameters to be real-valued, namely $x = x^*$, $y = y^*$, and $z = z^*$. The additional constraint $x^2 + y^2 + z^2 = 1$ is also needed. Hence the corresponding control manifold is a two-dimensional sphere. Under these conditions, the system presents a doubly degenerate subspace with vanishing eigenenergy. The system is initialized
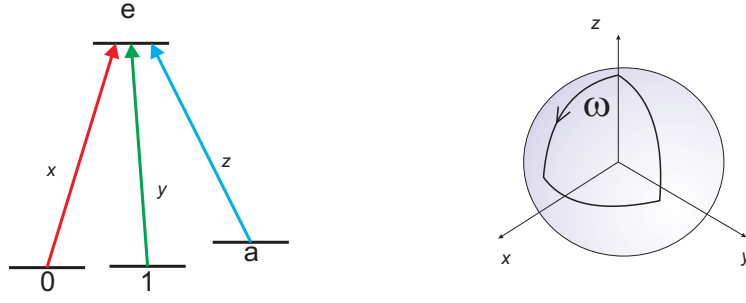
Figure 5.1: On the left: structure of the levels of the single trapped ion, with the relevant laser fields. On the right: a loop on the control manifold.

with $x = y = 0$, hence the initial Hamiltonian corresponds to the *North pole* on the control manifold. The computational space, defining the qubit, is determined as the linear span of the two *dark states*, $\mathcal{H}_0 = \mathrm{span}\{|0\rangle, |1\rangle\}$, which is initially decoupled.

It is easy to check that the corresponding connection one-form for the degenerate space is

$$A = \cos\vartheta\, d\varphi\, \sigma_y \tag{5.2}$$

expressed in polar coordinates on the two-sphere, namely

$$\tan\varphi = \frac{y}{x} \tag{5.3}$$

$$\cos\vartheta = \frac{z}{\sqrt{x^2 + y^2 + z^2}} , \tag{5.4}$$

where σ_y is the Pauli matrix in the computational subspace.

In correspondence with a *generic* path on the control manifold:

$$\gamma \;:\; t \in [0, T] \;\longrightarrow\; x(t),\; y(t),\; z(t), \tag{5.5}$$

one has to solve the Schrödinger equation (with $\hbar = 1$):

$$i\frac{d}{dt}|\psi(t)\rangle = H(t)|\psi(t)\rangle \tag{5.6}$$

with

$$H(t) = H|_\gamma = \frac{\Omega}{2}\left[x(t)|0\rangle\langle e| + y(t)|1\rangle\langle e| + z(t)|a\rangle\langle e| + \text{h.c.}\right], \tag{5.7}$$

and a suitable initial condition belonging to the computational subspace, $|\psi(0)\rangle = |\psi_{\text{in}}\rangle \in \mathcal{H}_0$. The solution, after the operational time T, is written as

$$|\psi_{\text{out}}\rangle = U|\psi_{\text{in}}\rangle , \tag{5.8}$$

where, formally:

$$U = \mathbf{T}\exp\left(-i\int_0^T H(t)dt\right) . \tag{5.9}$$

On the other hand, in the adiabatic limit, the evolution in the computational space, is completely described by the connection one-form in (5.2). In correspondence with an *adiabatic loop* on the control manifold

$$\gamma_{\text{ad}} \;:\; t \in [0, T] \;\longrightarrow\; x(t),\; y(t),\; z(t), \tag{5.10}$$

satisfying $\gamma_{\mathrm{ad}}(T) = \gamma_{\mathrm{ad}}(0)$, and

$$\sup_{t\in[0,T]} \frac{|\dot{\gamma}_{\mathrm{ad}}(t)|}{\Omega|\gamma_{\mathrm{ad}}(t)|} \ll 1 \; ; \tag{5.11}$$

one obtains that

$$|\psi_{\mathrm{out}}\rangle = W|\psi_{\mathrm{in}}\rangle \; , \tag{5.12}$$

where

$$W = \mathbf{P}\exp\left(-i\int_{\gamma_{\mathrm{ad}}} A\right) \; . \tag{5.13}$$

Thus, taking the connection as in (5.2), we can write

$$W = \exp\left(-i\int A\right) = \exp\left(i\int \cos\vartheta d\varphi \sigma_y\right) = \exp\left(-i\omega\sigma_y\right), \tag{5.14}$$

where ω is the solid angle spanned by the loop γ_{ad}.

In particular we focalize on the special class of loops identified in [Fl06] and further studied in [Tr06, Fl06', Lu07']. The peculiarity of that family of loops is that they present perfect fidelity at finite operational time, i.e. long before the adiabatic regime is reached. These perfect revivals of the fidelity appears in correspondence with special values of the operational time T (see also the chapter 3 for a review). The presence of the so-called *optimal working times* is a peculiar feature of a specific gate and loop which does not play any particular role in the discussion of the adiabatic regime. Nevertheless, by taking in consideration that class of holonomic gates, we are allowed to make a direct comparison between different effects of cancelation, due to *dynamical* or *geometric* features.

5.1.1 Adiabaticity of the path

A crucial point concerning holonomic computation is the assumption that the adiabatic limit is reached. Only in the adiabatic limit one can assume that the physical evolution of the quantum system is properly described by a holonomic transformation, or geometric phase. Although quantum holonomies can also appear in correspondence with non-adiabatic cyclic transformation (see chapter 2 and the references therein), only in the adiabatic limit a cyclic Hamiltonian yields a cyclic evolution. On the other hand, it is as well apparent that the transformation achieved in the adiabatic limit is an idealization, corresponding with an ideal gate. From that point of view, it is the adiabatic theorem that ensures that the ideal transformation is approached by the real one under suitable conditions.

In the absence of the instrumental noise, the holonomic computation requires the adiabaticity of the loop. On the other hand, one has to consider how the presence of the noise can affect the adiabaticity conditions. In the generic case, the noise can *preserve* or even *destroy* the adiabaticity of the unperturbed loop. Abstracting from the details of the noise model, the effects of the noise on the adiabaticity of the loop can depend on two physical quantities: the operational time of the gate T and the noise typical time τ. Notice that here τ does not indicate the correlation time of the noise, but the typical time under which the noisy component in the path changes. In order to have a (semi)quantitative measure of the adiabaticity of the unperturbed or noisy path, we consider the following quantity:

$$\alpha = \sup_{t\in[0,T]} \frac{|\dot{\gamma}(t)|}{\Omega|\gamma(t)|} \; , \tag{5.15}$$

where Ω is the relevant Bohr's frequency. More precisely, this quantity defines an *an-adiabaticity* parameter: in the *adiabatic regime* (both in the ideal and noisy case) one has $\alpha \ll 1$, conversely for $\alpha \gg 1$ one is in the opposite regime of *fast noise* which yields a highly non-adiabatic path. The quantity in (5.15) will be used in the following sections to characterize a given path in the parameter space with respect of its adiabaticity.

5.1.2 Noise models

In the previous chapter, we have discussed the geometric argument of robustness of holonomic gates using an over simplified model, which nevertheless is able to grasp all the essential features of the holonomic gates. On the other hand, for any feasible application, the geometric behavior of a gate is not given *a priori*, but is a consequence of dynamical constraints and appears only in special physical situations. An essential request for a gate to behave geometrically is that the adiabatic limit is reached, i.e. the adiabatic approximation is justified. Though, for a certain value of the operational time, that is true for the unperturbed gate, in order to exploit the geometric argument of robustness, one has to require that the loop is still adiabatic even when the noise is present. In other words, one has to require that the gate presents a fully geometric behavior *also* in the presence of the noise.

In the previous chapter, describing the *standard argument* of robustness of holonomic computation, and its *refinements*, we considered a typical time describing the noise component. The typical time-scale was the correlation time of the noise. That is the relevant time-scale to describe the geometric effects of cancelation of the consequences of the noise. It is important to notice that the correlation time is no more the relevant parameter when considering the feasibility of the adiabatic approximation for the noisy loop. For instance, let us considered the random processes used in the previous chapter, both the telegraphic noise and the Ornstein-Uhlenbeck process have a finite correlation time, nevertheless a loop perturbed with this noise models can never be adiabatic. For instance, the sample paths generated by the telegraphic noise are not continuous, while even though the Ornstein-Uhlenbeck process generates continuous paths, they are not differentiable. As it is easy to check, the (an-)adiabaticity parameter introduced in (5.15) is unbounded for those models of noise. In the discussion of the toy-model in chapter 4, the use of the telegraphic noise and the Ornstein-Uhlenbeck process was justified by the fact that the geometric character of the physical transformation was assumed *a priori* and was not a consequence of the adiabatic limit. In the present chapter, in which we consider the physical conditions under which the system evolves geometrically, it is worth introducing another model of noise that can produce *adiabatic sample-paths*.

In order to do that, we consider a noise determined by its *power spectrum*. In other words, we are going to consider a noise with exponentially decaying two-times correlation function,

$$C(t) = \varepsilon e^{i\eta t - \Gamma t}, \tag{5.16}$$

and a corresponding Lorentzian power spectrum

$$S(\omega) = \frac{1}{\pi} \frac{\omega}{(\omega - \eta)^2 + \Gamma^2} \tag{5.17}$$

with band width Γ and typical correlation time $\tau = \Gamma^{-1}$. Formally, one can write the random process as

$$\epsilon(t) = \varepsilon \int_0^{+\infty} d\omega \sqrt{S(\omega)} e^{i(\omega t + \phi_\omega)}, \tag{5.18}$$

where ϕ_ω are random phases. We can take advantage of the expression in (5.18) in order to simulate a random process by means its power spectrum. In particular, we introduce a frequency cut-off at $\omega = 2\Gamma$. Furthermore, we make the assumption that the noisy path is still closed. This assumption is rather unphysical, but it simplifies both the numerical calculation that the interpretation of the results. Indeed, in that setting, the term which corresponds to the fact that the noisy path is in general non-closed (see the analytical discussion in the chapter 4) does not appear, and the effect of the noise is to induce a *continuous deformation* of the loop. That assumption corresponds to select only the frequencies which are integer multiple of the fundamental frequency of the loop, leading to the expression:

$$\epsilon(t) = \frac{\varepsilon}{\mathcal{N}} \sum_{k=0}^{k\nu<2\Gamma} \sqrt{S(\omega)} e^{i(k\nu t + \phi_\omega)} , \qquad (5.19)$$

where $\mathcal{N}$ is a normalization factor. If the gate operational time is T, the fundamental frequency is $\nu = 2\pi/T$. The random process is thus determined by its amplitude ε, its band width Γ and the drift frequency η.

We are going to consider two different settings.

In the first case we take only the real part of (5.19): this choice preserves the control manifold, since the control parameter are real even in the noisy case. In this case, the noise component can be written in the following way:

$$\epsilon(t) = \frac{\varepsilon}{\mathcal{N}'} \sum_{k=0}^{k\nu<2\Gamma} \sqrt{S(\omega)} \cos\left(k\nu t + \phi_\omega\right) . \qquad (5.20)$$

Notice that the physical interpretation of that assumption is that the noise affects only the *amplitude* of the laser fields, without introducing any *de-tuning*. As example, some sample loops, including the ideal loop, corresponding to $\eta = 0$ and several values of ε and Γ are showed in figure 5.2.

The second setting corresponds to a complex-valued noise, which is interpreted as a noise affecting both the *amplitude* and the *de-tuning* of the laser fields. One can compute the noise component using the expression in (5.19). In that case, the control parameters do not belong any more to the *ideal* control manifold.

5.2 Numerical analysis

One can distinguish between two different mechanisms that account for a cancelation of the effects of the noise in holonomic gates. The first kind of cancelation is due to the geometric behavior of the gate in the adiabatic limit. As pointed out above, a crucial point is that the adiabatic approximation holds true, not only for the ideal unperturbed loop, but also for the perturbed one in presence of noise. If that condition is not verified, one cannot apply any argument of robustness which relies on the geometric character of the gate. On the other hand, if the noisy path is highly non-adiabatic, one can observe as well an effect of cancelation which has a dynamical instead of geometric nature. This second kind of *dynamical* cancelation was also discussed in [Lu07'] and reviewed in the chapter 3. Here we recall those argumentations and add new examples and discussions.
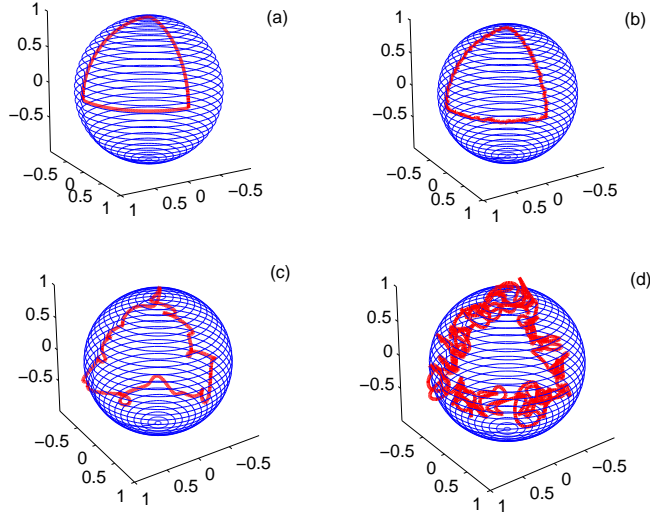
Figure 5.2: Several sample loops. Unperturbed loop (a). Noisy loops with $\varepsilon = 0.01\Omega$ and $\Gamma = 100\Omega$ (b); $\varepsilon = 0.1\Omega$ and $\Gamma = 10\Omega$ (c); $\varepsilon = 0.1\Omega$ and $\Gamma = 50\Omega$.

In the following sections, we are going to present some results obtained with a numerical analysis of the case study under consideration. We consider the ideal loop

$$\gamma \;:\; t \in [0, T] \;\longrightarrow\; \gamma(t/T) = (x(t/T), y(t/T), z(t/T)), \tag{5.21}$$

which in polar coordinates reads as follows:

$$\begin{aligned}
\vartheta(s) &= \begin{cases} 3s\pi/2 & s \in [0, 1/3] \\ \pi/2 & s \in [1/3, 2/3] \\ 3\pi/2\,(1-s) & s \in [2/3, 1] \end{cases} \\
\varphi(s) &= \begin{cases} 0 & s \in [0, 1/3] \\ 3\pi/2\,(s - \frac{1}{3}) & s \in [1/3, 2/3] \\ \pi/2 & s \in [2/3, 1] \, . \end{cases}
\end{aligned} \tag{5.22}$$

That coincides with the ideal loop discussed in the chapter 2. The ideal loop, that spans a solid angle $\omega = \pi/2$, gives rise, in the adiabatic limit to the ideal *geometric* evolutor

$$W = -i\sigma_y \tag{5.23}$$

acting in the computational subspace.

We consider a noise affecting the path, giving rise to the noisy loop

$$\gamma_{\mathrm{n}}(t) = \begin{cases} x_{\mathrm{n}}(t) = x(t) + \epsilon_x(t) \\ y_{\mathrm{n}}(t) = y(t) + \epsilon_y(t) \\ z_{\mathrm{n}}(t) = z(t) + \epsilon_z(t) \, . \end{cases} \tag{5.24}$$

Hence, the equation for the quantum evolutor $U(t)$

$$i\frac{d}{dt}U(t) = H_{\mathrm{n}}(t)U(t) \tag{5.25}$$

90

is numerically solved with the initial condition $U(0) = P_0$ where P_0 indicates the projector on the computational subspace $\mathcal{H}(0)$. The Hamiltonian in (5.25) corresponds to the noisy loop, namely:

$$H_{\mathrm{n}}(t) = \frac{\Omega}{2} \left[x_{\mathrm{n}}(t)|0\rangle\langle e| + y_{\mathrm{n}}(t)|1\rangle\langle e| + z_{\mathrm{n}}(t)|a\rangle\langle e| + \mathrm{h.c.} \right] . \tag{5.26}$$

Finally, the *average gate fidelity* $\mathcal{F}(\mathcal{E}, W)$ between the ideal adiabatic (noiseless) transformation and the actual dynamical evolution in the presence of noise is computed (*the definition of this quantity is recalled in the appendix B*). Eventually, a completely positive map $\mathcal{E}$ is defined as

$$\mathcal{E} \ : \ \rho \ \longrightarrow \ \langle U(T)\rho U(T)^\dagger \rangle_{\mathrm{noise}}, \tag{5.27}$$

where the average is taken over the realizations of the noise.

5.2.1 Real-valued noisy loop

In this section, we consider a noise which affects only the amplitude of the laser fields, hence modeled by a real-valued noisy component in the control parameters:

$$\epsilon_j(t) = \frac{\varepsilon}{\mathcal{N}'} \sum_{k=0}^{k\nu<2\Gamma} \sqrt{S(\omega)} \cos\left(k\nu t + \phi_{\{\omega,j\}}\right) , \tag{5.28}$$

with a Lorentzian power spectrum, and $j = x, y, z$. Some sample paths arising from that kind of noise are shown in the figure (5.2).

Non-adiabatic noise

For the first five values of the optimal operational time, figure 5.3 shows the behavior of the gate in the presence of noise. The amplitude is fixed to $\varepsilon = 0.1\Omega$. In the figure 5.3a, the average gate fidelity is plotted, while in the figure 5.3b, the (an-)adiabaticity parameter defined in (5.15) is plotted for the corresponding working times. These quantities are plotted as functions of the ratio Γ/Ω. The plot shows the revival of the fidelity which happens for fast noises, while the lowest value of the fidelity is reached in correspondence with a noise with a *resonant* frequency. It is also important to notice the high value of the (an-)adiabaticity parameter showed in figure 5.3b, from which it is apparent that in this regime the perturbed loop is highly non-adiabatic.

In the regime of fast noise, the effects of cancelation are related to the average of the *fast* degree of freedom of the noise over the *slow* internal dynamics of the system. In this regime, no connection is expected to exist with the geometry of the noisy loop spanned by the system during the time evolution (see also the discussion in [Lu07'] and in chapter 3).

Adiabatic noise

In the adiabatic setting, one needs to compare the efficacy of the actual gate with the one of the geometric gate. To be more specific, one can assume that the adiabatic approximation is justified not only for the ideal noiseless loop, but also for the noisy one. Hence, given a noisy loop, it spans a certain solid angle ω to which the corresponding holonomic transformation

$$W_{\mathrm{n}} = e^{-i\omega\sigma_y} \tag{5.29}$$
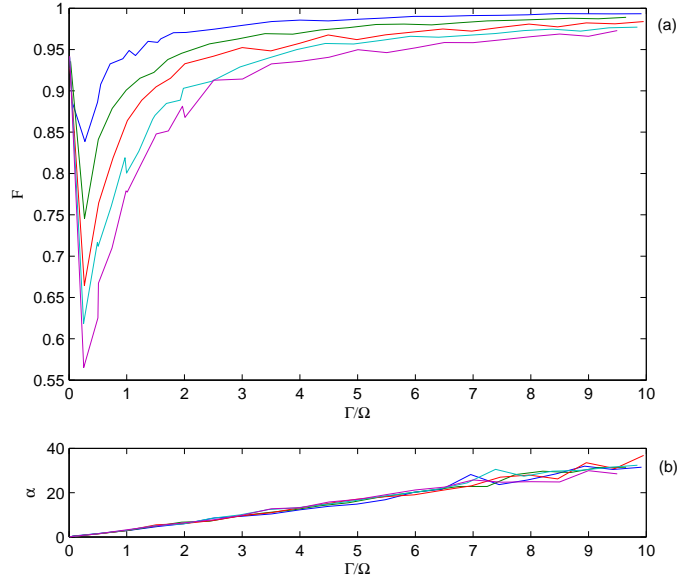
Figure 5.3: (a) Average gate fidelity as a function of the re-scaled typical frequency of the noise Γ/Ω, plotted for the first five value of the optimal working time, from the first optimal working time (blue line) to the fifth one (violet line). (b) The corresponding an-adiabaticity parameter as a function of the re-scaled frequency of the noise.

is associated. Since the solid angle ω, is itself a random variable, determined by the noise, one has to take the average over the realizations of the noise, which leads to definition of the following completely positive map

$$\mathcal{L} \; : \; \rho \; \longrightarrow \; \langle W_{\mathrm{n}} \rho W_{\mathrm{n}}^{\dagger} \rangle_{\mathrm{noise}} \, . \tag{5.30}$$

Finally, one can compute the average gate fidelity between the ideal geometric gate W and the completely positive map in (5.30), denoted as $\mathcal{F}(W, \mathcal{L})$. We will refer to that quantity as the *geometric fidelity*. In other words, one has to compare two average gate fidelities: the first fidelity is between the ideal gate (adiabatic limit, no noise) and the actual gate (computed by numerically solving the Schrödinger equation in presence of noise); the second fidelity compares the ideal gate with a fictitious gate which is the one that would be obtained for a perfectly adiabatic noisy loop. It is worth to notice that, in the presence of adiabatic noise, the fidelity which is expected to approach the unit is $\mathcal{F}(\mathcal{E}, \mathcal{L})$, whilst that cannot be said for the average gate fidelity $\mathcal{F}(W, \mathcal{E})$. Also, we expect that in the adiabatic regime $\mathcal{F}(W, \mathcal{E}) \simeq \mathcal{F}(W, \mathcal{L})$.

Coming back to the equation (5.30), the completely positive map can be written as

$$\rho \; \longrightarrow \; \mathcal{L}(\rho) = \sum_{\omega} p_{\omega} e^{-i\omega\sigma_y} \rho e^{i\omega\sigma_y}, \tag{5.31}$$

where p_{ω} is the probability (or relative frequency) of the solid angle valued ω.

Using the definition in (5.30), it can be immediately checked that the *geometric fidelity* has the following expression:

$$\mathcal{F}(W, \mathcal{L}) = \langle \sin^2 \omega \rangle_{\mathrm{noise}} \, . \tag{5.32}$$

92
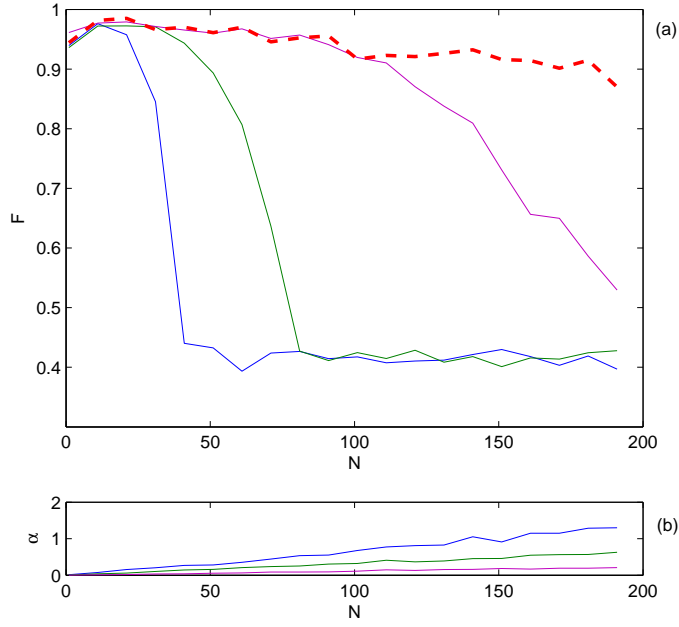
Figure 5.4: (a) Comparison between the average gate fidelity between the ideal gate and the actual gate (solution of the Schrödinger equation) for several values of the operational time: $\Omega T = 500$ (blue line), $\Omega T = 1000$ (green line), $\Omega T = 3000$ (violet line) and the average gate fidelity between the ideal gate and the fictitious geometric gate (dashed red line) as a function of the average number N of fluctuations of the noise. (b) The corresponding an-adiabaticity parameter for several values of the operational time as a function of N.

For small amplitude of the perturbations, if $\omega \simeq \pi/2 + \delta$, one can write

$$\mathcal{F}(W, \mathcal{L}) \simeq \langle \sin^2 (\pi/2 + \delta) \rangle_{\text{noise}} \simeq 1 - \langle \delta^2 \rangle_{\text{noise}} . \tag{5.33}$$

The figure 5.4a shows the *geometric fidelity* together with the *average gate fidelity* for several values of the operational time as functions of the average number of statistical independent fluctuations of the noise, $N = \Gamma T$. The plot refers to values of the operational time ranging from $\Omega T = 500$ to $\Omega T = 3000$. The average gates fidelity can be compared with the geometric fidelity. The geometric fidelity depends only on N and is it independent of the operational time T. The dynamical transformation is expected to coalesces with the geometric transformation only if the noise is adiabatic, hence the average gate fidelity follows the geometric fidelity only for small values of the an-adiabaticity parameter, which is plotted in figure 5.4b.

In contrast with the case of the dynamical cancelations, as long as the noisy loop remains adiabatic, the relevant parameter to describe both the gate in the presence of the noise is the number of fluctuations N. On the other hand, the adiabaticity of the loop is determined by the noise typical frequency, high values of the band width of the noise do break the adiabaticity of the loop, that situation corresponding to high values of the an-adiabaticity parameter in figure 5.4b. Also, for a higher value of the operational time, the same number of noise fluctuations is reached in correspondence of a slower noise.
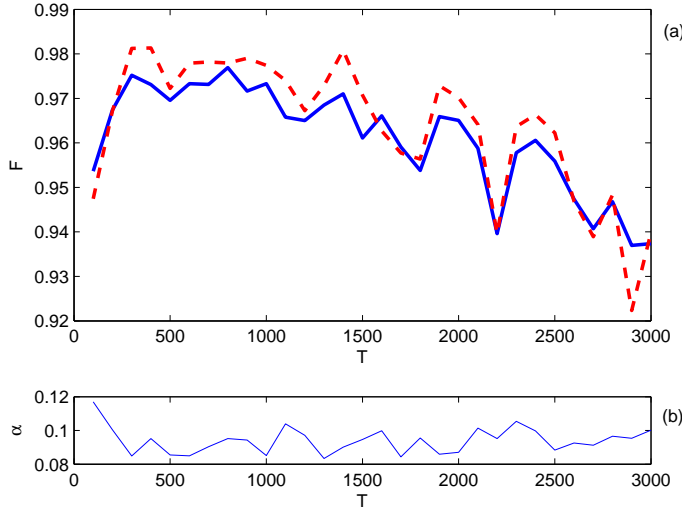
Figure 5.5: (a) Comparison between the average gate fidelity between the ideal gate and the actual gate (solution of the Schrödinger equation) (solid blue line) and the average gate fidelity between the ideal gate and the fictitious geometric gate (dashed red line). (b) The corresponding an-adiabaticity parameter as a function of the operational time. $\varepsilon = 0.1\Omega$, $\Gamma = 0.03\Omega$

It is worth noticing, in the pattern of the geometric fidelity, the existence of the first-order geometric effect of cancelation of the noise (leading to increase in the fidelity), together with the second order contribution that enhances the effects of the noise and is relevant for higher values of N (leading to decreasing fidelity).

A different point of view is described by the plot in figure 5.5a, where the gate fidelity and the geometric fidelity are plotted as functions of the operational time, for fixed values of the amplitude ε and the band width Γ. The amplitude and the typical frequency of the noise are chosen in order to guarantee the adiabaticity of the noisy loop, as can be checked in 5.5b where the corresponding an-adiabaticity parameter is plotted. The plot in figure 5.5a shows how, for a fixed noise, the gate fidelity is a function of the operational time. The gate has a completely geometric behavior in that setting, hence one can observe the effect of the noise both at the first and the second order. Notice that for fixed Γ, the number of independent fluctuations of the noise N is proportional to the operational time T, hence the expected behavior of the gate fidelity is of the following form:

$$\mathcal{F} \simeq 1 - a\frac{\varepsilon^2}{\Gamma T} - b\varepsilon^4 \Gamma T \ , \tag{5.34}$$

which is compatible with the pattern in figure 5.5a. The geometric fidelity is also plotted in figure 5.6 as a function of both the amplitude of the noise and the number of statistically independent fluctuations.

5.2.2 Complex-valued noisy loop

Here we take in consideration a more general noise, which affects both the amplitude and the de-tuning of the laser fields, hence it is modeled by a complex-valued noisy component in the control

94
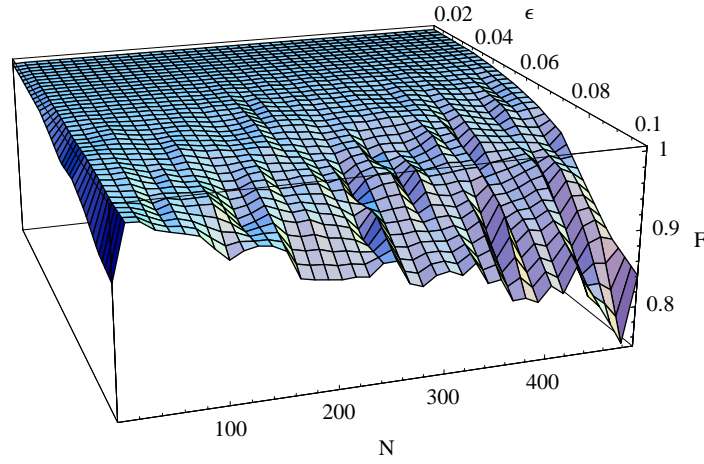
Figure 5.6: Average gate fidelity of the geometric gate as a function of both the amplitude of the noise ε and the average number of fluctuations of the noise N.

parameters:

$$\epsilon_j(t) = \frac{\varepsilon}{\mathcal{N}} \sum_{k=0}^{k\nu < 2\Gamma} \sqrt{S(\omega)} e^{i(k\nu t + \phi_{\{\omega,j\}})}, \qquad (5.35)$$

with a Lorentzian power spectrum, and $j = x, y, z$.

With respect to that kind of noise, the *average gate fidelity* is plotted in the figure 5.7 as a function of the operational time, for a fixed value of the noise band-width, $\Gamma = 0.03\Omega$, and for several values of its amplitude, ranging from $\varepsilon = 0.01\Omega$ to $\varepsilon = 0.1\Omega$. The plot shows the *typical behavior* of the fidelity in the *adiabatic regime*, where the different trends, corresponding to the first and second order perturbative terms, are clearly shown. Finally, the presence is apparent, for a given noise, of an *optimal operational time* which presents the maximum gate fidelity. That *optimal working point* appears in correspondence with the maximum of the fidelity in equation (5.34).

5.3   About the optimal working point

One of the most interesting features of the holonomic approach to computation is its believed robustness against parametric noise affecting the control parameters. We have seen that that can be motivated by the *standard argument* of robustness of geometric gates, which was reviewed in chapter 2. That argument is based on the first-order contribution of the noise on the geometric phase.

A possible strategy to minimize the effects of the noise is suggested by the standard argument of robustness. Given an experimental setting, one deals with some source of noise, which is characterized by the amplitude ε and the correlation time τ, or the band width $\Gamma \simeq \tau^{-1}$. The geometric behavior, depends only on the number of fluctuations $N \simeq \Gamma T$.

Hence the value of N can be changed by changing the operational time T. By modifying the value of the operational time, one could in principle be able to find a working time for the quantum logic gate which is *optimal* with respect to the issue of robustness under the given parametric noise. In other words, one has to find the value of T which *maximize the gate fidelity*.

Considering only the first-order terms in the perturbative expansion, one is led to conclude that the ideal optimal point is reached for high values of the T (ideally, the fidelity reaches one in the limit
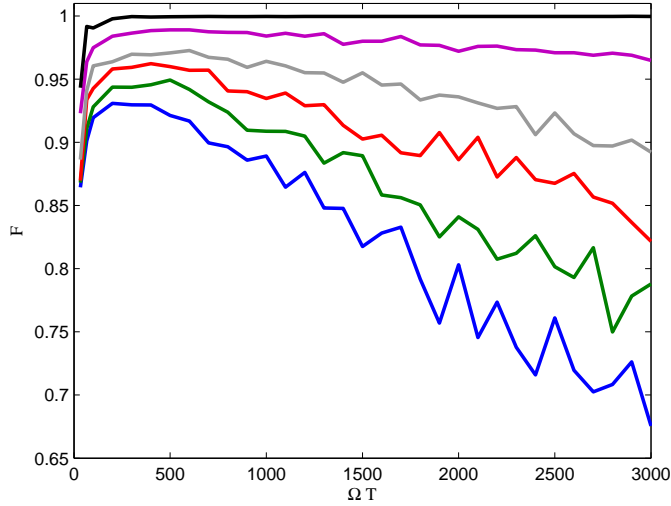
Figure 5.7: Average gate fidelity in presence of a noise affecting both amplitude and de-tuning as a function of the adimensional operational time ΩT. The noise has bandwidth $\Gamma = 0.03\Omega$. The amplitude of the noise are $\varepsilon = 0.01\Omega$, $\varepsilon = 0.05\Omega$, $\varepsilon = 0.07\Omega$, $\varepsilon = 0.08\Omega$, $\varepsilon = 0.09\Omega$, and $\varepsilon = 0.1\Omega$.

$\Omega T \to \infty$). On the other hand, taking into account the second-order in the perturbative expansion, one obtains a *refinement of that strategy*. The pattern of the average gate fidelity shown in the plots confirms the results obtained in the chapter 4 using the toy-model. According to them, the best strategy to optimize the fidelity of the holonomic gate is not to approach the limit $N \to \infty$, but rather to find an optimal value $N = N_{\mathrm{opt}}$, which corresponds to an *optimal operational time $T = T_{\mathrm{opt}}$*, that maximizes the fidelity in (5.34).

5.4 Trade off between geometric and dynamical cancelation

In the previous sections, we have distinguished between geometric and dynamical effects of cancelation of the noise. For the sake of simplicity and readability, we have described the dynamical cancelation for fast gates — at the first five optimal operational working times — while the geometric effects are illustrated for adiabatic gates corresponding to longer operational time. It is worth re-marking that the two different effects are not determined by the specific value of the operational time, conversely the presence of the one or the other (or none of the two) is only determined by the typical frequency of the perturbation.

In other words, geometric effects (of the first or higher order) appear for adiabatic noisy loop, while the dynamical effects of cancelation happen for non-adiabatic one. Hence the relevant parameter which discriminates between the two regimes is the an-adiabaticity parameter (5.15), which is determined by both the value of the operational time and the typical time-scale of the noise. In other words, for an ideally adiabatic holonomic gate, one can observe both dynamical and geometric effects of cancelation, depending on the value of the typical frequency of the noise.

To discuss that issue, we have considered a (quasi)monochromatic perturbation, with drift frequency η and band width $\Gamma \ll \eta$. The behavior of the system under this kind of perturbation is shown in the figure 5.8a, in which the average gate fidelity and the geometric fidelity are compared, together
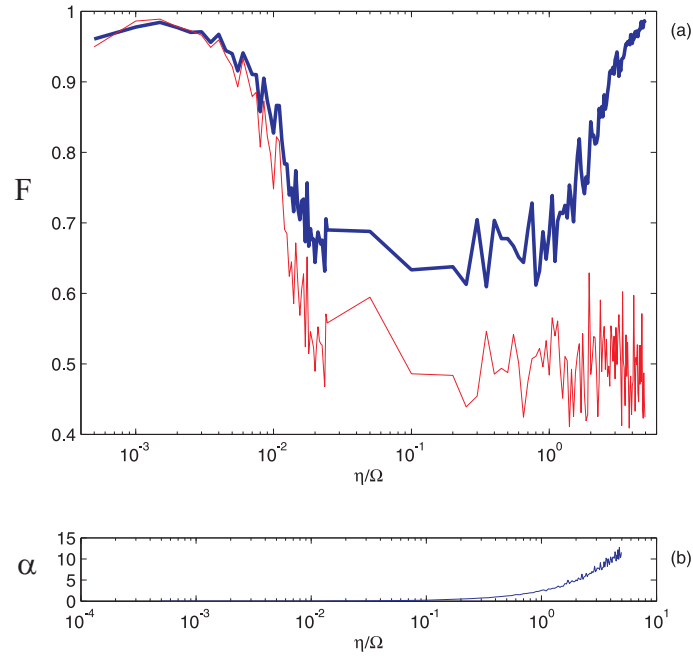
Figure 5.8: (a) Average gate fidelity of the actual gate (blue tick line) compared with the average fidelity of the geometric gate (narrow red line) as a function of the rescaled typical frequency of the noise η/Ω for a quasi monochromatic perturbation. (b) the corresponding (an-)adiabaticity parameter. The plot shows the trade off between geometric (for $\eta \ll \Omega$) and dynamical (for $\eta \gg \Omega$) cancelation effects. The operational time is fixed at $\Omega T = 2000$ and the amplitude of the noise is $\varepsilon = 0.1\Omega$.

with the corresponding an-adiabaticity parameter in figure 5.8b. In the adiabatic regime (corresponding to $\alpha \ll 1$, or $\eta/\Omega \ll 1$), the gate fidelity follows the fidelity of the geometric gate. On the other hand, in the highly non-adiabatic regime (corresponding to $\alpha \gg 1$, or $\eta/\Omega \gg 1$) the two patterns become different. While the geometric fidelity approaches $1/2$, the gate fidelity approaches one for of the dynamical effects of cancelation.

Conclusions

Dans la vie tout début a une fin
Tout n'est que souvenir
Donc efforcer vous pour que ça soit un bon souvenir

(it should be) a Senegalese motto.

The main result presented in this Thesis is based on a *simple* as well as *subtle* observation. The so-called *standard argument* of robustness of holonomic gates (or geometric phases) in the presence of *parametric noise* is based on a perturbative analysis which is truncated at the *first-order* in the noise amplitude. That argument can lead to the individuation of a *strategy* to obtain holonomic gates which are *optimal* from the point of view of *fault-tolerance*.

It is thus natural to ask about the role played by the *higher-order* terms in the perturbative expansion of the noisy geometric phase. With the help of some specific models, we have analyzed the terms which are of the second-order in the amplitude of the noise. We have shown that these contributions cannot be in general neglected since they can play a *relevant role* with respect of the issue of robustness. The contributions of the noise in the geometric phase have a *precise as well as simple interpretation* both at the first and at the second perturbative order.

In particular, our considerations and results lead to a *refinement* of the *optimal strategy* which takes into account also the higher order contributions in the perturbative expansion of the geometric phase. We think that this observation can be of certain interest for the realization of a *fault-tolerant quantum computation*.

Appendix A

About perturbations and noise

In order to study the behavior of holonomic gates and geometric phases in the presence of classical noise we need, for both the analytical and numerical calculations, suitable models describing the parametric noise.

From our point of view, a model for a noise component in the control parameters is a random process $\epsilon(t)$ characterized by its correlation functions. One can consider the two-times correlation function:

$$C(t, s) = \langle \epsilon(t)\epsilon(s) \rangle \tag{A.1}$$

where the average is taken over the realizations of the process. For a stationary process $C(t, s) = C(|t - s|)$. The random function can also be characterized by means of its power spectrum:

$$S(\omega) = \int_0^{+\infty} C(\tau) \cos(\omega\tau) d\tau . \tag{A.2}$$

If the stochastic process has differentiable sample paths, one can consider the function:

$$K(t, s) = \langle \dot{\epsilon}(t)\dot{\epsilon}(s) \rangle , \tag{A.3}$$

which is the two-times correlation of the derivative of the process. In that case, one can write the following identity:

$$K(t, s) = \frac{\partial^2}{\partial s \partial t} C(t, s) . \tag{A.4}$$

In the calculations presented in the chapter 4, we make use of the hypothesis that the relation (A.4) holds true. If this is the case, we may say that the sample paths of the random process are differentiable in a *weak* sense.

Exponential decay of correlations

For a stationary process with exponential two-times correlation function

$$C(t, s) = e^{-k|t-s|} \tag{A.5}$$

we have

$$K(t, s) = k \left[2\delta(t - s) - k \right] e^{-k|t-s|} \tag{A.6}$$

Ornstein-Uhlenbeck process

A Ornstein-Uhlenbeck process $\beta(t)$ is a stochastic process (see for instance [Ga83]) that fulfills the following differential equation:

$$d\beta(t) = -k\beta(t)dt + \sqrt{D}\xi(t)dt, \tag{A.7}$$

where $\xi(t)$ is a delta-correlated noise, D and k are respectively the diffusion and damping coefficient. For a stationary process, the two-times correlation function reads as follows:

$$C(t,s) = \frac{D}{2k}e^{-k|t-s|}. \tag{A.8}$$

On the other hand, we have:

$$\langle\dot{\beta}(t)\dot{\beta}(s)\rangle = k^2\langle\beta(t)\beta(s)\rangle + D\langle\xi(t)\xi(s)\rangle - k\sqrt{D}\left[\langle\xi(t)\beta(s)\rangle + \langle\beta(t)\xi(s)\rangle\right]. \tag{A.9}$$

To evaluate the last term, notice that:

$$\langle\xi(s)\dot{\beta}(t)\rangle = -k\langle\xi(s)\beta(t)\rangle + \sqrt{D}\langle\xi(s)\xi(t)\rangle. \tag{A.10}$$

Hence, putting $Z(t,s) := \langle\xi(s)\beta(t)\rangle$ we find:

$$\frac{\partial}{\partial t}Z(t,s) = -kZ(t,s) + \sqrt{D}\delta(t-s), \tag{A.11}$$

which has solution:

$$Z(t,s) = \sqrt{D}e^{-k(t-s)}\theta(t-s). \tag{A.12}$$

(Where θ indicates the heavy-side function.) We have

$$\langle\xi(t)\beta(s)\rangle + \langle\beta(t)\xi(s)\rangle = Z(t,s) + Z(s,t) = \sqrt{D}e^{-k|t-s|}, \tag{A.13}$$

that yields:

$$\langle\dot{\beta}(t)\dot{\beta}(s)\rangle = D\delta(t-s) - \frac{Dk}{2}e^{-k|t-s|}. \tag{A.14}$$

Finally, one can write

$$K(t,s) = \frac{\partial}{\partial t \partial s}C(t,s). \tag{A.15}$$

Telegraphic noise

For the numerical calculations, we also consider a telegraphic noise. In that case, the random process $\epsilon(t)$ can assume two values, say $\{-\varepsilon, \varepsilon\}$ with equal probability. The function has a probability per unit time π of changing its value. It follows that the probability of having n changes in a time τ is given by the Poisson distribution:

$$P_n(\lambda) = e^{-\lambda}\frac{\lambda^n}{n!}, \tag{A.16}$$

where $\lambda = \pi\tau$. Hence one obtains that:

$$\epsilon(t)\epsilon(t+\tau) = \begin{cases} \varepsilon^2 & \text{for } n \text{ even} \\ -\varepsilon^2 & \text{for } n \text{ odd} \end{cases} \tag{A.17}$$

102

The corresponding two-times correlation function has an exponential decay:

$$\langle \epsilon(t)\epsilon(s) \rangle = \varepsilon^2 \sum_n (-1)^n e^{-\lambda} \frac{\lambda^n}{n!} = \varepsilon^2 e^{-2\lambda} = \varepsilon^2 e^{-2\pi|t-s|}. \tag{A.18}$$

In the chapter 3, we make use of a simplified version of the standard definition of the telegraphic noise. In that case there is a typical time scale τ_{step} which characterized the process. As a consequence, the process is no more invariant under continuous time translation, but it is symmetric only under finite translations (by integer multiples of the typical time τ_{step}). The two-times correlation function can be written as an exponential only for a sufficiently large time interval, namely

$$C(t,s) \simeq e^{-|t-s|/\tau_{\text{step}}} \text{ for } |t-s| \gg \tau_{\text{step}} . \tag{A.19}$$

Some useful integrals

In the following we calculate some integrals which are useful for the discussion in the chapter 4. Taking in consideration the case in which the two-times correlation function decays exponentially

$$C(t-s) = e^{-k|t-s|}, \tag{A.20}$$

and

$$K(t-s) = k\left[2\delta(t-s) - k\right]e^{-k|t-s|}, \tag{A.21}$$

it is straightforward to obtain the following relations:

$$\int_0^\tau ds \int_0^\tau dt\, C(t-s) = \frac{\tau}{k} - \frac{2}{k^2}\left(1 - e^{-k\tau}\right) \tag{A.22}$$

$$\int_0^\tau ds \int_0^\tau dt\, K(t-s) = 2\left(1 - e^{-k\tau}\right) \tag{A.23}$$

$$\int_0^\tau ds \int_0^\tau dt\, t\, K(t-s) = \tau\left(1 - e^{-k\tau}\right) \tag{A.24}$$

$$\int_0^\tau ds \int_0^\tau dt\, C(t-s)K(t-s) = k\tau + \frac{1}{2}\left(1 - e^{-2k\tau}\right) \tag{A.25}$$

$$\int_0^\tau ds \int_0^\tau dt\, t\, s\, K(t-s) = \tau^2 - \frac{2}{k^2} + 2\frac{k\tau+1}{k^2}e^{-k\tau}, \tag{A.26}$$

that are taken in consideration in the chapter 4.

Quasi-monochromatic perturbation

In the chapter 5, in order to obtain an adiabatic noise, we consider the following *formal* expansion of the stochastic process:

$$\epsilon(t) \simeq \varepsilon \int_0^{+\infty} d\omega \sqrt{S(\omega)} e^{i(\omega t + \phi_\omega)}, \tag{A.27}$$

where $S(\omega)$ is the corresponding power spectrum, and ϕ_ω are randomly chosen initial phases. The integral in (A.27) can be ill-defined, nevertheless, one can consider the expression

$$\epsilon(t) \simeq \frac{\varepsilon}{\mathcal{N}} \sum_{k=0}^{k\nu<k_0} \sqrt{S(\omega)} e^{i(k\nu t + \phi_\omega)}, \tag{A.28}$$

103

where $\mathcal{N}$ is a normalization factor, and we have introduced a fundamental frequency ν and a cutoff at $\nu_0 = k_0 \nu$.

In particular, taking a Lorentzian power spectrum:

$$S(\omega) = \frac{1}{\pi} \frac{\Gamma}{(\omega - \omega_0)^2 + \Gamma^2} \tag{A.29}$$

we also consider a quasi-monochromatic perturbation, obtained in correspondence with $\Gamma \ll \omega_0$.

Appendix B

Figures of merit

One of the tasks faced in the present Dissertation is to make comparison between pairs of quantum states, or between pairs of quantum transformation. In order to make a quantitative comparison, one needs to identify a definition of a suitable "distance" between a pair of quantum states or transformation.

In order to compare two pure states $|\psi\rangle$ and $|\phi\rangle$ of a quantum system, one can consider the overlap

$$F(\psi, \phi) = |\langle \phi | \psi \rangle|, \tag{B.1}$$

which is know as quantum *fidelity*. The fidelity is insensible to a global phase, hence it is defined on the corresponding pure state density matrix and we can as well write

$$F(\psi, \phi) = \sqrt{\operatorname{tr}\left(|\phi\rangle\langle\phi|\psi\rangle\langle\psi|\right)}. \tag{B.2}$$

The generalization to mixed states is not as intuitive as it can be imagined to be. The following is the correct definition of the mixed state fidelity:

$$F(\rho, \sigma) = \operatorname{tr}\left(\sqrt{\sqrt{\rho^{1/2}\sigma\rho^{1/2}}}\right), \tag{B.3}$$

which finds its proper justification in the Uhlmann's theorem [Uh76, Jo94]. If $[\rho, \sigma] = 0$, the quantity in (B.3) reduces to the classical fidelity

$$f(p, q) = \sum_k \sqrt{p_k q_k}, \tag{B.4}$$

where q_k and p_k are respectively the eigenvalues of ρ and σ.

In our discussions, we often need to compare the output states $|\psi_{out}\rangle$ corresponding to an ideal, noiseless, transformation, with the output $|\psi_{noise}\rangle$ of a non-ideal, noisy gate. Since one is mainly interested in the transformation by itself, and not in one output state in particular, it is needed to consider all the possible input states. Among several possibilities, we have chosen the quantity known as *average gate fidelity* as a figure of merit to compare quantum transformations. (Another possible choice could have been the *worst case fidelity*.)

Following the discussion of Michael Nielsen in [Ni02], we define the average gate fidelity between a *quantum channel*[1] $\mathcal{E}$ and an unitary transformation U as

$$\mathcal{F}(U, \mathcal{E}) = \int d\psi \langle \psi | U^\dagger \mathcal{E}(|\psi\rangle\langle\psi|) U |\psi\rangle, \tag{B.5}$$

---

[1] a completely positive and trace-preserving map [NC00]

where $d\psi$ is the normalized Fubini-Studi measure over the set of (input) states. In order to evaluate the quantity in equation (B.5) it is indeed *not necessary* to explicitly compute the average over the set of input states. An useful formula was provided in [Ni02] (see also [Bo02, Ho99]), which allows to compute it directly without passing through the average over the set of input states. For a quantum system with d levels, given an orthogonal basis $\{X_\alpha\}_{\alpha=0...d^2-1}$ in the space of Hilbert-Schmidt operators, hence satisfying

$$\mathrm{tr}[X_\alpha^\dagger X_\beta] = d\delta_{\alpha\beta}, \tag{B.6}$$

one can write the following formula:

$$\mathcal{F}(U,\mathcal{E}) = \frac{\mathrm{tr}\left[UX_\alpha^\dagger U^\dagger \mathcal{E}(X_\alpha)\right] + d^2}{d^2(d^2+1)}. \tag{B.7}$$

Example 4 (Average gate fidelity for sigle-qubit transofrmations) *For a qubit system, $d = 2$, and one can chose X_α to be composed by the Pauli matrices together with the identity matrix, and write (B.7) in the following way:*

$$\mathcal{F}(U,\mathcal{E}) = \frac{1}{2} + \frac{1}{12}\sum_{k=1,2,3}\mathrm{tr}\left[U\sigma_k U^\dagger \mathcal{E}(\sigma_k)\right]. \tag{B.8}$$

Analogously, if one is dealing with a two-dimensional computational space $\mathcal{H}_0 = \mathrm{span}\{|0\rangle, |1\rangle\}$, which is a subspace of a larger space in which the dynamics is defined, one can consider the Pauli matrices σ_α in the computational basis:

$$\begin{aligned}
\sigma_0 &= |0\rangle\langle 0| + |1\rangle\langle 1| \\
\sigma_1 &= |0\rangle\langle 1| + |1\rangle\langle 0| \\
\sigma_2 &= i|0\rangle\langle 1| - i|1\rangle\langle 0| \\
\sigma_3 &= -|0\rangle\langle 0| + |1\rangle\langle 0|
\end{aligned} \tag{B.9}$$

In this case the formula (B.7) reads:

$$\mathcal{F}(U,\mathcal{E}) = \frac{1}{3} + \frac{1}{12}\mathrm{tr}\left[U\sigma_0 U^\dagger \mathcal{E}(\sigma_0)\right] + \frac{1}{12}\sum_{k=1}^{3}\mathrm{tr}\left[U\sigma_k U^\dagger \mathcal{E}(\sigma_k)\right]. \tag{B.10}$$

Bibliography

[AB59] Y. Aharonov and D. Bohm, *Significance of Electromagnetic Potentials in the Quantum Theory* Phys. Rev. **115** 485 (1959).

[AA87] Y. Aharonov, J. Anandan, *Phase change during a cyclic quantum evolution* Phys. Rev. Lett. **58** 1593 (1987).

[An88] J. Anandan, *Non-adiabatic non-abelian geometric phase* Phys. Lett. A **133** 171 (1988).

[An06] P. Aniello, C. Lupo and M. Napolitano, *Exploring Representation Theory of Unitary Groups via Linear Optical Passive Devices* Open Sys. & Information Dyn. **13** 415 (2006).

[An07] P. Aniello, C. Lupo, M. Napolitano and M. G. A. Paris, *Engineering multiphoton states for linear optics computation* Eur. Phys. J. D **41** 579 (2007).

[An07'] P. Aniello, C. Lupo, *A new class of separability criteria for bipartite quantum systems* arXiv:quant-ph/0711.3390.

[Ba95] A. Barenco, C. H. Bennet, R. Cleve, D. P. DiVincenzo, N. Margolus, P. Shor, T. Sleator, J. A. Smolin and H. Weinfurter, *Elementary gates for quantum computation* Phys. Rev. A **52** 3457 (1995).

[Be04] G. Benenti, G. Casati and G. Strini, *Principles of Quantum Computation and Information* (World Scientific, Singapore, 2004).

[Be84] M. V. Berry, *Quantal Phase Factors Accompanying Adiabatic Changes* Proc. R. Soc. Lond. A **392** 45 (1984).

[BF28] M. Born and V. Fock, *Beweis des Adiabatensatzes* Z. Phys. **51** 165 (1928).

[Bo02] M. D. Bowdrey, D. K. L. Oi, A. J. Short, K. Banaszek and J. A. Jones, *Fidelity of Single Qubit Maps* Phys. Lett. A **294** 258 (2002).

[BP02] H. P. Breuer, F. Petruccione, *The Theory of Open quantum Systems* (Oxford University Press, Oxford, 2002).

[Ca95] A. R. Calderbank and P. W. Shor, *Good quantum error-correcting eodes exist* Phys. Rev. A **54** 1098 (1996).

[Ca03] A. Carollo, I. Fuentes-Guridi, M. França Santos and V. Vedral, *Geometric Phase in Open System* Phys. Rev. Lett. **90** 160402 (2003).

[Ca04] A. Carollo, I. Fuentes-Guridi, M. França Santos and V. Vedral, *Spin-$1/2$ Geometric Phase Driven by Decohering Quantum Fields* Phys. Rev. Lett. **92** 020402 (2004).

[CJ04] D. Chruscinski, A. Jamiołkowski, *Geometric Phases in Classical and Quantum Mechanics* (Birkhauser Boston, 2004).

[Ci95] J. I. Cirac, P. Zoller, *Quantum Computations with Cold Trapped Ions* Phys. Rev. Lett. **74** 4091 (1995).

[Ci00] J. I. Cirac, P. Zoller, *A scalable quantum computer with ions in an array of microtraps* Nature **404** 579 (2000).

[DP03] G. De Chiara, G. M. Palma, *Berry Phase for a Spin $1/2$ Particle in a Classical Fluctuating Field* Phys. Rev. Lett. **91** 090404 (2003).

[DJ92] D. Deutsch and R. Jozsa, *Rapid solutions of problems by quantum computation* Proc. R. Soc. Lond. A **439** 553 (1992).

[Du01] L.-M. Duan, J. I. Cirac, P. Zoller, *Geometric Manipulation of Trapped Ions for Quantum Computation* Science **292** 1695 (2001).

[Di95] D. P. DiVincenzo, *Two-bit gates are universal for quantum computation* Phys. Rev. A **51** 1015 (1995).

[Ek98] R. Cleve, A. Ekert, C. Macchiavello, and M. Mosca, *Quantum algorithms revisited* Proc. R. Soc. Lond. A **454** 339 (1998).

[Fa05] P. Facchi, S. Tasaki, S. Pascazio, H. Nakazato, A. Tokuse and D. A. Lidar, *Control of decoherence: Analysis and comparison ofthree different strategies* Phys. Rev. A **71** 022302 (2005).

[Fa00] G. Falci, R. Fazio, G. M. Palma, J. Siewert and V. Vedral, *Detection of geometric phases in superconducting nanocircuits* Nature **407** 355 (2000).

[Fa03] L. Faoro, J. Siewert and R. Fazio, *Non-Abelian Holonomies, Charge Pumping, and Quantum Computation with Josephson Junctions* Phys. Rev. Lett. **90** 028301 (2003).

[Fi06] S. Filipp, *New Aspects of the Quantum Geometric Phase* Ph.D. dissertation (2006).

[Fl06] G. Florio, P. Facchi, R. Fazio, V. Giovannetti and S. Pascazio, *Robust gates for holonomic quantum computation* Phys. Rev. A **73** 022327 (2006).

[Fl06'] G. Florio, *Decoherence in Holonomic Quantum Computation* Open Sys. & Information Dyn. **13** 263 (2006).

[Fu05] I. Fuentes-Guridi, F. Girelli, E. Livine, *Holonomic Quantum Computation in the Presence of Decoherence* Phys. Rev. Lett. **94** 020503 (2005).

[Ga83] C. W. Gardiner, *Handbook of Stochastic Methods* (Springer, Berlin, 1983).

[Go96] D. Gottesman, *A Class of quantum error-correcting codes saturating the quantum Hamming bound* Phys. Rev. A **54** 1862 (1996).

[Ho99] M. Horodecki, P. Horodecki and R. Horodecki, *General teleportation channel, singlet fraction, and quasidistillation* Phys. Rev. A **60** 1888 (1999).

[Jo94] R. Jozsa, *Fidelity for Mixed Quantum States* J. Mod. Opt. **41** 2315 (1994).

[Ka51] T. Kato, *On the Adiabatic Theorem of Quantum Mechanics* J. Phys. Soc. Jap. **5** 435 (1951).

[Ki03] A. Yu. Kitaev, *Fault-tolerant quantum computation by anyons* Annals Phys. **303** 2 (2003); arXiv:quant-ph/9707021.

[Li98] D. A. Lidar, I. L. Chuang, and K. B. Whaley, *Decoherence-Free Subspaces for Quantum Computation* Phys. Rev. Lett. **81** 2594 (1998).

[Lu05] C. Lupo, V. I. Man'ko, G. Marmo, E. C. G. Sudarshan, *Partial scaling transform of multiqubit states as a criterion of separability* J. Phys. A **38** 10377 (2005).

[Lu06] C. Lupo, V. I. Man'ko, G. Marmo, *Bell's inequalities in the tomographic representation* J. Phys. A **39** 12515 (2006).

[Lu07] C. Lupo, V. I. Man'ko, G. Marmo, *Qubit-portraits of qudit states and quantum correlations* J. Phys. A **40** 13091 (2007).

[Lu07'] C. Lupo, P. Aniello, M. Napolitano and G. Florio, *Robustness against parametric noise of nonideal holonomic gates* Phys. Rev. A **76** 012309 (2007).

[Lu07+] C. Lupo, *On the realignment criterion and beyond* arXiv:quant-ph/0705.2328.

[Ma92] K. B. Marathe, G. Martucci, *The Mathematical Foundations of Gauge Theories* (North-Holland, Amsterdam, 1992).

[Me62] A. Messiah, *Quantum Mechanics*, (North-Holland, Amsterdam, 1962) vol. 2.

[Mo99] K. Mølmer, A. Sørensen, *Multiparticle Entanglement of Hot Trapped Ions* Phys. Rev. Lett. **82** 1835 (1999).

[Mo95] C. Monroe, D. M. Meekhof, B. E. King, W. M. Itano, and D. J. Wineland, *Demonstration of a Fundamental Quantum Logic Gate* Phys. Rev. Lett. **75** 4714 (1995).

[Na05] M. Nakahara, *Geometry, topology and physics*, 2nd Ed., (IoP publishing, Bristol, 2005).

[NC00] M. A. Nielsen, I. L. Chuang, *Quantum Computation and Quantum Information* (Cambridge University Press, Cambridge, 2000).

[Ni02] M. A. Nielsen, *A simple formula for the average gate fidelity of a quantum dynamical operation* Phys. Lett. A **303** 249 (2002).

[Og99] R. W. Ogburn, J. Preskill, *Topological Quantum Computation* Lecture Notes in Computer Science, edited by C. P. Williams (Springer, Berlin/Heidelberg, 1999).

[Pa99] J. Pachos, P. Zanardi and M. Rasetti, *Non-Abelian Berry connections for quantum computation* Phys. Rev. A **61** 010305(R) (1999).

[Pa01] J. Pachos, P. Zanardi, *Quantum Holonomies for Quantum Computing* Int. J. Mod. Phys. B **15** 1257 (2001).

[Pa56] S. Pancharatnam, Proc. Indian Acad. Sci. A **44** 247 (1956), reprinted in *Collected works of S. Panchartnam* (Oxford Univ. Press, London, 1975).

[Pa06] D. Parodi, M. Sassetti, P. Solinas, P. Zanardi, N. Zanghì, *Fidelity optimization for holonomic quantum gates in dissipative environments* Phys. Rev. A **73** 052304 (2006).

[Pr98] J. Preskill, *Fault-tolerant quantum computation* in "Introduction to Quantum Computation", edited by S. Popescu, T. P. Spiller and H.-K. Lo (World Scientific, London, 1998), arXiv:quant-ph/9712048.

[Ro99] Ch. Roos, Th. Zeiger, H. Rohde, H. C. Nägerl, J. Eschner, D. Leibfried, F. Schmidt-Kaler, and R. Blatt, *Quantum State Engineering on an Optical Transition and Decoherence in a Paul Trap* Phys. Rev. Lett. **83** 4713 (1999).

[SB88] J. Samuel and R. Bhandari, *General Setting for Berry's Phase*, Phys. Rev. Lett. **60** 2339 (1988).

[SL05] M. S. Sarandy, D. A. Lidar, *Adiabatic Quantum Computation in Open Systems* Phys. Rev. Lett. **95** 250503 (2005).

[SL05+] M. S. Sarandy, D. A. Lidar, *Adiabatic approximation in open quantum systems* Phys. Rev. A **71**, 012331 (2005); *Abelian and non-Abelian geometric phases in adiabatic open quantum systems* Ibid. **73** 062101 (2006).

[Sh95] P. W. Shor, *Scheme for reducing decoherence in quantum computer memory* Phys. Rev. A **52** 2493 (1995).

[Si83] B. Simon, *Holonomy, the Quantum adiabatic Theorem, and Berry's Phase* Phys. Rev. Lett. **51** 2167 (1983).

[So03] P. Solinas, P. Zanardi, N. Zanghì and F. Rossi, *Holonomic quantum gates: A semiconductor-based implementation* Phys. Rev. A **67** 062315 (2003).

[So04] P. Solinas, P. Zanardi and N. Zanghì, *Robustness of non-Abelian holonomic quantum gates against parametric noise* Phys. Rev. A **70** 042316 (2004).

[So99] A. Sørensen, K. Mølmer, *Quantum Computation with Ions in Thermal Motion* Phys. Rev. Lett. **82** 1971 (1999).

[St96] A. Steane, *Multiple Particle Interference and Quantum Error Correction* Proc. R. Soc. Lond. A **452** 2551 (1996).

[Tr06] A. Trullo, P. Facchi, R. Fazio, G. Florio, V. Giovannetti, S. Pascazio, *Robustness of optimal working points for non-adiabatic holonomic quantum computation* Las. Phys. **16** 1478 (2006).

[Uh76] A. Uhlmann, *The "transition probability" in the state space of a $*$-algebra* Rep. Math. Phys. **9** 273 (1976).

[WZ84] F. Wilczek and A. Zee, *Appearance of Gauge Structure in Simple Dynamical Systems* Phys. Rev. Lett. **52** 2111 (1984).

[Wi98] D. J. Wineland, C. Monroe, W. M. Itano, D. Leibfried, B. E. King, D. M. Meekhof, *Experimental issues in coherent quantum-state manipulation of trapped atomic ions* J. Res. Natl. Inst. Stand. Technol. **103** 259 (1998).

[Wu05] L.-A. Wu, P. Zanardi, D. A. Lidar, *Holonomic quantum computation in decoherence-free subspaces* Phys. Rev. Lett. **95** 130501 (2005).

[ZR97] P. Zanardi and M. Rasetti, *Noiseless Quantum Codes* Phys. Rev. Lett. **79** 3306 (1997).

[ZR99] P. Zanardi, M. Rasetti, *Holonomic Quantum Computation* Phys. Lett. A **264** 94 (1999).